

THE CONTRIBUTION BY THE WATER TABLE TO CROP WATER USE

by

Ahmad Ali Hassan

B. Sc. Agric. Engg. (Hons.) (BAU, Bangladesh)

M. Engg. (AIT, Thailand)

A thesis submitted in fulfilment of the requirements
for the degree of Doctor of Philosophy
in
Agricultural Engineering

The University of Newcastle upon Tyne
July 1990

Abstract

The contribution by the water table to crop water use was evaluated in the absence of surface water application from lysimetric studies in a glasshouse during 1988, 1989 and 1990. The water table contribution was measured for beans, barley and lettuce in the presence of constant water tables 60, 90 and 120 cm deep. The water table contributed to about 27.0, 16.4 and 11.4% of evapotranspiration of barley with water tables 60, 90 and 120 cm deep, respectively. The contribution in lettuce was found to be 34.7, 13.5 and 6.0% for the 60, 90 and 120 cm water tables, respectively. The water table could not contribute to the evapotranspiration of beans because the initial soil moisture suction profile was not in equilibrium, and there was always a zero-flux plane above the water table.

Capillary upward flux from the water table was also measured using Darcy's equation and by direct measurement. For this, unsaturated hydraulic conductivity was determined in the laboratory from diffusivity over a wide range of moisture content. Conductivity values were also evaluated *in situ* using Darcy's equation. *In situ* and laboratory conductivity values were well fitted by Gardner's (1958) conductivity function but not by that of Rijtema (1965).

Root water uptake was evaluated using the extraction-term approach. A very small proportion of roots near the water table was absorbing water from the capillary fringe in the case of a deep-rooted crop (barley) for all water table depths. Lettuce, a shallow-rooted crop, was absorbing water from the water table although roots were confined to the top 5 cm depth for all water table depths.

A simulation model (CAPROW) was developed to account for capillary rise from constant water tables. The model can also predict soil moisture content, root water uptake and inflow to roots provided soil physical parameters and relevant data are known.

Parameters needed to run the model were determined from the bean experiment with the water table at 60 cm depth. CAPROW was used to simulate results for water tables at 90 and 120 cm under three different crops.

Model predictions of soil moisture contents at harvest agreed well with the measured values. The predicted cumulative upward flux in barley and lettuce under two different water table treatments agreed closely with the measured values. The contribution by the water table to water use by barley was found to be 16.4 and 11.4% for 90 and 120 cm water table depths, respectively. Corresponding simulated values were 15.5 and 10.4%. For lettuce, measured contributions from the water table to evapotranspiration were 13.5 and 6.0%. Corresponding simulated values were 15.7 and 6.7%.

Acknowledgements

This research was carried out under the supervision of Prof. J. R. O'Callaghan and Dr. D. A. Rose. The author acknowledges with gratitude their invaluable help, guidance and constant inspiration throughout the duration of this work.

The author thanks Dr. D. L. Rimmer for chemical analysis of the soil, and fertilizer recommendations.

The author appreciates the help rendered by Anne Pickering and other staffs in Moor Bank glasshouse.

Acknowledgement is also due to the Commonwealth Scholarship Commission for its financial support and the Bangladesh Institute of Nuclear Agriculture for granting study leave.

The author thanks his mother, wife, brothers and sisters for their inspiration and patience throughout the study.

Contents

Abstract	ii
Acknowledgements	iv
1 STATEMENT OF PROBLEM	1
1.1 General:Water Demand by Plants	1
1.1.1 Evapotranspiration	2
1.1.2 Photosynthesis	2
1.1.3 Nutrient Transport	3
1.2 Sources of Water Supply to Plants	3
1.3 Transfer Process from Storage to Plant Roots	4
1.4 Groundwater Contribution to Crop Water Demand	7
1.4.1 Groundwater through Capillary Fringe to Roots	8
1.4.2 Groundwater through Capillary Fringe to Surface	8
1.5 Problem to be Investigated	9
2 BACKGROUND AND LITERATURE SURVEY	11
2.1 Unsaturated Flow	11
2.1.1 Soil Moisture Characteristics	11
2.1.2 Determination of Unsaturated Hydraulic Conductivity	13
2.1.2.1 Laboratory Methods	13
2.1.2.2 Field Methods	14
2.1.3 Prediction of Unsaturated Hydraulic Conductivity	15
2.1.4 Hysteresis of the Hydraulic Conductivity	15
2.1.5 The Dynamics of Capillary Rise	16
2.1.6 Capillary Potential and Capillary Rise	16
2.1.7 Steady Evaporation in Presence of Water Table	17
2.2 Water Table Effect on Yield and Water Use	21
2.3 Experiments on Water Table Contribution	24
2.4 Water Uptake by Roots	27
3 THEORY	31
3.1 Theory of Unsaturated Flow	31
3.1.1 Soil Water Potential	31

3.1.2	Soil Moisture Characteristic	32
3.1.3	Hydraulic Conductivity	34
3.1.3.1	Hydraulic Conductivity from Diffusivity	36
3.1.3.2	Hydraulic Conductivity from Unsteady Drainage Flux	37
3.1.3.3	Hydraulic Conductivity from Water Depletion	39
3.1.3.4	$K(\psi)$ Empirical Equation	39
3.1.4	Capillary Rise	40
3.1.4.1	Plane of Zero Flux	41
3.1.5	Water Uptake by Roots	41
4	MATERIALS AND METHODS	43
4.1	Materials	43
4.1.1	Experimental Site	43
4.1.2	Soil	43
4.1.3	Crops	43
4.1.4	Lysimeters	43
4.1.5	Mariotte Siphon	44
4.1.6	Tensiometers	44
4.1.7	Resistance Blocks	46
4.2	Methods	46
4.2.1	Soil Analysis	46
4.2.2	Soil Moisture Characteristic	46
4.2.2.1	Haines Method	46
4.2.2.2	Pressure Plate Apparatus	47
4.2.2.3	Resistance Block	47
4.2.2.4	Vacuum Desiccator Method	47
4.2.3	Unsaturated Hydraulic Conductivity	48
4.2.3.1	Diffusivity Measurement	48
4.2.3.2	Drainage Flux Method	50
4.2.3.3	Soil-water Depletion Method	50
4.2.4	Root Length Measurement	51
4.3	Experimental	52
4.3.1	Runner Bean Experiment (June to October, 1988)	52
4.3.2	Barley Experiment (April to July, 1989)	53
4.3.3	Lettuce Experiment (March to May, 1990)	54

5	MODELLING	56
5.1	Capillary Upward Flux	56
5.1.1	Computational Procedure	57
5.1.2	Boundary Conditions	57
5.2	Root Water Uptake	58
5.2.1	Computational Procedure	58
5.2.2	Boundary Conditions	59
5.3	Inflow to Roots	59
5.4	Description of the Computer Model	60
5.5	Model Input Parameters	60
6	RESULTS AND DISCUSSION	63
6.1	Soil Properties	63
6.1.1	Bulk density	63
6.1.2	Mechanical Composition of Soil	63
6.1.3	Soil Moisture Characteristics	64
6.1.4	Hydraulic Conductivity	69
6.1.5	Soil Moisture Suction	75
6.2	Hydraulic Head Gradient and Plane of Zero Flux	90
6.3	Soil Moisture Extraction	103
6.4	Soil Water Flux	114
6.5	Capillary Rise from Water Table	134
6.6	Root Water Uptake	145
6.6.1	Sink Term and Suction	154
6.6.2	Inflow Rate to Roots	159
6.7	Water Table Contribution, Yield and Water Use of Crops	163
6.8	Separation of Evaporation and Transpiration	172
6.9	Simulation	173
7	SUMMARY AND CONCLUSIONS	184
7.1	Soil Properties	184
7.2	Capillary Contribution	184
7.3	Root Water Uptake	185
7.4	Model Prediction	185
7.5	Future Extension	186

APPENDIX A	187
APPENDIX B	188
REFERENCES	194

List of Figures

1.1	Soil-plant-water-atmosphere systems.	5
4.1	Schematic of lysimetric soil-water-plant system that operates on the Mariotte siphon principle (not to scale).	45
5.1	Flow chart of the operations of programme CAPROW.	61
6.1.	(a) Moisture characteristic curve for lysimeter WT-60.	66
6.1.	(b) Moisture characteristic curve for lysimeter WT-90.	67
6.1.	(c) Moisture characteristic curve for lysimeter WT-120.	68
6.2.	(a) Hydraulic conductivity versus soil moisture suction for WT-60.	72
6.2.	(b) Hydraulic conductivity versus soil moisture suction for WT-90.	73
6.2.	(c) Hydraulic conductivity versus soil moisture suction for WT-120.	74
6.3.	(a) Suction from tensiometers in lysimeter WT-60 (Bean).	79
6.3.	(b) Suction from tensiometers in lysimeter WT-90 (Bean).	80
6.3.	(c) Suction from tensiometers in lysimeter WT-120 (Bean).	81
6.4.	(a) Suction from tensiometers in lysimeter WT-60 (Bar- ley).	82
6.4.	(b) Suction from tensiometers in lysimeter WT-90 (Bar- ley).	83
6.4.	(c) Suction from tensiometers in lysimeter WT-120 (Bar- ley).	84
6.5.	(a) Suction from tensiometers in lysimeter WT-60 (Let- tuce).	85
6.5.	(b) Suction from tensiometers in lysimeter WT-90 (Let- tuce).	86
6.5.	(c) Suction from tensiometers in lysimeter WT-120 (Let- tuce).	87
6.6.	Calibration of resistance block.	88

6.7. Diurnal variation of tensiometer reading from lysimeter	
WT-60 (Bean).	89
6.8. (a) Variation of hydraulic gradient with time for WT-60	
(Bea).	94
6.8. (b) Variation of hydraulic gradient with time for WT-90	
(Bea).	95
6.8. (c) Variation of hydraulic gradient with time for WT-120	
(Bea).	96
6.9. (a) Variation of hydraulic gradient with time for WT-60	
(Barley).	97
6.9. (b) Variation of hydraulic gradient with time for WT-90	
(Barley).	98
6.9. (c) Variation of hydraulic gradient with time for WT-120	
(Barley).	99
6.10. (a) Variation of hydraulic gradient with time for WT-60	
(Lettuce).	100
6.10. (b) Variation of hydraulic gradient with time for WT-90	
(Lettuce).	101
6.10. (c) Variation of hydraulic gradient with time for WT-120	
(Lettuce).	102
6.11. (a) Water content versus time for WT-60 (Bean).	105
6.11. (b) Water content versus time for WT-90 (Bean).	106
6.11. (c) Water content versus time for WT-120 (Bean).	107
6.12. (a) Water content versus time for WT-60 (Barley).	108
6.12. (b) Water content versus time for WT-90 (Barley).	109
6.12. (c) Water content versus time for WT-120 (Barley).	110
6.13. (a) Water content versus time for WT-60 (Lettuce).	111
6.13. (b) Water content versus time for WT-90 (Lettuce).	112
6.13. (c) Water content versus time for WT-120 (Lettuce).	113
6.14. (a) Measured flux versus time for WT-60 (Bean).	116
6.14. (b) Measured flux versus time for WT-90 (Bean).	117

6.14. (c) Measured flux versus time for WT-120 (Bean).	118
6.15. (a) Hydraulic conductivity as a function of depth for WT- 60 (Bean).	119
6.15. (b) Hydraulic conductivity as a function of depth for WT- 90 (Bean).	120
6.15. (c) Hydraulic conductivity as a function of depth for WT- 120 (Bean).	121
6.16. (a) Measured flux versus time for WT-60 (Barley).	122
6.16. (b) Measured flux versus time for WT-90 (Barley).	123
6.16. (c) Measured flux versus time for WT-120 (Barley).	124
6.17. (a) Hydraulic conductivity as a function of depth for WT- 60 (Barley).	125
6.17. (b) Hydraulic conductivity as a function of depth for WT- 90 (Barley).	126
6.17. (c) Hydraulic conductivity as a function of depth for WT- 120 (Barley).	127
6.18. (a) Measured flux versus time for WT-60 (Lettuce).	128
6.18. (b) Measured flux versus time for WT-90 (Lettuce).	129
6.18. (c) Measured flux versus time for WT-120 (Lettuce).	130
6.19. (a) Hydraulic conductivity as a function of depth for WT- 60 (Lettuce).	131
6.19. (b) Hydraulic conductivity as a function of depth for WT- 90 (Lettuce).	132
6.19. (c) Hydraulic conductivity as a function of depth for WT- 120 (Lettuce).	133
6.20. (a) Capillary rise as a function of time (Barley).	137
6.20. (b) Water use from soil profile and water table against time for WT-60 (Barley).	138
6.20. (c) Water use from soil profile and water table against time for WT-90 (Barley).	139
6.20. (d) Water use from soil profile and water table against time for WT-120 (Barley).	140

6.21. (a) Capillary rise as a function of time (Lettuce).	141
6.21. (b) Water use from soil profile and water table against time for WT-60 (Lettuce).	142
6.21. (c) Water use from soil profile and water table against time for WT-90 (Lettuce).	143
6.21. (d) Water use from soil profile and water table against time for WT-120 (Lettuce).	144
6.22. (a) Measured sink term versus time for WT-60 (Bean).	147
6.22. (b) Measured sink term versus time for WT-90 (Bean).	148
6.22. (c) Measured sink term versus time for WT-120 (Bean).	149
6.23. (a) Measured sink term versus time for WT-60 (Barley).	150
6.23. (b) Measured sink term versus time for WT-90 (Barley).	151
6.23. (c) Measured sink term versus time for WT-120 (Barley).	152
6.24. Measured sink term versus time for lettuce at 5 cm depth.	153
6.25. (a) Sink term as a function of suction (Bean).	155
6.25. (b) Sink term as a function of suction (Barley).	156
6.25. (c) Sink term as a function of suction (Lettuce).	157
6.25. (d) Sink term hypothesis as a function of suction (after Feddes and Zaradny, 1978.)	158
6.26. Evapotranspiration as a function of time (Bean).	169
6.27. Evapotranspiration as a function of time (Barley).	170
6.28. Evapotranspiration as a function of time (Lettuce).	171
6.29. (a) Measured and simulated water content as a function of depth for WT-60 at harvest (Bean).	175
6.29. (b) Measured and simulated water content as a function of depth for WT-90 at harvest (Bean).	176
6.29. (c) Measured and simulated water content as a function of depth for WT-120 at harvest (Bean).	177
6.30. (a) Measured and simulated water content as a function of depth for WT-60 at harvest (Barley).	178

6.30. (b) Measured and simulated water content as a function of depth for WT-90 at harvest (Barley).	179
6.30. (c) Measured and simulated water content as a function of depth for WT-120 at harvest (Barley).	180
6.31. (a) Measured and simulated water content as a function of depth for WT-60 at harvest (Lettuce).	181
6.31. (b) Measured and simulated water content as a function of depth for WT-90 at harvest (Lettuce).	182
6.31. (c) Measured and simulated water content as a function of depth for WT-120 at harvest (Lettuce).	183

List of Tables

1.1	Nomenclature.	6
2.1	Comparison of measured and maximal evaporation rates with theoretically predicted rates for steady evaporation from uniform soil columns of sand and loess (Hadas and Hillel, 1968).	20
2.2	Annual rainfall, class A pan evaporation and evapotranspira- tion with different degree of plant cover and water table depth (Stewart et al., 1969).	22
2.3	Water table effect on grainyield, plant height, grain moisture content with of maize under irrigated and rainfed condition (Alvino and Zebri, 1986).	22
2.4	A summary of water table effect on total E , yield, and fresh bio-mass for different crops.	24
2.5	Summary of some experiments to measure groundwater con- tribution.	27
2.6	Inflow of water into roots, cm^3 (water) cm^{-1} (root) d^{-1} (Gregory, 1988).	30
6.1	Bulk density of soil in lysimeters (Mean \pm s.d., $n = 5$).	63
6.2	Mechanical composition of soil (Mean \pm s.d., $n = 3$).	64
6.3	Calculation of capillary conductivity in lysimeter with water table at 60 cm depth (from Bean experiment).	70
6.4	Summary of time at which tensiometers failed (days from sow- ing) at different depths for different water table treatments under beans.	76
6.5	Summary of time at which tensiometers failed (days from sow- ing) at different depths for different water table treatments under barley.	77
6.6	Summary of time at which tensiometers failed (days from sow- ing) at different depths for different water table treatments under lettuce.	78
6.7	Summary of time at which zero-flux plane moved for different water table treatments under beans.	91

6.8	Summary of time at which zero-flux plane moved for different water table treatments under barley.	92
6.9	Summary of time at which zero-flux plane moved for different water table treatments under lettuce.	93
6.10	Components of the water balance equation (mm) for different water tables after harvest of bean (1988).	134
6.11	Components of the water balance equation (mm) for different water tables after harvest of barley (1989).	135
6.12	Components of the water balance equation (mm) for different water table after harvest of lettuce (1990).	136
6.13	Root length density (R_l) and inflow to roots (I_r) in each lysimeter for bean (Mean \pm s.d.,n=3).	160
6.14	Root length density (R_l) and inflow to roots (I_r) in each lysimeter for barley (Mean \pm s.d.,n=3).	161
6.15	Root length density (R_l) and inflow to roots (I_r) in each lysimeter for lettuce (Mean \pm s.d.,n=3).	162
6.16	Fresh bean yield, top fresh yield, drymatter yield and pro- portion, water use and efficiency for different water table treatments.	165
6.17	Yield of barley, top fresh yield, drymatter yield and propor- tion, water use and efficiency for different water table treat- ments.	166
6.18	Fresh lettuce yield, drymatter yield and proportion, water use and efficiency for different water table treatments.	166

Chapter I

STATEMENT OF PROBLEM

1.1 General:Water Demand by Plants

All plant growth depends upon a supply of water, and normally the need is satisfied through roots that extract water from the soil in which the plants grow. Often water availability is a major control to plant growth in both ecological and physiological contexts. Water in soil fulfils the demand of the plant in three different major ways.

- First, water transpired through plant leaves and evaporated from soil maintains a balance with the atmospheric demand. Otherwise, normal plant growth is stunted.
- Second, it is a major constituent of plant protoplasm, sometimes making up as much as 95% of the total weight of the plant. Most organic substances in protoplasm, including carbohydrates, proteins and nucleic acids are hydrated in their natural state and removal of water adversely affects their physical and chemical properties. When protoplasm is dehydrated it stops activity and below a certain water content it is killed. Amongst the processes directly affected by dehydration is photosynthesis, where water takes part in a number of chemical reactions.
- Third, nutrients can be obtained from the soil by the plant only in aqueous solution. Water acts as a solvent in which minerals and other solutes enter plant cells and move from cell to cell and organ to organ. The permeability of most cell walls and membranes to water results in a continuous liquid phase extending throughout the plant in which translocation of solutes of all kinds occurs.

1.1.1 Evapotranspiration

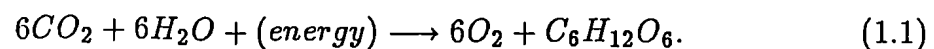
Evapotranspiration (E), a combined term for the evaporation of water from soil or plant surfaces and transpiration from plant leaves, is a complex of interactions between soil, plant and the atmosphere. Plants transpire over 90% of the extracted water from the soil to satisfy the atmospheric demand. The occurrence of evaporation or transpiration requires three conditions to be satisfied.

- First, the evaporating surface must have a supply of water.
- Second, there should be a source of energy to vaporise water.
- Third, a mechanism should be available to transfer the vapour away from the surface.

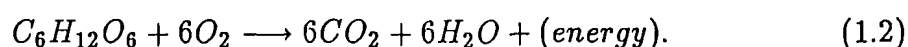
Soil pores in the root zone act as a reservoir of water and the energy is supplied by the ultimate source, the sun. The transfer mechanism consists of molecular and turbulent diffusion processes. For evaporation from the soil, the vaporization of water takes place at the soil surface. Where a water table occurs close to the surface, continual flow may take place from the capillary fringe (a region of saturation or near saturation above the water table, frequently referred to imprecisely as the capillary fringe) underneath depending on whether the surface soil is saturated or not. But for transpiration, the conversion of liquid water to vapour phase takes place at the walls of the mesophyll and epidermal cells of leaves. The mechanics of water supply to these surfaces at which vaporization occurs, therefore, forms an important part of evapotranspiration process.

1.1.2 Photosynthesis

Photosynthesis is a process where carbon dioxide, after reacting with water in the presence of sunlight, is converted into carbohydrates by the chloroplasts. The basic reaction of this photosynthetic process can be summarized as:



When the reduced carbon atoms in the sugars i.e. carbohydrates, are oxidized during respiration, energy is released and water is again formed as follows:



It is apparent from these two equations that the water in plant cells is an essential metabolic intermediate in the same way as are nitrogen, phosphorus or potassium.

Photosynthetic tissues contain water sometimes making up as much as 95% of the total weight of plant. A very small portion of this water (0.2%) is used in photosynthesis and the rest is retained in the plant for transpiration. Slatyer (1967) pointed out that the rate at which stress is applied will affect the response in respiration rate. Chang (1968) stated that the rate of photosynthesis declines noticeably after a reduction of approximately 30% in the water content of leaves and ceases when 60% of leaf moisture is lost.

1.1.3 Nutrient Transport

The absorption of mineral nutrients is as important as the absorption of water. But the uptake of nutrients from the soil and then their translocation to different organs of the plant is not possible without the presence of water.

There are two different processes whereby nutrients are transferred from the bulk of soil to the root surface. These processes are mass flow (convection) and diffusion. Mass flow occurs because water is absorbed by roots to meet the loss by transpiration from the shoot; as the water moves to the roots so dissolved ions are also carried to the root surface. Diffusion occurs when ions move along a concentration gradient established between the root surface and the body of soil; ions diffuse towards the root if they are taken up faster than they are carried to the surface by mass flow and away from the root if the converse pertains.

1.2 Sources of Water Supply to Plants

The evaporative demand of the atmosphere can be met by water from different sources e.g. precipitation, irrigation, soil water store and groundwater. Different

sources of water that fulfil crop water need can be well understood if the soil-water-plant atmosphere system is considered as shown in Fig.1.1 (Nomenclature in Table 1.1).

Precipitation may be of different forms e.g. solid(snow) and liquid. Its distribution is not uniform for each and every location. Various factors influence its distribution, frequency, amount and depth. This is the main source of water for the soil-water-plant atmosphere system. The average annual rainfall and its average seasonal distribution are first indicators of possible water availability.

Rainfall, after its interception by foliage and infiltration by the soil, contributes to soil moisture storage in the unsaturated zone of the soil. Water storage capacity is the maximal amount of water that soil can retain after gravitational water drains off naturally under field conditions when wetted from above and evaporation is absent. Again, depending on the soil moisture storage capacity, there is interflow and deep percolation to the water table for groundwater storage. Irrigation is practised in situations where the rainfall and the available stored water in the soils fail to meet the water requirements of the crops.

1.3 Transfer Process from Storage to Plant Roots

The transfer of water from storage occurs when there is a gradient of water potential from the soil surrounding the root to the root xylem. The rate at which water transport occurs depends on the magnitude of the gradient in water potential and the resistance to water flow in the soil and the roots. Resistance to water movement in the soil depends mainly on the hydraulic conductivity. Resistance in roots depends mainly on the degree of suberization and the physical condition of the protoplasm and its resistance to water movement. Again the physical condition of the protoplasm depends on factors such as aeration and temperature.

The transport of water from the soil to the plant is not an independent process but is related to and largely controlled by the rate of water loss in transpiration, at least when water is readily available to the roots. Water movement through plants from soil to air is regarded as a series of linked processes in which the overall rate is controlled by the stage at which the greatest resistance to water movement occurs.

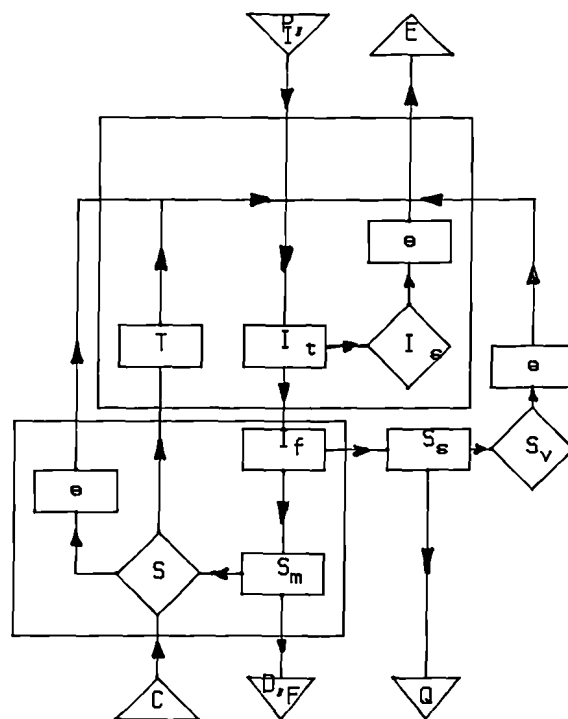


Fig. 1.1. Soil-water-plant-atmosphere systems.

Table 1.1. Nomenclature.

C	Capillary rise.
D	Percolation.
E	Evapotranspiration.
e	Evaporation.
F	Interflow.
I	Irrigation.
I _f	Infiltration.
I _s	Internal storage.
I _t	Interception.
P	Precipitation.
Q	Runoff.
S	Soil moisture storage.
S _s	Surface storage capacity.
S _m	Soil moisture storage capacity.
S _v	Surface storage.
T	Transpiration.

As long as the plant does not wilt, and as long as the influx of radiation and heat to the canopy results in change of phase only, it is possible to assume steady flow through the plant. Since van den Honert (1948) it has been popular to use resistance analogues to describe the steady-state fluxes in the soil-plant-atmosphere continuum (SPAC) in the form:

$$E = \frac{-\Delta\phi_1}{R_1} = \frac{-\Delta\phi_2}{R_2} = \frac{-\Delta\phi_3}{R_3} = \frac{-\Delta\phi_4}{R_4} \quad (1.3)$$

where

E = transpiration rate,

$\Delta\phi_1, \Delta\phi_2, \Delta\phi_3, \Delta\phi_4$ = potential drop in the soil towards the roots, the soil and root xylem, root xylem to the leaves, leaves and atmosphere, respectively, and

R_1, R_2, R_3, R_4 = resistances in soil, root, xylem, and leaves, respectively.

Experimental and theoretical studies of soil moisture extraction by roots (Molz, 1976; Nimah and Hanks, 1973; Reicosky and Ritchie, 1976) suggest that different resistance terms can be important: the root resistance term most probably tending to predominate in wet soils with high hydraulic conductivity, and the soil's hydraulic resistance tending to gain importance as the extraction process continues and causes progressive depletion of soil moisture.

1.4 Groundwater Contribution to Crop Water Demand

At the beginning of the cropping season, the process of evaporation will predominate and this will reduce soil wetness and thus increase the matric suction at the surface. This, in turn, will generally cause soil water to be drawn upward from the layers beneath which have been wetted by the capillary fringe from the water table. At a later stage, transpiration will predominate and the soil will dry because water will be taken up by roots. As the surface layers have become drier from the initial evaporation process, so the crop roots will penetrate lower layers to extract water for its demand. Sometimes, when there is a shallow water table, the roots of deep-rooted crops approach the water table.

1.4.1 Groundwater through Capillary Fringe to Roots

In the presence of a water table, water uptake is not necessarily related to root distribution, and a small quantity of roots near the capillary fringe can absorb most of the water (Reicosky et al. 1972). But "single root" models (e.g. Molz, 1975) suggest that dimensions and density of roots are important.

The uptake of water required to meet crop water demand can be limited by factors in the soil, as well as in the plant. It is well known that soil hydraulic conductivity decreases as water content decreases, but few data are available on the actual magnitude of its effect on water uptake by plant roots. Unsaturated hydraulic conductivity is one of the major limiting factors in water uptake by plant roots (Reicosky et al., 1972). The amount of water absorbed from the upper part of the soil is negligible compared with that absorbed from lower layers. Therefore, downward root growth becomes important for transporting water from the capillary fringe to roots.

1.4.2 Groundwater through Capillary Fringe to Surface

When a water table occurs close to the surface, upward flow may occur from the saturated zone or capillary fringe through the unsaturated soil to the surface. If this flow is more or less steady, continued flow caused by evapotranspiration can occur without materially changing the soil moisture content. The steady rate of capillary rise depends on the depth of the water table and on the suction at the soil surface (Gardner, 1958) in the absence of a crop. This suction is dictated largely by the external conditions, since the greater the atmospheric evaporativity, the greater the suction at the soil surface upon which the atmosphere is acting. The suction at the soil surface can become very large. But the increase in flux in the soil depends on the depth of the water table. Even the driest and most evaporative atmosphere cannot steadily extract water any faster than the soil profile can transmit. The maximal transmitting ability of the profile depends on the hydraulic conductivity of the soil in relation to the suction (Marshall and Holmes, 1988; Hillel, 1980).

As the water table goes deeper and the suction at the soil surface increases, the evapotranspiration rate approaches a limiting value regardless of how high the

external evaporativity may be (Gardner, 1958; Hillel, 1980). In that case crop will be under moisture stress and need irrigation (Hillel, 1980).

1.5 Problem to be Investigated

A shallow water table contributes significantly to the evaporative demand of crops. Several reports (Misra et al., 1969; Modgal et al., 1968; Sharma and Singh, 1971) suggest that crops responded very little to irrigation mainly because of the shallow water table in the experimental area.

Successful exploitation of the water table depends on several factors that include water table depth, soil water retention and transmission properties, evapotranspiration demand and plant root system (Rijtema, 1959; Van Bavel et al., 1968; Raats and Gardner, 1974; van Bakel, 1981). Even if the water table is at 120 to 150 cm depth, a crop may not need irrigation (Torres and Hanks, 1989).

Again for exploiting the water table, it is necessary to consider the quality of water. In areas of shallow water table of good quality, crops can extract water directly from capillary fringe which thus meets the crop water demand. In saline soils, the upward flux from shallow water tables may transport salt to the soil surface. Under arid conditions, where saline soils may exist, the groundwater contribution could lead to an accumulation of salts in the root zone. It is therefore necessary to maintain a deeper water table (Talsma, 1963; Kovda et al., 1973) so that crop growth is not restricted due to salinity.

So the capillary rise from the water table, in terms of quantity and quality, is an important phenomenon in water table management schemes. Fluctuations of the water table and ground water storage are partly due to the upward flux. Again some soil water models need to know the capillary rise from the water table to determine the amount of water leaving the groundwater to satisfy crop water demand and transport of salt to the soil surface (Gardner, 1958; Hillel, 1980; Marshall and Holmes, 1988).

Bearing in mind the above facts, I conducted the study with the following objectives:

1. To determine the amount of groundwater contributing to the evaporative demand of shallow, medium and deep-rooted crops through the capillary fringe from constant, shallow water tables.
- ✱ 2. To devise a method for calculating the upward flux.
3. To investigate the differences of root penetration for differing water table depths.
4. To devise a simulation model of capillary rise including water uptake by the roots for the optimal management of the water table to crop production.
5. To apply the model in 4 to predict what might happen with other water table depths in the same soil and crops, and other crops, where root demand might be different.

Chapter II

BACKGROUND AND LITERATURE SURVEY

2.1 Unsaturated Flow

2.1.1 Soil Moisture Characteristics

The relationship between matric potential (ψ) and water content θ is called a soil moisture characteristic or moisture release curve, $\theta(\psi)$, (Childs, 1940).

The determination of the soil moisture characteristic is a routine procedure. In addition to having a practical value in the tensiometric measurement and control of soil water, its utility is recognised in the mathematical description of transient water flow problems (Richards et al., 1956).

The existence of hysteresis or nonsingularity between the drying and wetting characteristics has been discussed by Haines (1930) and Richards (1931). Hysteresis has been the subject of many investigators, e.g. Youngs (1960) and Poulouvasilis (1962). But a single characteristic curve which can describe the whole phenomenon (drying and wetting simultaneously) has neither been shown nor investigated (Youngs, 1960; Poulouvasilis, 1962).

Hysteresis in many models is ignored because insufficient data are available to take it into account. There are some empirical models (Gillham et al., 1976; Hoa et al., 1977) in which it is assumed that scanning curves in the $\theta(\psi)$ relation can be scaled from the main hysteresis loop. But these are not as acceptable as the theoretical models (Poulouvasilis, 1962; Topp, 1971; Kool and Parker, 1987) which are based on the domain theory of capillary hysteresis. In the case of a drying cycle, one uses the desorption curve $\theta(\psi)$ with no consideration of the hysteresis effect (Marshall and Holmes, 1988).

The desorption soil moisture characteristic, $\theta(\psi)$ is usually obtained by starting with initially saturated soil and removing water until a desired matric potential is reached. There are several methods of determining $\theta(\psi)$ relations (Klute, 1986).

The static availability of soil water to the plant roots is determined by the potential of soil water in the boundary layer closely surrounding the roots. The methods useful in determining soil water potential are tensiometer, moisture block and thermocouple psychrometer (Slavik, 1974).

Several authors (Jamison and Kroth, 1958; Bartelli and Peters, 1959; Lund, 1959; Salter et al., 1966; Shaykewich and Zwarich, 1968; Gupta and Larson, 1979) have reported empirical relationships between soil texture and water content on soil moisture characteristics. Visser (1969a) reported there are very few quantitative studies on soil properties related to the form of the soil moisture characteristic.

Several empirical models have been proposed for the soil moisture characteristic curve, and one of them (Cowan, 1965) is the simple logarithmic function (Equation 2.1) which describes only a limited range of θ , not the entire range.

$$\ln(\psi) = l + m\theta \quad (2.1)$$

where

ψ = the water potential,

θ = volumetric water content, and

l, m = parameters for a given soil.

McQueen and Miller (1974) and many others have provided good evidence that this function can yield a useful description of the draining soil moisture characteristics, the $\theta(\psi)$ function.

Visser (1969b), Gardner et al. (1970), Rogowski (1971), Jacobsen (1973), and Clapp and Hornberger (1978), however, have illustrated that the power function $\psi = p\theta^q$ is a useful model for the soils they examined. Clapp and Hornberger (1978) suggested that the exponent q was dependent on texture.

Williams et al. (1983) reported a small error of prediction in using Equation (2.1) for the soil moisture characteristic compared to direct laboratory determination. The standard error of the mean for the actual estimate of moisture content ranged from ± 0.009 to ± 0.029 .

2.1.2 Determination of Unsaturated Hydraulic Conductivity

Application of soil water flow theory to many practical problems requires estimates or measurements of hydraulic conductivity or soil water diffusivity for unsaturated soil over the water content range of interest (Green et al., 1986). While soil moisture content and hydraulic conductivity are crucial parameters for determining soil water flow, their theoretical description and measurement remain a continuous and sometimes difficult challenge for many workers (Sposito, 1986). Numerous methods have been developed to evaluate soil hydraulic properties using both laboratory and field methods (Klute, 1972; Ragab et al., 1981; Bouma, 1983; Alexander and Skaggs, 1986; Hillel and Benyamini, 1973).

2.1.2.1 Laboratory Methods

(a) *Steady-state Head Control Method* - In the steady-state method (Klute and Dirksen, 1986) of determining $K(\theta)$, a time-invariant, one-dimensional flow of the liquid phase is established in a soil sample at a given water content. The volumetric flux density and the hydraulic gradient are measured, and the conductivity is calculated from the ratio of flux density/gradient. The conductivity obtained is related to the measured matric potential and water content.

(b) *Hydraulic Conductivity from Diffusivity* - Bruce and Klute (1956) and Gardner (1956) have used Darcy's equation in terms of the diffusivity (Buckingham, 1907; Childs and Collis-George, 1950; Sposito, 1986) using the following transport diffusion equation.

$$\frac{\partial \theta}{\partial t} = \frac{\partial}{\partial z} \left[D(\theta) \frac{\partial \theta}{\partial z} \right] + K(\theta) \quad (2.2)$$

in which $D(\theta)$ is the soil water diffusivity and $K(\theta)$ is the hydraulic conductivity, written here for one-dimensional vertical flow.

Gardner (1962) reduced the transport diffusion equation to a linear parabolic equation by assuming $D(\theta)$ constant. This assumption is based on the fact that for a small change in θ , $D(\theta)$ is approximately constant; and that over this small range, the $\theta(\psi)$ relation of the soil is linear. In that case, Equation (2.2) becomes for horizontal flow:

$$\frac{\partial \theta}{\partial t} = -D(\theta) \left[\frac{\partial^2 \theta}{\partial x^2} \right] \quad (2.3)$$

or

$$\frac{\partial \psi}{\partial t} = -K(\psi) \left[\frac{\partial^2 \psi}{\partial x^2} \right] \quad (2.4)$$

However, literature has revealed that generally in soils $K(\psi)$, $K(\theta)$ functions decrease sharply with decrease of moisture content (Doering, 1965; Klute, 1972). Some modifications of the unsteady flow equations were developed in determining $K(\psi)$, $K(\theta)$ indirectly by evaluating $D(\theta)$ first in the laboratory (Ragab et al., 1981).

Rose (1963a, 1968b) applied the principles of evaporation of water from a soil column under isothermal conditions. The soil aggregate column remained essentially semi-infinite, which enabled the evaluation of $D(\theta)$.

Gardner (1962) reported that $D(\theta)$ can be calculated directly from the outflow rate from a large one-step change in pressure, $\Delta\psi$ by assuming constant diffusivity over the entire length of the soil sample. This one-step outflow method has been shown to agree with other methods (Doering, 1965; Acharya and Daudet, 1980). Recently the one-step outflow method has been involved in generating data for parameter estimation (Kool et al., 1985; Parker et al., 1985).

2.1.2.2 Field Methods

A larger area of measurement and preservation of field structure are inherent advantages of field methods over laboratory methods (Green et al., 1986).

(a) *Unsteady Drainage Flux Method* - This is also called the instantaneous profile method after Watson (1966). The drainage flux method was first used in the field by Richards et al. (1956). It was developed further by Nielsen et al. (1964), Rose et al. (1965) and van Bavel et al. (1968). Watson (1966) improved upon the analysis of data by replacing the computation of differences in time

and depth by the presumably more accurate instantaneous profile method. This method is elaborated in this study (Section 3.1.3.2).

(b) *Unit Hydraulic Gradient Method* - $K(\theta)$ is determined from the periodic measurement of $\theta(z, t)$ during the redistribution of water in the soil profile following infiltration (Green et al., 1986). In addition to the assumption of negligible lateral flow in the soil layer, a unit hydraulic gradient is also assumed, i. e. $\frac{\partial H}{\partial z} = -1$ (Ragab et al., 1981). The assumption of unit gradient during redistribution of soil water without evaporation following infiltration in a uniform soil was introduced by Black et al. (1969). This assumption was used in the determination of hydraulic conductivity of unsaturated soil by Nielsen et al. (1973).

2.1.3 Prediction of Unsaturated Hydraulic Conductivity

The solution of unsaturated flow problems requires the predetermination of soil hydraulic properties such as the relationship of matric potential, ψ with the moisture content, and the dependence of hydraulic conductivity, K upon the moisture content.

Empirical formulae (Wind, 1955; Gardner, 1958; Brooks and Corey, 1964; Averjanov, 1950; Rijtema, 1965) can be applied to predict K when some measured data of either $K(\psi)$ or $K(\theta)$ are available (Muallem, 1986) for the following reasons:

1. To allow a closed-form analytical solution for some unsaturated flow problems.
2. To simplify the computational procedure of numerical solution, save computer time, and improve accuracy.
3. To systematically extrapolate the measured curve.
4. To minimize the measurements required for statistical representation of the hydraulic conductivity distribution in the field.

2.1.4 Hysteresis of the Hydraulic Conductivity

The $\theta(\psi)$, $K(\psi)$ or $K(\theta)$ relations are not unique functions but depend on the history of wetting and drying processes to which the porous medium was subjected

(Davidson et al., 1966). The hysteresis in $K(\psi)$ is orders of magnitude bigger than hysteresis in $\theta(\psi)$ (Nielsen and Biggar, 1961; Topp, 1969; Poulouvasilis, 1970; Talsma, 1970; Vachaud and Thony, 1971).

It is preferable to use the $K(\theta)$ relation rather than the $K(\psi)$ for many practical uses in which wetting and drying processes are involved, if hysteresis is to be neglected (Mualem, 1986). Mualem (1974, 1976b) proposed methods that allow prediction of hysteresis in $K(\psi)$ as well as $K(\theta)$. When drying from an initially wet profile however, the $K(\psi)$ function (Gardner, 1958; Hillel, 1980) can be used, because there is no hysteresis.

2.1.5 The Dynamics of Capillary Rise

Parlange and Aylor (1972) examined the dynamics of capillary rise of water in a long column of porous medium when its base is suddenly immersed in water. Initially, the column had a uniform water content. They have used the following one-dimensional equation for the rise of water into the porous medium.

$$\frac{\partial z}{\partial t} + \frac{\partial}{\partial \theta} \left(D \frac{\partial \theta}{\partial z} \right) = \frac{dK}{d\theta} \quad (2.5)$$

The boundary conditions of Equation (2.5) were as follows:

$$\begin{aligned} t = 0, \quad z \geq 0, \quad \theta = \theta_0 = 0 \\ t > 0, \quad z = 0, \quad \theta = \theta_1 = 1. \end{aligned}$$

Philip's (1966) numerical solution to the same equation describes only the early stage of the capillary rise, typically less than 10% of the complete rise, whereas the solution of Parlange and Aylor (1972) describes the whole phenomenon.

2.1.6 Capillary Potential and Capillary Rise

The capillary potential concept, introduced by Buckingham (1907), assumed a capillary force field generated by the attraction of moist soil for water. He defined a capillary potential, the gradient of which is equal in magnitude to the capillary

force. Shortly after Buckingham, Green and Ampt (1911, 1913) also introduced the capillary force concept of soil moisture. The introduction of a potential function gave rise to the study of soil moisture as a dynamic system. The capillary potential may be considered as a pressure potential due to the differential pressures on either side of the liquid-gas interface in the menisci of the water-films (Gardner et al., 1922).

The rise of water in soil from the water table is termed capillary rise. This term derives from the capillary model (Keen, 1919) which considers the soil as a bundle of capillary tubes, predominantly wide in case of sandy soil and narrow in clay soil. Accordingly, the equation relating to the equilibrium height of capillary rise to the radii of pores is as follows:

$$h = \frac{2\gamma \cos \alpha}{r\rho g} \quad (2.6)$$

where

h = capillary rise,

γ = surface tension,

r = the capillary radius of pores,

ρ = density of water,

g = the acceleration due to gravity, and

α = the contact angle which is usually considered as zero.

2.1.7 Steady Evaporation in Presence of Water Table

The steady-state upward flow of water from a water table through the soil profile to an evaporation zone was first studied by Moore (1939). Theoretical solutions of the flow equation for the process of evaporation from the soil surface in the presense of a water table were given by several workers including Gardner (1958), Anat et al. (1965) and Ripple et al. (1972).

Shaykewich and Stroosnijder (1977) used the concept of matric flux potential for determining the steady upward flux. They defined the matric flux potential as follows:

$$M(h) = \int_{h_0}^h K(h)dh \quad (2.7)$$

where

M = matric flux potential at pressure head h ,

h = pressure head at the centre of the effective root zone, and

h_0 = the pressure head at the water table = 0, and

$K(h)$ = unsaturated hydraulic conductivity function.

Memon et al. (1986) used Gardner's (1958) one-dimensional unsaturated flow equation for steady-state evaporation. They derived the relation in calculating the upward flux in finite difference form as:

$$z_{i+1} = \frac{M_{i+1} - M_i}{q + [K(h_{i+1}) + K(h_i)]/2} \quad (2.8)$$

where

h = soil water pressure head,

z = vertical distance from soil surface.

In Equations (2.7) and (2.8), Rijtema's conductivity function was used as:

$$K(h) = ae^{-c\psi} \quad (2.9)$$

where a and c are arbitrary constants.

Philip (1957b), Gardner (1958), Ripple et al. (1972), Zhang (1968), Hadas and Hillel (1968), and Marshall and Holmes (1988) used similar approaches to calculate the steady upward flux starting with Darcy's equation. According to them, the equation describing steady upward flow is:

$$q = K(\psi)\left(\frac{d\psi}{dz} - 1\right) \quad (2.10)$$

or

$$q = D(\theta) \frac{d\theta}{dz} - K(\psi) \quad (2.11)$$

where

q = flux equal to steady evaporation rate,

ψ = suction,

K = hydraulic conductivity,

D = hydraulic diffusivity,

θ = volumetric water content, and

z = height above the water table.

An empirical equation for $K(\psi)$ given by Gardner (1958) used by some investigators, is:

$$K(\psi) = a(\psi^n + b)^{-1} \quad (2.12)$$

where a, b and n are constants which must be determined for each soil. Accordingly, Equation (2.10) becomes (Hillel, 1980):

$$q = \frac{a}{\psi^n + b} \left(\frac{d\psi}{dz} - 1 \right) \quad (2.13)$$

Disregarding the constant b in Equation (2.12), Gardner (1958) obtained the equation:

$$q_{max} = A a/d^n \quad (2.14)$$

where

d = depth of the water table below the soil surface,

a, n = constants of Equation (2.12),

A = constant which depends on n , and

q_{max} = the limiting rate at which the soil can transmit water from the water table to the evaporation zone at the surface.

A number of workers (Wind, 1955; Visser, 1959; Talsma, 1963) accorded the above theory. Hadas and Hillel (1968), however, found that experimental values deviated from the predicted behaviour (Table 2.1).

Table 2.1 — Comparison of measured and maximal evaporation rates with theoretically predicted rates for steady evaporation from uniform soil columns of sand and loess (Hadas and Hillel, 1968).

Soil	Water table depth cm	Measured rates $mm\ d^{-1}$	Calculated rates ($mm\ d^{-1}$) according to		
			Anat et al. (1965)	Gardner (1958)	
				Original	Modified
Rehovot sand	120	0.2	0.28	0.39	0.38
	70	2.0	2.40	2.40	2.0
	35	19.0	38.40	34.40	31.0
Gilat loess	120	8.0	4.2	8.2	8.1
	70	20.0	7.7	24.0	21.0

Anat et al. (1965) developed a modified set of equations employing dimensionless variables. Their theory also leads to a maximal evaporation rate q_{max} varying inversely with the water table depth d to the power of n :

$$q_{max} = [1 + \frac{1.886}{(n^2 + 1)}]d^{-n} \quad (2.15)$$

where the parameters are same as in Equations (2.12) to (2.14).

Hillel (1980) reported that a shallow water table may be present at a constant or variable depth or it may be absent or too deep to affect evaporation. Where a water table occurs close to the surface, steady-state flow may take place from the saturated zone beneath, through the unsaturated layer to the surface.

2.2 Water Table Effect on Yield and Water Use

Evapotranspiration results in a moisture loss from the capillary fringe when the water table is near the ground surface (Lembke, 1969).

Wind (1959) conducted a field experiment concerning capillary rise of moisture in a heavy clay soil. The water table was 45 cm below the soil surface. He calculated the rate of capillary rise using a water balance approach. The capillary fringe contributed about 150 mm of water over a period of 160 days. He concluded that under favourable circumstances, a delivery of 3-4 mm per day from water table to surface is possible.

Hartmann and de Boodt (1973) reported that for a shallow root zone (20 cm) of Tuberous Begonia, at the beginning of a dry period, the water table should be less than 100 cm deep if one wants to avoid irrigation daily. They also found for a root zone of 60 cm, that irrigation may be delayed even when the water table is 140 cm deep because of the groundwater contribution.

Nikolski (1977) reported that the amount of irrigation water required to maintain an optimal average water content in the root zone for maximum crop yield depends on the water table depth as well as evapotranspiration.

Stewart et al. (1969) reported that the annual evapotranspiration of Tifway bermuda grass, grown on Arzel fine sand with 30, 60 and 90 cm water tables, was proportional to the amount of plant cover. They also reported that evapotranspiration increased with grass cover at water table depths of 60 and 90 cm but decreased slightly with cover when the water table depth was 30 cm (Table 2.2). They also added that the ratio between evapotranspiration from no grass or a partial grass and full grass cover was related to the depth of water table, amount, frequency and distribution of rainfall.

In the Netherlands, the water use of crops is affected by the upward flow from the relatively shallow water table through the capillary fringe (van Bakel, 1981).

The grain yield of maize decreased as the water table depth increased with the change being more rapid in rainfed than in irrigated conditions (Alvino and Zerbi, 1986). Grain moisture content and individual seed weight were linearly related to

Table 2.2 — Annual rainfall, class A pan evaporation and evapotranspiration with different degree of plant cover and water table depth (Stewart et al., 1969).

Year	Water table depth cm	Rainfall cm	Class A pan evaporation cm	Evapotranspiration			
				Full sod cm	2/3 sod cm	1/3 sod cm	No sod cm
1965	60	137.0	171.8	104.3	84.0	65.3	39.0
1966	90	184.5	157.0	87.5	77.8	68.0	48.0
1967	30	171.0	173.3	104.8	110.5	112.8	115.8

Table 2.3 — Water table effect on grainyield, plant height, grain moisture content with of maize under irrigated and rainfed condition (Alvino and Zebri, 1986).

Water table depth cm	Irrigated				Rainfed			
	Yield	Grain moisture	Sterile	Plant	Yield	Grain moisture	Sterile	Plant
	t/ha	content %	plants %	height cm	t/ha	content %	plants %	height cm
60	10.0	18.5	17.0	2.7	7.5	18.4	20.0	2.6
80	8.0	17.7	16.0	2.6	6.0	17.7	23.0	2.5
120	7.5	17.3	15.0	2.5	4.5	17.2	26.0	2.4

water table depth. The difference in yield between the water regimes was due to the water table depth and to the percentage of sterile plants above the deep water table. Plant height decreased as water table depth increased (Table 2.3).

Alfalfa produced nearly as much forage under arid condition without irrigation as with six irrigations per year when the water table was 150 to 270 cm below

the soil surface (Campbell et al., 1960). But they reported that appreciable salt accumulation occurred in the 90 to 210 cm soil zone.

The evapotranspiration E and water use efficiency (WUE) of celery was studied by Shih and Rahi (1985), who reported that both are inversely related to the water table depth. For sorghum, E and WUE were also inversely related to water table depths (Shih, 1986) at 30, 60 and 85 cm with three replications. Similar studies on maize were reported by Shih (1985). He reported that E and water-to-yield ratio were inversely related to water table depth. The maize grew equally well with 60 and 85 cm water tables.

The water demand of the crop which is determined by the climate, is not always fulfilled. If a reduction in E partially determined by soil physical factors appears, the yield of the crop also decreases. For that reason, the effect of the soil properties in relation to the depth of the water table needs to be studied to calculate the maximum amount of water available for E (Feddes, 1968).

A summary of the water table effect on total E , yield, and fresh bio-mass for different crops is presented in Table 2.4.

Table 2.4 — A summary of water table effect on total E , yield, and fresh bio-mass for different crops.

Crop	Water table depth cm	Total E in depth mm	Total marketable yield $kg\ m^{-2}$	Total fresh biomass $kg\ m^{-2}$	Reference
<i>Maize</i> *	30	273	1.74	6.32	Shih (1985)
	60	231	2.17	7.35	
	85	183	2.29	7.11	
<i>Sorghum</i> †	30	450.6	0.52	4.64	Shih (1985)
	60	397.5	0.93	9.65	
	85	347.6	1.33	14.28	
<i>Celery</i> †	30	551.9	10.17	15.77	Shih and Rahi (1985)
	60	470.5	10.35	17.70	
	85	352.1	9.90	15.24	

2.3 Experiments on Water Table Contribution

Ragab and Amer (1986) followed two independent procedures: the first involved the use of Darcy's equation to calculate the upward capillary flux and the second, based on the soil water balance, assumed the water table contribution to be the difference between estimated E and measured soil water depletion. Both procedures estimated the water table contribution to be in the range of 19-22 cm, which amounted to about 40% of E over the 75-day growth period of maize.

* 1980

† 1981

Lal and Sharma (1974) estimated the water table contribution to E of wheat by studying the soil moisture depletion created by plants grown in bottomed and bottomless drums which were sunk in a crop field during 1969-70 and 1970-71 at Pantnagar, India. They found that the total E in the bottomed drums was 511.0 mm as against 319.6 mm in the bottomless drums for an upward flow of water. Thus the amount of water contributed by ground water table was 191.4 mm, which amounted to 37.5 % of the total consumptive use where the depth of water table varied from a maximum of 171 and 177 cm to a minimum of 126 and 132 cm in 1969-70 and 1970-71, respectively.

Wallender et al. (1979) reported that water supplied to a growing crop by capillary rise from a shallow water table can be an important resource. According to them, several thousand hectares in the western San Joaquin Valley in California have a perched water table created by irrigation and a slowly permeable subsurface zone. When irrigations were made according to a schedule that is optimum for soils without a shallow water table, cotton has shown stunted plant growth that is a characteristic of waterlogging. They used two independent procedures to evaluate the contribution of a perched water table to the evapotranspiration demand of cotton and to develop an irrigation schedule that uses the resources efficiently. The procedures were the water budget method and the chloride translocation technique. Both procedures estimated the water table contribution to be near 36 cm for the growing season.

Stuff and Dale (1978) reported the capillary rise past a 105 cm deep root-zone boundary estimated as the difference between estimated E and changes in soil moisture under maize on a tile-drained Typic Argiaquoll at West Lafayette, Indiana, during three growing seasons, 1971-73. Capillary rise supplied an average of 27% of E in periods with little or no precipitation. Their computer model estimated capillary rise to furnish about 17% of the total E over a 100-day period from 49 days before silking to 50 days after. As the monitoring of soil moisture in crop root zone becomes a part of the agricultural advisory and crop production forecasts, models must be adapted to consider capillary rise from shallow water tables.

Benz et al. (1985) investigated the water table contribution for alfalfa using the

water balance approach with non-weighing lysimeters. Four constant water table depths and three surface-irrigation levels were the independent variables. Sources of water to meet evaporative demands were rainfall, irrigation and the water table, in addition to water stored in soil. The highest alfalfa yield in both years was 8.0 t/ha and occurred in the first harvest in 1979 with 155 cm water table depth and 1.3 irrigation level ($1.3 \times \text{calculated } E$). Rainfall, surface irrigation and water table contributed 48.6, 24.7, and 26.7%, respectively, of the total actual E . The shallowest (46 cm) water table depth had the highest E and lowest yields compared to the other water table depths i.e. 101, 155, and 210 cm. The data showed that capillary rise from a range of water table depths from 101 to 210 cm contributed to the water use of alfalfa, thus decreasing surface irrigation requirements.

Benz et al. (1985) also investigated the effects of the water table and irrigation on maize and sugarbeet. The effects of four shallow constant water table depths and three surface-irrigation levels on their yields and actual E were evaluated by them in non-weighing lysimeters installed in the field. The average seasonal E was about 519 mm for maize and about 591 mm for sugarbeet after combining data from all water table depths and irrigation levels. About 63% of total E was provided by the water table in one lysimeter with the lowest surface-irrigation level and a 155 cm water table. Subirrigation from shallow water tables (101, 155, and 210 cm) contributed to E in sizeable quantities if rainfall and surface-irrigation were inadequate. Both maize and sugarbeet yields were much lower for the shallowest (46 cm) water table treatment, because of inadequate aeration.

A summary of some experiments to measure the water table contribution is presented in Table 2.5.

Table 2.5 — Summary of some experiments to measure groundwater contribution.

Croptype	Water table depth cm	Soil type	Growing period days	Groundwater contribution % <i>E</i>	Reference
Maize	25–55	clay-loam (non-saline)	75	40.0	Ragab and Amer (1986)
Wheat	126–171* 132–177†	silt-loam		37.5	Lal and Sharma (1974)
Cotton	212–266	calcareous loam	126	59.0-70.0	Wallender et al. (1979)
Maize	125–200	silt-loam	100	27.0	Stuff and Dale (1978)
Alfalfa	155	sandy loam		26.7	Benz et al. (1985)
Maize and Sugarbeet	155	do		63.0	Benz et al. (1985)

2.4 Water Uptake by Roots

Plants rely upon their roots for water extracting ability to cope with the evaporative demand impressed by the prevailing moisture (Narda and Curry, 1981). Several mathematical models have been developed in the past to describe water uptake by plant root systems (Lambert et al., 1976). In general, two distinctly different approaches, (i) the microscopic or single-root approach and (ii) the macroscopic or extraction-term approach, have been followed.

* 1969-70

† 1970-71

In the microscopic approach, root distribution is considered to be uniform. Single-root models also suggest that dimensions and density of roots are important. The microscopic approach (Hillel et al., 1975) is based on the solution of the non-linear diffusion equation:

$$\frac{\partial \theta}{\partial t} = \frac{1}{r} \frac{\partial}{\partial r} \left[r D(\theta) \frac{\partial \theta}{\partial r} \right] \quad (2.16)$$

where

r = radial distance from the axis of the root,

θ = volumetric soil water content of soil,

t = time, and

D = hydraulic diffusivity.

The solution of the Equation (2.16) is attempted by analytical means (Philip, 1957a; Gardner, 1960; Cowan, 1965) or numerical means (Molz et al., 1968; Lambert and Penning de Vries, 1973). Many of the later studies (Lang and Gardner, 1970; Whisler et al., 1970) were motivated by the theoretical analysis performed by Gardner (1960) and Cowan (1965). A more sophisticated approach to the description of flow within a single plant was done by Molz and Hornberger (1974) and Molz and Ikenberry (1974) as cited by Feddes et al. (1974). The problem of microscopic studies is that of determining the correct boundary condition. Moreover, it is difficult to test single-root models experimentally since it is not yet possible to measure water potential at the soil-root interface (Narda and Curry, 1981). Thus, because of these difficulties with the microscopic approach, there has been a tendency to describe water uptake by the macroscopic approach.

In the macroscopic or the extraction term approach, water uptake by roots is represented by a volumetric sink term added to the continuity equation (discussed in detail in section 3.1.5). Macroscopic models have been employed by number of investigators (Ogata et al., 1960; Gardner, 1964; Rijtema, 1965; Rose and Stern, 1967; Van Bavel et al., 1968; Whisler et al., 1968; Molz, 1971; Molz and Remson, 1970, 1971; Feddes, 1971; Feddes and Rijtema, 1972; Reicosky et al., 1972; Nimah and Hanks, 1973; Stone et al., 1973; Feddes et al., 1974; Hillel et al., 1975; Feddes et al., 1976; Hillel and Talpaz, 1976; Willatt and Taylor, 1978).

Narda and Curry (1981) developed a model called SOYROOT which is a combination of a root growth sub-model and the macroscopic model. They defined their model as:

$$U_i = L_i \cdot u_i \cdot f(\theta) \cdot f(r) \quad (2.17)$$

$$\sum_{i=1}^n U_i = T \quad (2.18)$$

where

U_i = total water uptake by the plants from the i th soil cell,

L_i = total length of roots in the i th soil cell,

u_i = water uptake rate per unit length of root,

$f(\theta)$ = soil moisture dependent function to account for the diminished rate of uptake by the roots due to decreased moisture content in the soil cell,

$f(r)$ = net root effectiveness function to account for the death of the roots in the soil cell and loss in absorptive power of the roots due to aging,

T = transpiration by plants, and

n = number of soil cells from which transpired water is being extracted.

According to them, the model is applicable to homogeneous soil from which surface evaporation is prevented.

Following Taylor and Klepper (1978), water uptake (U_i) from a soil volume (V_i) can be determined from:

$$U_i = (V_i)(L_{vi})(q_i)(\psi_{si} - \psi_p + \psi_{zi} + \sum \psi_{fi}) \quad (2.19)$$

where

L = root length in layer,

q = average root water uptake rate in V ,

ψ_{si} = difference of water potential between soil and plant xylem at the soil surface,

ψ_p = xylem potential at the soil surface,

ψ_{zi} = water potential loss due to evaporation, and

ψ_{fi} = decrease in potential due to frictional forces within the root.

During a growing season, water uptake is initially confined to the surface layers of the soil, but as the root system penetrates deeper into the soil and the upper layers become dry, so the zone of maximum root activity moves downward and water uptake from the upper layers becomes less important (Gregory, 1988). Typical values for the inflow of water into root systems are presented in Table 2.6.

Table 2.6 — Inflow of water into roots, cm^3 (water) cm^{-1} (root) d^{-1} (Gregory, 1988).

Crop	Inflow	Range	Source
Soybean	3.0×10^{-2}	$0.5 - 5 \times 10^{-6}$	Allmaras et al., 1975.
Onion	2.2×10^{-2}		Dunham and Nye, 1973.
Winter wheat	2.0×10^{-3}	$0.7 \times 10^{-3} - 2.5 \times 10^{-3}$	Gregory et al., 1978.
Ryegrass	7.0×10^{-4}		Lawlor, 1972.
Cotton			Taylor and Klepper, 1971.
		early season 0.1-3.1 late season 0.03-0.86	

Chapter III

THEORY

3.1 Theory of Unsaturated Flow

Changes in moisture content throughout the soil profile depend on the flow of water in the unsaturated zone above the water table. Under natural conditions, the soil surface or the plough layer dries out during dry weather and plant growth. A potential gradient will then develop and water will move in the upward direction. This so called capillary rise or groundwater contribution is very important for the supply of water to the crops especially in soils with low water holding capacity.

The capillary upward flux from the water table depends on the location of the plane of zero flux. Upward flux from the water table occurs only when the hydraulic gradient is negative, i.e. $dH/dz < 0$ at the water table.

3.1.1 Soil Water Potential

The water potential function ψ that describes the energy status of water consists of several components as follows:

$$\psi = \psi_m + \psi_g + \psi_o + \psi_p \quad (3.1)$$

where

ψ_m = matric potential, arising from local interacting forces between soil and water,

ψ_g = gravitational potential, arising from the gravitational forces,

ψ_o = osmotic potential, arising from osmotic forces, and

ψ_p = pneumatic potential, arising from changes in external gas pressure.

The potentials are defined relative to the reference state of water at atmospheric pressure at zero datum elevation. The potential is often expressed as

energy per unit weight of soil water. Then potential has the dimension of length. As the pneumatic potential in natural soil does not differ from the atmospheric pressure, $\psi_p = 0$. As the influence of osmotic potential is small, ψ_o is negligible.

Since ψ_o and ψ_p are negligible, the water potential ψ deals only with matric and gravitational potentials. It is usual, in that case, to refer to ψ as the hydraulic potential H and to $-\psi_m$ as the soil moisture suction $-\psi$.

Assuming the z -axis downward directed and the origin at the ground surface, $\psi_g = -z$, so Equation (3.1) becomes:

$$H = -\psi - z \quad (3.2)$$

where

$-\psi$ = soil moisture suction head,

z = vertical co-ordinate downward directed, and

H = hydraulic head.

3.1.2 Soil Moisture Characteristic

The soil moisture characteristic is the relationship between the soil moisture content θ and the soil water potential ψ or suction $-\psi$.

As the soil moisture characteristic is related to the pore size distribution, structure and texture, such a relationship is different for each soil. The relationship between suction and water content is not unique but hysteretic. It depends on the wetting and drying cycle of the soil. When the soil wets from air-dryness or dries from saturation, the characteristics are called primary wetting or drying curves. The wetting curve always has a lower water content for a given suction than does the drying curve. The characteristics that result from drying a partially wet soil or wetting a partially dry soil are called scanning curves. They lie between the primary wetting and drying loops. An explicit analytical treatment of hysteresis has been worked out (Poulovassilis, 1962; Mualem and Miller, 1979), and hysteresis is sometimes included in water flow models (Gillham et al., 1979). If there is only desorption, single-valued functions like $K(\psi)$ and $\theta(\psi)$ can be used.

$\theta(\psi)$ relations are usually obtained by desorption starting initially with saturated soil and removing water until a desired suction is reached. It is possible to apply suctions by porous ceramic plates up to 20 bars (Marshall and Holmes, 1988). For further higher suctions, one has to use the vapour equilibrium method.

The relationship between humidity and water potential is useful in describing the vapour phase in soils. It provides a means for measuring the higher suctions at low moisture contents. Soil exposed to an atmosphere that is in vapour equilibrium with an aqueous solution at the same temperature will absorb or lose water vapour until its liquid is also in equilibrium with the vapour, e , of the solution (Marshall and Holmes, 1988). Soil water potential can then be calculated from e/e_o by means of Equation (3.3).

$$\psi_m = \frac{RT}{M_w g} \ln \frac{e}{e_o} \quad (3.3)$$

where

ψ_m = water potential of soil,

R = universal gas constant,

T = thermodynamic temperature,

M_w = molar volume of water,

g = acceleration of free fall,

e = vapour pressure of soil air, and

e_o = vapour pressure of saturated air at the same temperature as the soil.

Because the vapour pressure of water increases greatly with temperature, adequate control of temperature is required and this becomes a limiting aspect of the method as e/e_o approaches unity. It is unsuited to the range of e/e_o from 0.98 to 1.0 (Marshall and Holmes, 1988). But special thermocouple psychrometers can be used to measure in this range.

The values of suction ($-\psi$) range from 0.0 (when all pores are filled with water) to 10^7 cm (oven-dry). To present this range easily in a graph, Schofield (1935) introduced the quantity p^F , defined as

$$p^F = \log_{10} \psi \quad (3.4)$$

with ψ the soil moisture potential (negative) expressed in (positive) cm of water column.

At low suctions capillary forces are dominant, while at high suctions, adsorption is most important. Therefore in the low suction range ($0 \leq p^F \leq 2.7$), where the structure is of influence on the water retention properties, undisturbed soil samples are ususally used. In the higher suction range, disturbed samples may be used. But if undisturbed samples are easy to collect, they can be used for both ranges.

The soil moisture characteristic $\theta(\psi)$ can be described using ψ as a function of θ . In this case the curve can be divided into three line segments e.g. higher moisture content or low suction, medium moisture content or medium suction, and low moisture content or higher suction (Feddes et al., 1978). So ψ as a function of θ can be represented by three segments as:

$$\psi = e^{a_1(b_1 - \theta)} \quad \text{for} \quad \theta_1 \leq \theta \leq \theta_s \quad (3.5)$$

$$\psi = e^{a_2(b_2 - \theta)} \quad \text{for} \quad \theta_2 \leq \theta \leq \theta_1 \quad (3.6)$$

$$\psi = e^{a_3(b_3 - \theta)} \quad \text{for} \quad \theta_3 \leq \theta \leq \theta_2 \quad (3.7)$$

where θ_s = saturation moisture content.

3.1.3 Hydraulic Conductivity

The hydraulic conductivity depends on pore size distribution, porosity, structure, and moisture content of soil. Therefore, as soils differ in their physical properties, so hydraulic conductivity K will be different for each soil.

For saturated (groundwater) flow, the total soil pore space is available for water flow. With unsaturated flow, part of the pore space is filled with air so that K must be smaller than for saturated flow because of decreased cross-sectional area

for flow and smaller pores. So for unsaturated flow K is not a constant but depends on the soil moisture content because $\theta = f(\psi)$. So the hydraulic conductivity K can be described as:

$$K = K(\theta) \quad \text{or} \quad K = K(\psi) \quad (3.8)$$

The soil moisture flow in the soil system is described by Darcy's equation as:

$$q = -K \nabla H \quad (3.9)$$

where

q = volumetric flux,

K = hydraulic conductivity, and

H = hydraulic head.

In order to get a complete mathematical description for unsaturated flow, the continuity equation, which expresses the law of conservation of matter, is applied:

$$\frac{\partial \theta}{\partial t} = -\nabla \cdot q \quad (3.10)$$

where

θ = volumetric moisture content, and

t = time.

Combining Equation (3.9) and Equation (3.10) yields the general equation of motion which describes the flow of water in the liquid phase in unsaturated soil:

$$\frac{\partial \theta}{\partial t} = \nabla \cdot (K \nabla H) \quad (3.11)$$

If flow is considered to take place only in the horizontal direction, the appropriate governing equation from Equation (3.11) is

$$\frac{\partial}{\partial x} \left(K \frac{\partial \psi}{\partial x} \right) = \frac{\partial \theta}{\partial t} \quad (3.12)$$

By the chain rule of differentiation

$$\frac{\partial \psi}{\partial x} = \frac{d\psi}{d\theta} \frac{\partial \theta}{\partial x} \quad (3.13)$$

So equation (3.12) can be written as

$$\frac{\partial}{\partial x} \left[D(\theta) \frac{\partial \theta}{\partial x} \right] = \frac{\partial \theta}{\partial t} \quad (3.14)$$

which is the diffusion equation (Marshall and Holmes, 1988). D is the soil water diffusivity defined by the relation

$$D(\theta) = K(\theta) / (d\theta/d\psi) \quad (3.15)$$

The conductivity from the Equation (3.15) can be written as follows:

$$K(\theta) = D(\theta) \frac{d\theta}{d\psi} \quad (3.16)$$

where

D = soil water diffusivity,

K = unsaturated hydraulic conductivity, and

$d\theta/d\psi$ = slope of the soil moisture characteristic curve.

3.1.3.1 Hydraulic Conductivity from Diffusivity

By solving the diffusion equation (3.14), for the following boundary conditions,

$$\theta = \theta_i \quad 0 \leq x \leq L \quad t = 0$$

$$\theta = \theta_f \quad x = 0 \quad t > 0 \quad (3.17)$$

$$\partial\theta/\partial x = 0 \quad x = L \quad t > 0$$

Gardner (1962) derived an expression for soil water diffusivity $D(\theta)$ as:

$$D(\theta) = \frac{4L^2}{\pi^2(\theta - \theta_f)} \frac{d\theta}{dt} \quad (3.18)$$

assuming that for a small change in θ , $D(\theta)$ is approximately constant. In Equation (3.18),

$D(\theta)$ = hydraulic diffusivity,

L = the length of the sample,

θ = volumetric water content,

$d\theta/dt$ = instantaneous outflow rate, and

θ_f = final equilibrium volumetric water content.

(a) *One-step Outflow Method* - In this method soil is exposed to a step change in pressure, usually from zero to 1000 cm water. Considerable time is saved in the analysis of each soil sample because the size of the pressure step is limited only by the bubbling pressure of the plate.

(b) *Evaporation Method* - The outflow method is limited by the bubbling pressure of the plate. To extend the method to higher moisture suctions, an evaporation method can be used. It follows the same principle of diffusivity. Soil is dried in a closed chamber in which air of constant humidity circulates (Rose, 1968b).

All diffusivities can be converted to conductivities using Equation (3.16).

3.1.3.2 Hydraulic Conductivity from Unsteady Drainage Flux

Measurement of hydraulic conductivity during the unsteady drainage flux condition *in situ* is based on the Darcian analysis of transient soil water content and hydraulic head profiles during vertical drainage within the profile as functions of depth and time. Isothermal conditions are assumed to exist in the soil profile during the course of drainage, so neglecting the effect of any temperature changes that might occur.

The equation (Green et al., 1986) describing one-dimensional, isothermal, non-hysteretic, unsaturated flow of water during drainage is:

$$\frac{\partial \theta(z, t)}{\partial t} = \frac{\partial}{\partial z} \left[K(\theta) \frac{\partial H(z, t)}{\partial z} \right] \quad (3.19)$$

where

$\theta(z, t)$ = transient volumetric water content,

$H(z, t)$ = hydraulic head,

$K(\theta)$ = hydraulic conductivity,

z = vertical distance co-ordinate, and

t = time.

When z is positive downward with respect to ground surface reference then

$$H(z, t) = -\psi(z, t) - z \quad (3.20)$$

where $-\psi(z, t)$ = transient soil water suction head.

The initial condition for Equation (3.19) is the soil moisture profile at the moment infiltration of water at the soil surface ceases. With the surface covered thereafter to prevent evaporation, the upper boundary condition for drainage is zero-flux at $z = 0$. With this condition, Equation (3.19) is integrated with respect to z , between the limits of $z = 0$ and any desired depth (z) to obtain for a given time:

$$\int_0^{z_1} \frac{\partial \theta(z, t)}{\partial t} dz = K(\theta) \frac{\partial H(z, t)}{\partial z} \Big|_{z_1} \quad (3.21)$$

or

$$\frac{\partial}{\partial t} \int_0^{z_1} \theta(z, t) dz = K(\theta) \frac{\partial H(z, t)}{\partial z} \Big|_{z_1} \quad (3.22)$$

$$\frac{\partial}{\partial t} \int_0^{z_1} \theta(z, t) dz = K(\theta) \frac{\partial H(z, t)}{\partial z} \Big|_{z_1} \quad (3.22)$$

Equation (3.21) or (3.22) can be used to determine $K(\theta)$ or $K(\psi)$ at desired values of z from θ and H profiles measured at frequent time intervals. The left-hand side, the drainage flux, is equal to the product of hydraulic conductivity $K(\theta)$ or $K(\psi)$ and hydraulic gradient.

3.1.3.3 Hydraulic Conductivity from Water Depletion

Hydraulic conductivity in the field can also be determined from flux and hydraulic gradient data when there is loss of water from evaporation and plant use.

Then, Equation (3.9) in conjunction with Equation (3.2) can be expressed as in Equation (3.23) and used to measure hydraulic conductivity.

The flux in Equation (3.23) is not the same for all depths (Wind, 1955; Feddes, 1968) but the sum of capillary rise from the groundwater level and the amount of moisture extracted from below the depth concerned.

$$q = C + M = K(\psi) \frac{d\psi}{dz} - 1 \quad (3.23)$$

where

q = upward flux,

C = capillary rise,

M = soil moisture extraction, and

K = hydraulic conductivity.

For short dry periods, with continuous flow upwards, one may use arithmetic average values of ψ and q to calculate conductivity or in any other calculations.

3.1.3.4 $K(\psi)$ Empirical Equation

From the hydraulic conductivity measurements, data-pairs θ, ψ and K , θ are available. An empirical equation can be fitted to the data to represent the hydraulic

A general function which seems to fit the available data very well is Gardner's (1958) type of equation :

$$K(\psi) = a(\psi^n + b)^{-1} \quad (3.24)$$

where a, b and n are constants. In general, the coarser the texture of the soil, the larger the values of n . For most soils investigated n values vary between 1 for heavy soils and 4 for very sandy soils (Gardner and Fireman, 1958).

3.1.4 Capillary Rise

The steady-state upward water flow from groundwater to an evaporation zone at the soil surface was first studied by Moore (1939). When dealing with unsaturated flow, it is usual to consider flow in the vertical z direction only. From Equations (3.2) and (3.11)

$$\begin{aligned} \frac{\partial \theta}{\partial t} &= \frac{\partial}{\partial z} \left[K \frac{\partial}{\partial z} (\psi - z) \right] \\ \frac{\partial \theta}{\partial t} &= \frac{\partial}{\partial z} \left(K \frac{\partial \psi}{\partial z} \right) - \frac{\partial K}{\partial z} \end{aligned} \quad (3.25)$$

When steady-state flow is in one direction only, it is convenient to work with Equation (3.25) in terms of potential head (ψ).

In order to solve Equation (3.25) for any given boundary conditions, the relation between K , ψ and θ must be known. Numerical methods of solutions are then often required.

For steady-state conditions, $\partial \theta / \partial t = 0$, and Equation (3.25) becomes, on integrating once,

$$q = K \left(\frac{d\psi}{dz} - 1 \right) \quad (3.26)$$

where q = constant of integration and represents the flux. Equation (3.26) is a restatement of Equation (3.9) using Equation (3.2).

From Equation (3.26), using expression (3.24), the capillary upward flux can be represented by

$$q = a(\psi^n + b)^{-1} \left(\frac{d\psi}{dz} - 1 \right) \quad (3.27)$$

where q is the capillary upward flux.

Equation (3.27) can be used to find fluxes if suction (ψ) distributions with respect to depths and times are known.

3.1.4.1 Plane of Zero Flux

When in a soil profile a positive and negative hydraulic gradient simultaneously occur, a zone or plane where hydraulic gradient, $dH/dz = 0$, will be present between the region of upward and downward flow (Arya et al, 1975; Hartmann, 1984; Hassan, 1986). In that plane, the flux q equals zero. That plane is often called the zero-flux plane.

In the presence of a water table, the plane of zero flux could be above or at the water table or not be present at all. If the zero-flux plane is above the water table, there will be no upward capillary rise from the water table. Rather there will be downward flux or drainage to the water table because $dH/dz > 0$ i.e. positive, from the soil profile below the zero-flux plane. Upward flux will be only above the zero-flux plane because of $dH/dz < 0$. In the presence of crops and no irrigation, the plane of zero flux will shift downward. After an elapse of time, the zero-flux plane will reach the water table where the hydraulic gradient $dH/dz < 0$. When that occurs, profiles above the water table will have $dH/dz < 0$ and continuous upward flux will occur from the water table thereafter.

3.1.5 Water Uptake by Roots

The water uptake by the roots is represented by a sink term, which simply is added to the continuity Equation (3.10) i.e.,

$$\frac{\partial \theta}{\partial t} = -\frac{\partial q}{\partial z} + S_z \quad (3.28)$$

where

θ = volumetric water content,

t = time,

q = soil water flux,

S = sink term that represents water uptake by plant roots, and

z = vertical co-ordinate downward directed.

Thus the sink term is the volume of water extracted from a unit volume of soil per unit time. Values of $\partial \theta / \partial t$ can be obtained from a graph of water content versus time at different depths. Eye-fitted curves can be drawn through data points for each depth, thus providing a family of curves for various depths.

$\partial q / \partial z$ can be determined graphically from a plot of soil water flux versus depth at different times. Fluxes at different depths can be calculated from flow Equation (3.26) under steady-state conditions assuming that a steady-state existed over a given time interval.

In other words, for a unit time interval and any compartment of unit depth, Equation (3.28) can be simplified as below to calculate the sink term S (numerically).

$$S_{(z,t+1)} = \theta_t - q_{z-1} + q_{z+1} - \theta_{t+1} \quad (3.29)$$

where

t = time, and

z = vertical co-ordinate downward directed.

Chapter IV

MATERIALS AND METHODS

4.1 Materials

4.1.1 Experimental Site

The experiment was conducted in Moor Bank glasshouse, University of Newcastle upon Tyne, to avoid any surface water application by rainfall.

4.1.2 Soil

Surface soil of Rivington Series from the University of Newcastle upon Tyne experimental farm, Cockle Park, was selected for the experiment. Soil was collected by scraping mechanically the surface of a cultivated field to a depth of 15 cm at the end of February, 1988. About six tonnes of soil were needed to fill three lysimeters. Soil from the farm was transported to the glasshouse and steam-sterilised to avoid any disease transferred to other plants in the glasshouse. The soil contained much large gravel and stones, which were removed (as far as possible) while filling the lysimeters manually. Soil analysis results are presented in section 4.2.1 and chapter 6 (section 6.1.2).

4.1.3 Crops

Three crops were used. Runner bean (*Phaseolus coccineus*), a medium rooted (50 - 70 cm) crop was grown from June to October, 1988. Barley (*Hordeum vulgare*), a deep rooted crop (100 - 150 cm) was grown from April to July, 1989. Lettuce (*Lactuca sativa*), a shallow rooted crop (30 - 50 cm) was grown from March to May, 1990.

4.1.4 Lysimeters

Lysimeters were constructed from bulk liquid containers of pvc (polyvinyl chloride) material. Three lysimeters, 106 cm in diameter and 145 cm deep, were sited

in the glasshouse. A 10 cm layer of fine gravel mixed with coarse sand was placed at the bottom of each lysimeter. They were then filled with soil. After filling each 15 cm layer, the soil was compacted manually to uniform bulk density. In addition to the manual compaction, the soil was stabilized by wetting the whole column from the bottom of the lysimeter to the soil surface and then draining to the water table. Wetting the profile from the bottom to the surface also helped to expel all air in the soil, and thus to alleviate any hysteresis effects due to air entrapment. Desired levels of water table were checked through a sight tube, 5 mm diameter, from the bottom gravel layer of lysimeter, Fig. 4.1.

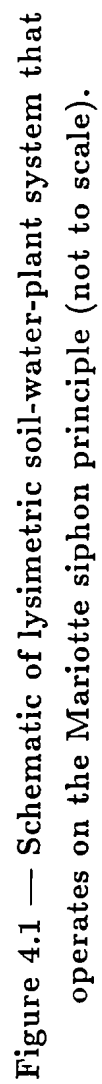
4.1.5 Mariotte Siphon

Water tables were controlled at three levels i.e. 60, 90 and 120 cm below the soil surface in the lysimeters by Mariotte siphons. The siphons supplied water through the bottom of the soil column as shown in Fig. 4.1. They were connected to each lysimeter at a point 135 cm below the soil surface. The siphon reservoirs measured the water that moved into the lysimeters to replace that used by the plants in the lysimeters. Water losses were recorded to the nearest 50 cm^3 . The records were taken daily.

4.1.6 Tensiometers

Each lysimeter had tensiometers inserted at different depths (5, 15, 30 and 45 cm for the water table at 60 cm ; 5, 15, 30, 45, 60 and 75 cm for the water table at 90 cm, and 5, 15, 30, 45, 60, 75, 90 and 105 cm for the water table at 120 cm) for daily measurement of soil moisture suction and hydraulic gradient.

Before installation, the tensiometer cups were checked for any cracks under a pressure of 1000 cm of water (one bar) using de-aired water. After installation, as shown in Fig. 4.1, they were purged of air and stoppered. Measurements of suctions were made daily at 8 a.m. However in order to check for diurnal variation in soil suction, additional readings were made at 12 noon and 4 p.m. on some days.



4.1.7 Resistance Blocks

Each lysimeter had resistance blocks inserted parallel to the soil surface at the same depths as the tensiometers. Resistances were recorded for each lysimeter when tensiometers failed to record suction because of air entry. Moisture content was inferred from the calibration curves of resistance blocks, determined on the same soil in the laboratory.

4.2 Methods

4.2.1 Soil Analysis

After the soil in the lysimeter was compacted and stabilized, triplicate samples were taken from each lysimeter and analyzed for particle size distribution using the pipette method (Avery and Bascomb, 1982). The average sand, silt, and clay content of the soil was 37.2, 59.3, and 3.5%, respectively. Thus, the texture is a sandy silt loam, using the classification of the Soil Survey of England and Wales (SSEW). Soil bulk density was also determined on five undisturbed core samples (Blake and Hartge, 1986) for each lysimeter. The average bulk density obtained from the measurement was $1.56 \pm 0.05 \text{ g cm}^{-3}$.

4.2.2 Soil Moisture Characteristic

The soil moisture characteristic is represented by p^F against volumetric moisture content in the range saturation (zero suction) to wilting point (15000 cm) following the desorption process (Reicosky et al., 1972) and higher than 15000 cm of water by the vacuum desiccator method (Marshall and Holmes, 1988).

Soil moisture characteristics were determined in the laboratory by measuring suction and water content. Different methods used in developing the curve are outlined below.

Volumetric water content was then inferred from the curve for any suction measured in the lysimeters when soil was drying.

4.2.2.1 Haines Method

This method of measurement is used for suctions below 125 cm of water (Jack-

son, 1962). Four undisturbed soil samples in pvc cores, 50 mm long and 30 mm diameter, were used. At zero suction, one sample was used to determine gravimetric moisture content and then converted to volumetric moisture content. After applying each suction, sufficient time was given to equilibrate. Finally, suctions were related to respective volumetric moisture contents. X

4.2.2.2 Pressure Plate Apparatus

This method of measurement was used for the higher suction range, 150 to 15000 cm of water (Richards, 1965). Undisturbed thin (10 mm) core samples in triplicate were used for each measurement. Sufficient time was allowed for incremental pressure application to equilibrate with the potential of the water in the soil samples. The soil moisture content was determined after equilibrium by a gravimetric method for the respective applied suction and converted to volumetric moisture content.

4.2.2.3 Resistance Block

Resistance blocks were calibrated in the laboratory in disturbed core (7.5 × 5.0 cm) samples. Cores with the blocks were left in a constant temperature room (18°C) to evaporate. Daily evaporation loss along with the resistance of the block were recorded. After obtaining the constant sample weight together with the constant resistance, the moisture content was determined for each resistance measurement. Resistance as a function of volumetric moisture content was plotted on a five-cycle semilogarithmic graph paper to produce calibration curves.

Resistance readings in the lysimeter were recorded along with temperature. The calibration curves were at 18°C. Temperatures in the glasshouse differed from those in the laboratory, and so the resistance measurements in lysimeters were adjusted for temperature variation in determining the moisture content from the calibration curve.

4.2.2.4 Vacuum Desiccator Method

Disturbed soil samples (10 mm) were saturated on a 15-bar ceramic plate. After overnight saturation, the samples in triplicate were placed in the pressure

chamber. The samples were under desorption at 10.0 bar. After 5-6 days when there was no outflow and the soil samples had attained equilibrium moisture content, they were taken out and weighed. After weighing samples with the containers were placed in vacuum desiccator containing solutes of known fixed relative humidity in sequence of the decreasing humidity. Different solutes used were K_2SO_4 , KNO_3 , KCl , NH_4NO_3 , CH_3COOK , and $NaOH$, having relative humidities (e/e_o) of 0.97, 0.92, 0.84, 0.70, 0.23, and 0.07, respectively. The desiccator was evacuated and left for 2-3 days for equilibrium. After that, samples were removed, weighed and returned to the desiccator over the next solute. Finally, soil samples were oven dried and volumetric moisture contents were determined. Soil moisture suctions were determined using Equation (3.3). Then these suctions were related to the measured moisture contents in pF curve (Fig. 6.1 a,b and c - vapour equilibrium).

4.2.3 Unsaturated Hydraulic Conductivity

4.2.3.1 Diffusivity Measurement

(a) *One-step Outflow Method* - Undisturbed soil samples were collected in triplicate in short brass rings 30 mm long and 54 mm diameter. The brass rings normally fit into the Tempe Pressure cell No. 1400 (Soil Moisture Equipment Inc., USA). The pressure cell was loaded with a previously saturated ceramic plate.

A single undisturbed core sample was loaded into the pressure cell along with its brass ring. The soil sample was then saturated slowly, over 3-4 days to expel all entrapped air, through the pressure plate which was allowed to imbibe de-aired water from a reservoir. After innundation, the pressure cell unit was connected to the compressed air line. The required pressures were controlled at 1000 cm of water using a mercury manometer.

A step-change in pressure of 1000 cm of water was applied to the pressure cell containing a saturated soil core in a constant temperature room ($18^\circ C$). Water outflow from the soil was measured in drops by means of a drop counter which was connected to a time-function recording chart. The number of outflow drops over the entire desorption could be read off from the chart. From the known volume of a single drop, the cumulative outflow was calculated as a function of time. The

apparatus described is a simplified version of that used by Acharya and Daudet (1980) and Bababe (1987).

At the end of each run, which lasted for 3-5 days, the gravimetric moisture content of the core sample at one bar suction was determined.

A plot of cumulative outflow versus the outflow time, t , was constructed with a smooth curve (eye - fitted) through the points.

The slope of the curve at a given time of outflow was evaluated graphically to obtain the water flow rate. These graphically determined rates were then plotted against cumulative outflow to yield another smooth curve (eye-fitted).

The values of instantaneous outflow were obtained from the latter curve. These in conjunction with the other measurable terms in diffusivity Equation (3.18) were used to calculate soil water diffusivity of each soil replicate, as a function of volumetric water content, $D(\theta)$. Hydraulic conductivity was then calculated using Equation (3.16).

(b) *Evaporation Method* - Triplicate undisturbed samples in pvc cores (7.5×5.0 cm) were placed in a closed chamber after desorption at a pressure of 1000 cm of water in pressure plate. A tray of silica gel was placed underneath the sample (which stood on a platform with other cores) to absorb moisture and maintain the humidity constant.

Relative humidity and temperature inside the chamber were recorded. They were 45% and 20°C , respectively throughout the experiment.

When the samples were placed in the chamber, initially evaporation losses were measured after every half an hour for a period of six hours. Later on, losses were measured after every 24 hours and continued until a constant weight was obtained. At the end of the drying period, which lasted for 11 days, the volumetric moisture contents of the samples were determined.

A plot of cumulative evaporation versus time t was constructed as the in one-step outflow method. The rest of the graphical analysis was done following the outflow method and diffusivity values at low moisture contents were determined. Subsequently, hydraulic conductivity values were obtained from Equation (3.16).

Thus, a wide range of diffusivity values, obtained combining the one-step out-flow and the evaporation method, enabled the determination of conductivity values (as shown in Figs. 6.2 a, b and c - laboratory method).

4.2.3.2 Drainage Flux Method

Hydraulic conductivity of the soil in the lysimeter was measured *in situ* using the unsteady drainage flux method (Green et al., 1986). The water table was raised to the soil surface in the lysimeter. Then the soil surface was covered to prevent evaporation so that water was draining vertically to the water table. Tensiometer readings were recorded after every 24 hours for all depths. Hydraulic heads (H) from tensiometric data for different positions were plotted against time. A smooth curve was drawn through the points. From the smooth curve of H versus t , H values were plotted for respective tensiometer depths (z) and a smooth curve was drawn. The hydraulic gradient $\partial H/\partial z$ was determined from the smooth curve of H versus z . The suction head ψ was determined from the H versus z curve and $\psi(z)$ values were recorded.

Soil water content profiles were not measured directly. $\psi(z)$ data points were converted to water content values $\theta(z)$ using the soil moisture characteristic $\psi(\theta)$ determined in the laboratory following the desorption and vapour equilibrium methods. $\theta(z)$ values were plotted against time (t), and a smooth curve was drawn for $\theta(z)$ versus t . Using the water content profile for a given time, the integral $\int \theta(z, t) dz$ was estimated by a trapezoidal approximation (Green et al., 1986).

A smooth curve was fitted through the data of $\int \theta(z, t) dz$ versus time and the derivatives $\partial[\int \theta(z, t) dz]/\partial t$ at different times were calculated. The time derivatives are the fluxes at fixed positions and times.

Unsaturated hydraulic conductivity values were then calculated by dividing the fluxes calculated above with the hydraulic gradients at the same positions and time.

4.2.3.3 Soil-water Depletion Method

Hydraulic conductivity of the soil in the lysimeters was calculated from the soil-water depletion measurements in the lysimeters following the procedure of

Wind (1955) and Feddes (1968) using Equation (3.23).

To apply the method, it was needed to know the amount of moisture depleted from the soil and the capillary rise from water table.

Moisture extraction was estimated from tensiometer readings. Suction heads were converted to volumetric moisture content using the soil moisture characteristics.

Depths of moisture depleted in each layer were calculated for periods of five days. The water table contribution for the same period was measured.

The total vertical flow for all depths for that particular period was calculated as a sum of capillary rise from the water table and the amount of moisture extracted from below the depth concerned. The upward flow q with respect to depth per day was calculated by dividing the total vertical flow at that depth by the time period. Average values of q and ψ were calculated for successive layers. Capillary conductivity values were calculated at each depth for the period using Equation (3.23) and shown as a function of suction in Figs. 6.2 a, b and c (Soil-water depletion).

4.2.4 Root Length Measurement

After harvesting each crop, soil samples containing roots were collected down to the water table at each 15 cm interval with the use of a root sampler (3.75 cm *dia* \times 15 cm *long*). Immediately after taking the first core, subsequent cores were taken from the same hole. Collected samples were kept in polythene bags. In this way triplicate soil samples were collected for each water table treatment. After collection, the samples were stored in a cold-room.

The samples were then dispersed in water by manual shaking and stirring. The soil with roots then passed through a 60-mesh sieve leaving the roots on the mesh. Microscopic stain, Congo Red (Gurr), was added to the clean roots to stain and left overnight. This made it easy to separate the roots distinctly.

After separation, root samples were randomly spread on a one cm square grid for counting. The total root length in each sample was estimated by the method

of Newman (1966) as modified by Marsh (1971) and Tennant (1975) and used by Malik et al. (1989). Root length was calculated from Equation (4.1).

$$L_r = C_f \times N \times G \quad (4.1)$$

where L_r is the total root length in the soil sample (cm), N is the number intersection counts, G is grid size, and C_f is the conversion factor which, for a one cm square grid, is 0.7857.

The root length density (R_l) was estimated by dividing the root length by the volume of the soil from which the roots were extracted, and expressed in $cm(root) cm^{-3}(soil)$. The inflow rates to roots could then be estimated by dividing the sink-term by R_l .

4.3 Experimental

4.3.1 Runner Bean Experiment (June to October, 1988)

The soil in the lysimeter was loosened to a depth of 20 cm using a hand shovel. After loosening the soil, lime was applied at the rate of 7.0 t/ha and thoroughly mixed in the soil to raise the pH from 5.7 to 7.0. Then N , P , K were applied at the rate of 150 kg N /ha, 125 kg P_2O_5 /ha, and 125 kg K_2O /ha, as the recommended doses after soil analysis.

24 bean seeds were dibbled to a depth of 5 cm in rows, 30 cm apart on 20 June 1988. Plants were thinned to a spacing of 30 cm between plants 20 days after sowing. There were 12 plants in each lysimeter.

When the plants were too tall to stand without support, cane sticks, 210 cm long, were inserted in the soil near each plant to provide support. When the plants were 180 cm tall, their tops were cut off to enhance branching.

On average, flowering started 35 days after sowing. Runner beans are insect (mostly bees) pollinated. Usually, bees suck pollen from flowers and carry it from flower to flower. Inside the glasshouse, there were few bees, so pollination was less and fewer pods were formed.

The first harvest of pods was on 16 September 1988, and there were subsequent harvests when the pods were mature enough for cooking. Yield was measured as fresh weight of harvested pods.

Finally, on 20 October 1988, when flowering and pod formation had ceased, the plant tops were cut just above the soil surface. The fresh weight of tops were recorded for each lysimeter. Fresh plant materials were dried in an oven at 60°C to find the moisture content.

After harvesting plant tops, triplicate soil samples were collected down to the water table to measure the moisture distribution gravimetrically. Other soil samples were collected with a 3.75 cm diameter and 15.0 cm long soil auger over every 15.0 cm interval down to the water table depth to measure root penetration and density.

During the period of experiment, tensiometer and siphon observations were recorded daily. Missing data of moisture content (in the case of tensiometer failure) was inferred from the plots of harvest time moisture content and moisture content before tensiometer failure (from p^F curve).

4.3.2 Barley Experiment (April to July, 1989)

The soil was loosened to a depth of 20 cm as in the bean experiment. N , P , K were applied at the rate of 75 kg N/ha , 40 kg P_2O_5/ha , and 60 kg K_2O/ha , respectively as the prescribed doses after soil analysis.

Barley seeds were sown in line on 9 April 1989. Row to row distance was 5 cm. Plants were thinned maintaining a spacing of 5 cm between plants 20 days after sowing. There were 350 plants in each lysimeter, a planting density of 400 m^{-2} .

On average, flowering started from 20 May 1989, and was uniform in all lysimeters. Grain filling started from 15 June 1989. Panicles of barley from each lysimeter were harvested after maturity on 29 July 1989.

After collecting panicles, plant tops were cut just above the soil surface. Fresh top weight and dry weight (oven dry at 60°C) were also recorded to measure the

moisture content. Seeds were separated from panicles and weights were recorded as grain yield.

After harvesting, triplicate soil samples were also collected as in the bean experiment to determine the root penetration and density in the soil down to water table.

During the experiment period, tensiometer and siphon readings were recorded daily as in bean experiment. When tensiometers failed, electrical resistance readings were recorded from the moisture blocks.

4.3.3 Lettuce Experiment (March to May, 1990)

Water tables in all the lysimeters were raised to the soil surface on 10th December 1989 and left covered to prevent evaporation. The water in each lysimeter drained to the water table with excess water draining out through the outflow hole (Fig. 4.1). This was done to have an equilibrium soil moisture profile.

The soil was loosened on 28 March 1990, to a depth of 20 cm as in bean and barley experiments. Only *N* was applied, at the rate of 100 kg *N*/ha as the prescribed dose after soil analysis. Lettuce seeds were sown on the same day. Row to row distance was 17.5 cm. Plants were thinned maintaining a spacing of 15 cm between plants 15 days after sowing. There were 42 plants in each lysimeter, a planting density of 45 m^{-2} . A high density of plants were maintained to have a complete soil cover for high evapotranspiration rate.

Lettuces were uprooted when leaves were grown enough to eat, using a hand shovel on 25 May 1990. Fresh top weight and root penetration length were recorded for each plant.

Five randomly selected plants, from each lysimeter, were dried (oven dry at 60°C to find the moisture content. Root length density was measured from the roots of same five plants.

After harvesting, soil samples were also collected as in previous experiments to determine the moisture content of the soil down to water table.

During the experiment period, tensiometer and siphon readings were recorded daily as in bean and barley experiments. When tensiometers failed, electrical resistance readings were recorded from the moisture blocks.

Chapter V

MODELLING

Several authors have reported that capillary rise from a water table is an important resource of water for crop production. There are different models of upward water flow (Gardner, 1958; Skaggs, 1978; Shaykewich and Stroosnijder, 1977) to take into account the capillary upward flux in the absence of crops.

Capillary rise is controlled by soil physical factors and environmental demand and also by crop factors such as the nature of the crop and the extent and proliferation of roots.

Several mathematical models have been developed to describe water uptake by plant roots. Some authors have used a microscopic approach (or the single root-model) where the root is considered as a hollow cylinder, of uniform radius, infinite length and having uniform water absorbing properties (Hillel et al., 1975; Molz and Hornberger, 1974; Molz and Ikenberry, 1974). Others have used a macroscopic approach (or the extraction term approach) where water uptake by the roots is represented by a volumetric sink term added to the continuity equation for flow of water in the soil (Reicosky et al., 1972; Nimah and Hanks, 1973; Stone et al., 1973; Feddes et al., 1974; Hillel et al., 1975; Feddes et al., 1976; Hillel and Talpaz, 1976; Willatt and Taylor, 1978).

The model developed here (CAPROW) accounts for capillary upward flux and root water uptake, simultaneously, in the presence of a water table.

5.1 Capillary Upward Flux

For monodirectional upward movement of water from an initially wet profile towards an evaporation zone at the soil surface, Equation (3.27) is applied (Gardner, 1958; Hillel, 1980).

5.1.1 Computational Procedure

The capillary upward flux at each incremental increase in depth can be calculated from Equation (3.26) as follows:

$$q_i^j = K_i^j(\bar{\psi}_i^j) \frac{\psi_i^j - \psi_{i+1}^j}{z_{i+1}^j - z_i^j} - 1 \quad (5.1)$$

where the “i” subscripts refer to depth and the “j” superscripts refer to time. The value of $K_i^j(\bar{\psi}_i^j)$ is computed at each incremental increase in depth using Equation (3.24) as follows:

$$K_i^j(\bar{\psi}_i^j) = \frac{a}{b + (\bar{\psi}_i^j)^n} \quad (5.2)$$

where $\bar{\psi}$ is the geometric mean of the matric suction of two adjacent layers i.e. the geometric mean of ψ_i^j and ψ_{i+1}^j , ψ_{i+1}^j and ψ_{i+2}^j , and so on. When the soil is drying, large differences in suction near the soil surface may result in a large difference in ψ used in calculating K (Haverkamp and Vauclin, 1979). The geometric mean is preferable to the arithmetic mean for representing log normally distributed data (Campbell, 1985). The log or geometric mean is a number much more representative of the data set. But between the water table and the layer just above water table, $\bar{\psi}$ was calculated as the mean of ψ at the water table ($\psi = 0$) and at 15 cm above water table. Otherwise the geometric mean would be zero and would refer to the saturated hydraulic conductivity, K_s , which, in the real situation, is not true. The computed capillary upward flux in this case would be higher than actually occurred.

5.1.2 Boundary Conditions

The water table is at a specified depth so that the bottom boundary is static. Therefore, $\psi = \psi_0 = 0$ and $\theta = \theta_s$ at the water table where θ_s = saturation water content.

The flow at the bottom boundary could be up or down depending on the location of the plane of zero flux. The plane of zero flux is determined from the

slope of the hydraulic gradient, dH/dz . The depth, where $dH/dz = 0$, is referred to as the zero-flux plane. Flow will be upwards above the zero-flux plane where $dH/dz < 0$. Flow will be downwards, i. e. deep percolation, to water table below the zero-flux plane where $dH/dz > 0$.

The initial condition with no flow is that ψ is equal to the height above the water table or mathematically $t = 0$, $\psi = -z$. As the initial water content is generally high, the soil water flux will not be limited by the soil water conditions but only by climatic conditions. As the soil continues to dry so the soil surface will eventually become air-dry. Then the evaporation from the soil surface will be less than that determined from climatic calculations. Soil evaporation will then be dependent on soil water flow in the top soil layers. Soil drying may also restrict plant root water uptake and subsequent transpiration as the soil water content approaches the wilting point. This condition will generally be found after a much longer time when soil evaporation falls below the potential rate.

5.2 Root Water Uptake

The general flow equation in one dimension with a sink term i.e. root water uptake, is given by Equation (3.28) and can be expressed as follows:

$$S_z = \int_0^z \int_{t_1}^{t_2} \frac{\delta \theta}{\delta t} dz dt + q_{z+1} - q_{z-1} \quad (5.3)$$

where S_z is the sink term at depth z , q is the capillary upward flux in the z direction, t is the time, and θ is the volumetric moisture content. Here the sink term is assumed as a macroscopic sink term, i.e. the volume of water extracted from a unit volume of soil per unit time.

5.2.1 Computational Procedure

The sink term at each incremental increase in depth can be calculated as follows:

$$S_{z_i}^j = \bar{D}_i^j \quad (5.4)$$

$$S_{z_i}^j = \bar{D}_i^j + q_{i+1}^j \quad (5.5)$$

$$S_{z_i}^j = \bar{D}_i^j + q_{i+1}^j - q_{i-1}^j \quad (5.6)$$

where \bar{D} is the average soil moisture depleted per day.

5.2.2 Boundary Conditions

Equation (5.4) applies when $q_{i+1}^j \leq 0.0$ and $i = 1$ which is the top boundary. Again Equation (5.5) is also for the first layer as Equation (5.4) when $q_{i+1}^j > 0.0$ and $i = 1$. In all other conditions Equation (5.6) is applied provided the moisture deficit is in the available range i.e. between field capacity and wilting point (-15,000 cm suction head assumed). If the matric suction (ψ) has exceeded the wilting point then the capillary upward flux in that situation is no longer available to plant roots and considered as zero water extraction (Feddes, 1978).

5.3 Inflow to Roots

Inflow rates to roots are related to the root length density and water extraction rate and calculated as the water uptake per unit root length density. It is expressed as the inflow to root as the ratio of volume of water extracted from the layer to the total length of the root in that layer. So inflow to the roots is expressed as:

$$I_r = \frac{S_z}{R_l} \times A_f \quad (5.7)$$

where

I_r = Inflow to roots,

S_z = Sink term,

R_l = Root length density,

A_f = Factor related to area and depth of layer (Appendix A).

5.4 Description of the Computer Model

The programme CAPROW is written in FORTRAN 77. The programme consists of a main programme as shown in the flow chart (Fig. 5.1). Steps in the programme are as follows:

1. Read data that includes depth of tensiometer bulbs including zero for surface, time (days) of tensiometer reading (IT), matric suction (H) from tensiometer, and root length density (RD).
2. Calculate volumetric moisture content, THETA (θ) from matric suction using Equations (3.5), (3.6) and (3.7), respectively for various boundary conditions.
3. Calculate moisture depleted in depth, AMD, mm for specific time interval (5 days) and then converted to moisture extraction, AMD1, $mm\ d^{-1}$ (AMD1 = D1 in Equations (5.4), (5.5), and (5.6). This is continued until $\theta > \theta_w$, where θ_w = volumetric water content at wilting point.
4. Calculate geometric mean of matric suction (GMH) for adjacent layers from matric suction (H) and then calculate unsaturated hydraulic conductivity AK, $mm\ d^{-1}$ using Equation (5.2). After calculation of hydraulic conductivity, capillary upward flux $Q(mm\ d^{-1})$ was calculated using Equation (5.1).
5. In calculating the sink term, only flux values (Q1) for suctions less than wilting point were considered and separated.
6. Sink term (S) was calculated using Equations (5.4), (5.5), and (5.6) respectively according to the boundary conditions outlined.
7. Root inflow rate (RI) was calculated using Equation (5.7).

The symbols written in describing the model activities steps are used in the main CAPROW program, printed in Appendix B.

5.5 Model Input Parameters

As mentioned in the flow chart, the parameters needed to to run the model

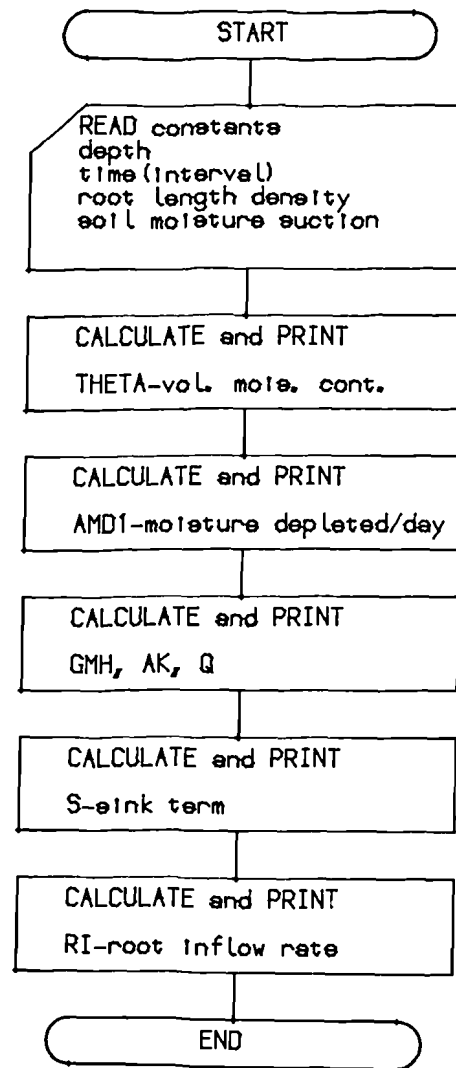


Fig. 5.1. Flow chart of the operations of programme CAPROW.

had to be determined. Although much data are available in the literature on $\theta - \psi$ and hydraulic conductivity (K) or diffusivity (D), it is difficult to apply and not relevant to the experiment. For these reasons, data for the water table at 60 cm from the runner bean experiment were used to determine some soil physical parameters to run the model.

The soil moisture characteristic was determined as outlined in chapter 4 (Section 4.2.2). The data were available over the wide range of water contents from saturation to oven-dry (Fig. 6.1a). The curve was divided into three segments to describe ψ as a function of θ as mentioned in Equations (3.5), (3.6), and (3.7), respectively. The constants were evaluated to give the best-fit line segment to the curve.

Hydraulic conductivity as a function $K(\psi)$ was determined from the bean experiment (water table at 60 cm) using laboratory and soil-water depletion methods as detailed in sections 4.2.3.1 and 4.2.3.3, respectively and then fitted to conductivity prediction Equation (3.24). The constants of the equation were evaluated. A wide range of matric suction data were available from tensiometer and resistance measurements. Resistance readings were converted to soil moisture contents as shown in Figs. 6.11 to 6.13.

Actual measurement of the root distribution at the end of the experiment was done to avoid destructive sampling during experiment.

To apply the model under field conditions, data on the parameters are needed under static water table conditions having similar soil physical properties. Only information on the water table contributions to various crops under different static water tables are available.

The model was used to simulate data available from lysimeters for a shallow water table fixed at 90 cm depth and a deep water table fixed at 120 cm depth.

Simulation was accomplished for specific static water table depths i.e. 90 cm and 120 cm, for shallow, medium, and deep rooted crops (Section 4.1.2).

Chapter VI

RESULTS AND DISCUSSION

6.1 Soil Properties

6.1.1 Bulk density

The bulk density of undisturbed core samples for three lysimeters are presented in Table 6.1.

Table 6.1 — Bulk density of soil in lysimeters (Mean \pm s.d., $n = 5$).

Water table depth below soil surface cm	Bulk density $g\ cm^{-3}$
60 (WT-60)	1.55 ± 0.07
90 (WT-90)	1.56 ± 0.05
120 (WT-120)	1.56 ± 0.05

It appears from Table 6.1 that compaction in each lysimeter was more or less uniform. Assuming that the particle density of the soil is $2.65\ g\ cm^{-3}$, the percent of solid space, from the relation of bulk density and particle density, is 58.70. In other words, the saturation water content should be $0.413\ cm^3(H_2O)\ cm^{-3}$ which shows excellent agreement with the measured value i.e. $0.415\ cm^3(H_2O)\ cm^{-3}$.

6.1.2 Mechanical Composition of Soil

The mechanical analysis of soil was done following the method described in chapter 4 (section 4.2.1). The percentage of the different constituents are as presented in Table 6.2.

Table 6.2 — Mechanical composition of soil (Mean \pm s.d., $n = 3$).

Soil (Sandy Silt loam) constituents	Percent
Sand	37.2 ± 0.6
Silt	59.3 ± 2.2
Clay	3.5 ± 0.3

6.1.3 Soil Moisture Characteristics

The average volumetric moisture content, θ of the experimental soils from the undisturbed samples are presented graphically in Figs. 6.1a, b, c. It is observed that the soil moisture characteristic is the same for each lysimeter. This indicates that soils in each lysimeter were uniform both in terms of soil composition and structure. This can be ascertained from Table 6.2.

The method of measuring the characteristic has been described in section 4.2.2. The saturated water content determined using Haines' funnel apparatus and found to be $0.415 \pm 0.01 \text{ cm}^3 \text{ cm}^{-3}$.

The soil moisture suction was assumed to be a single-valued function of soil moisture content for drying. Soil moisture characteristics have been shown to be non-singular (Davidson et al., 1966) because they are dependent upon the rate at which a given matric potential was established in either a wetting or drying process. But because the experimental concern was with the soils that were drying from an initial wet condition, the boundary drying curve can be used (Marshall and Holmes, 1988).

The soil moisture characteristic can be tabulated i. e. as a table of θ , or can be described as a function of $\theta(\psi)$. In this study, θ has been described as a function of ψ as shown in Fig. 6.1a. The empirical three-straight-line semilog models have fitted well the relationship between water content and soil water suction. de Jong et al. (1983) reported that the empirical two-straight-line models were found to be most suitable to relate soil water content to soil water

suction. Those two-straight-line models did not describe the entire range of θ . But in this study, three-straight-line models have described the entire range of θ (Fig. 6.1a). The number of straight-line models depends upon the nature of the curve. de Jong (1976) also reported that the second-degree polynomial model did not describe the relationship between water content and soil water suction satisfactorily. According to them, a third-degree polynomial described the data better than did the second-degree. But it was also unacceptable because it showed local maximum and minimum values within the observed data range. de Jong et al. (1983) reported that the power- curve model (chapter 2: section 2.1.1) of Gardner et al. (1970) gave acceptable results for fine-textured soils but was less satisfactory for medium- and coarse-textured soils. Straight-line semilog models are versatile in describing the characteristic curve and are used for predicting soil moisture content in the capillary rise and root water uptake model (CAPROW).

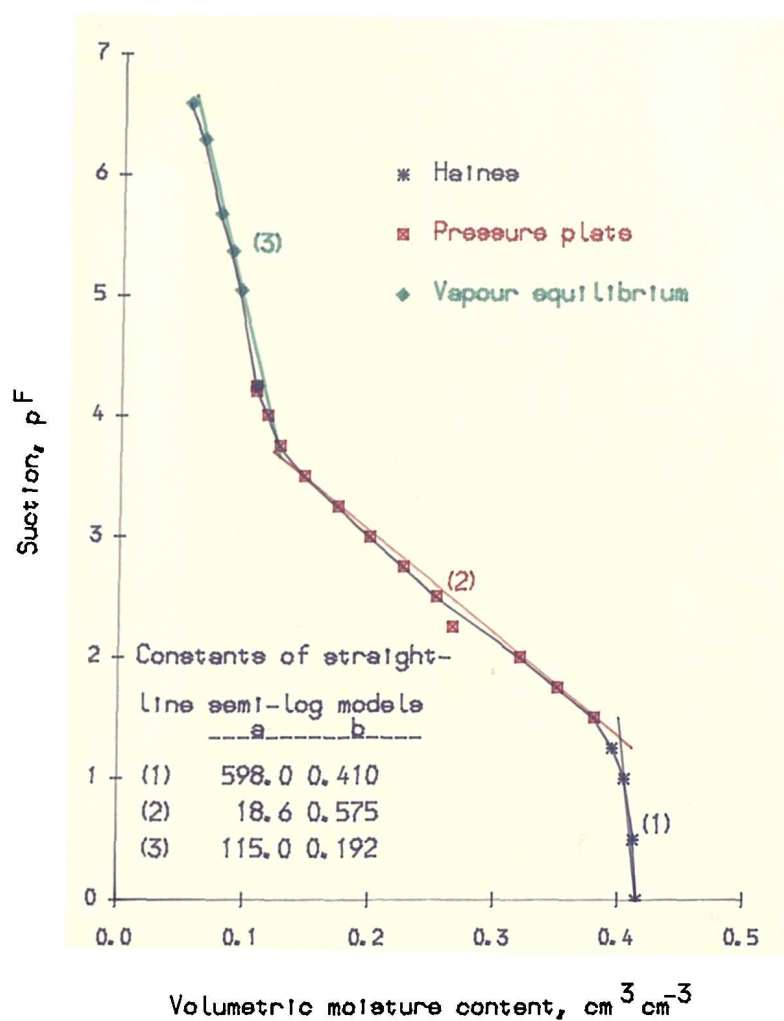


Fig. 6.1. (a) Moisture characteristic curve for lysimeter WT-60.

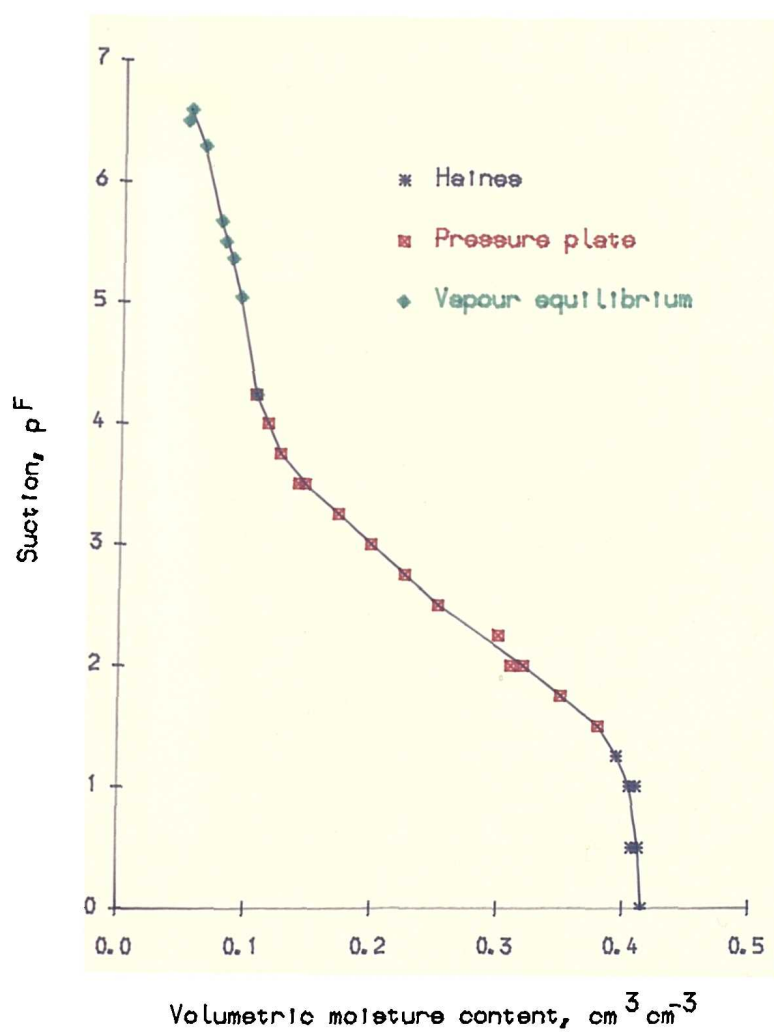


Fig. 6.1. (b) Moisture characteristic curve for lysimeter WT-90.

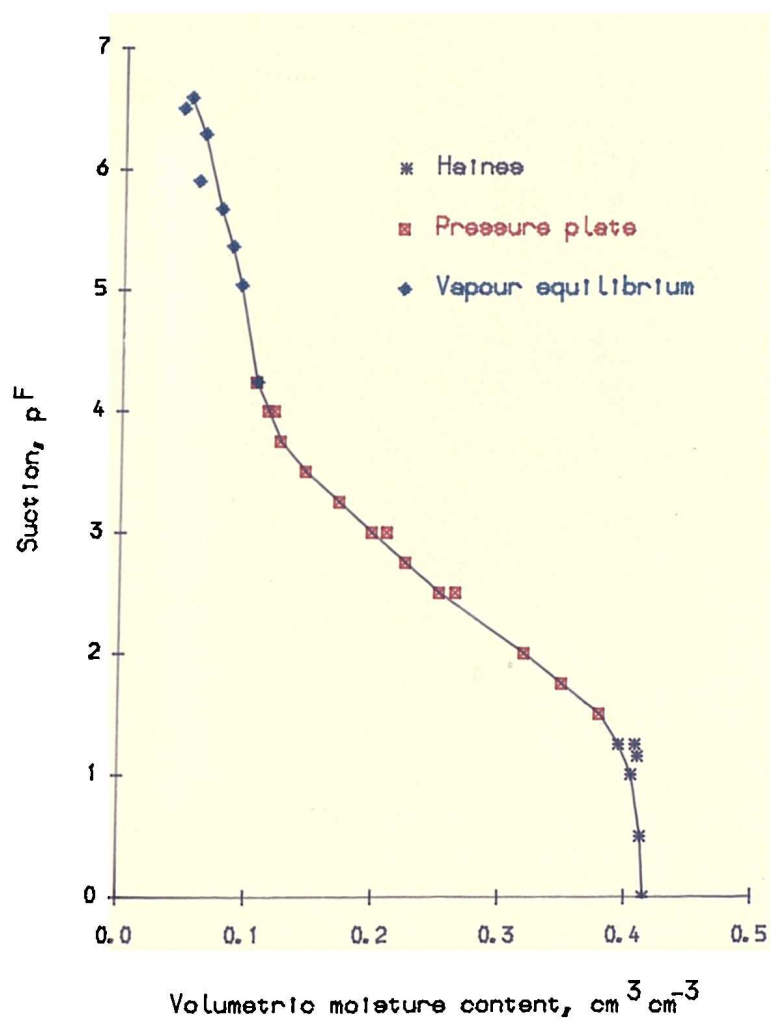


Fig. 6.1. (c) Moisture characteristic curve for lysimeter WT-120.

6.1.4 Hydraulic Conductivity

Hydraulic conductivities were determined, using methods detailed in section 4.2.3, for all the three lysimeters with different water tables.

In Table 6.3, an example of the calculation of the capillary conductivity from lysimeter data is given. The data are from the period 23-28 September 1988, from the water table at 60 cm depth using the method in section 4.2.3.3. In this period, the amount of capillary rise was 0.397 mm. The results of such calculation are shown in Figs. 6.2a, b and c along with the other three methods. Conductivity values obtained from diffusivity and soil-water depletion have shown good agreement compared to the drainage flux method. Conductivity values from drainage flux are slightly higher compared to the other two. Very few data were obtained from the drainage flux as shown in the figures because of a very slow drainage rate. The drainage flux method is not likely to be accurate in the high moisture range, especially for sandy soils (Hillel and Benyamini, 1973). They also reported that there are practical limits to extending the method in the very low moisture range, at which the rate of internal drainage may become so slow as to require a very long time (weeks or even months) for any perceptible change to occur.

The differences in conductivities could be due to covered soil surface and the absence of plant roots. Arya et al. (1975) observed differences between field and laboratory measured conductivities. According to them, the differences could be in part due to shear and compression of the soil cores during extraction. But they did not mention the rooting effect. Feddes (1968) showed good agreement between laboratory and field conductivity (obtained as in method in section 4.2.3.3) values in the presence of cabbage roots and a water table at 90 cm depth.

The relation between K and ψ is presented with the functions as in Equation (3.24), separately in Figs. 6.2a, b and c. The constants of the equations are calculated separately. The values of n were found to be in the range of investigated values, 1 to 4 (Gardner and Fireman, 1958).

It was tried to fit Rijtema's (1965) conductivity function (Fig. 6.2a).

$$K = K_0 \cdot e^{-c\psi} \quad (6.1)$$

Table 6.3 — Calculation of capillary conductivity in lysimeter with water table at 60 cm depth (from Bean experiment).

Depth in cm below surface	ψ_1 cm	ψ_2 cm	M $mm (5d)^{-1}$	$\bar{\psi}$ cm	$\sum \Delta q =$ C + M $mm (5d)^{-1}$	$\sum \Delta \bar{q}$ $mm d^{-1}$	$\sum \Delta \bar{q}$ $mm d^{-1}$	$\frac{\Delta \psi}{\Delta z} - 1$	K $mm d^{-1}$	$\bar{\psi}$ cm
5	2240	2950	0.65	2595	3.147	0.629				
							0.565	126.1	0.00448	1960
15	1200	1450	0.60	1325	2.497	0.50				
							0.440	69.7	0.00632	795
30	234	293	1.50	264	1.897	0.379				
							0.230	15.5	0.015	140
45	16.3	16.3	0.0	16.3	0.397	0.079				
							0.079	0.0893	0.885	8.17
60	0.0	0.0	0.0	0.0	0.397	0.079				

where

K = the hydraulic conductivity at matric suction, ψ ,

K_0 = the texture specific saturated hydraulic conductivity, and

c = a texture specific empirical constant.

Measurements have shown that the Equation (6.1) does not hold over the entire range of ψ values occurring in soils (Rijtema, 1965). The same function, if used for higher values of ψ , gives very low values of conductivities compared to measured values. If ψ exceeds a texture specific suction limit, ψ_{max} , an empirical equation (6.2) has to be used (Rijtema, 1965) to describe the relationship between K and ψ :

$$K = a\psi^{-1.4} \quad \text{if } \psi > \psi_{max} = 50 \text{ cm} \quad (6.2)$$

where

a = texture specific empirical constant, and

ψ_{max} = texture specific suction limit.

After fitting the curve to data, it is observed that Equation (6.2) does not fit (see Fig. 6.2a) as well as Gardner's equation (3.24).

The $K(\psi)$ function (Equation 3.24), with evaluated constants from laboratory and soil-water depletion methods, is used in calculating the conductivity for all depths throughout the experiments.

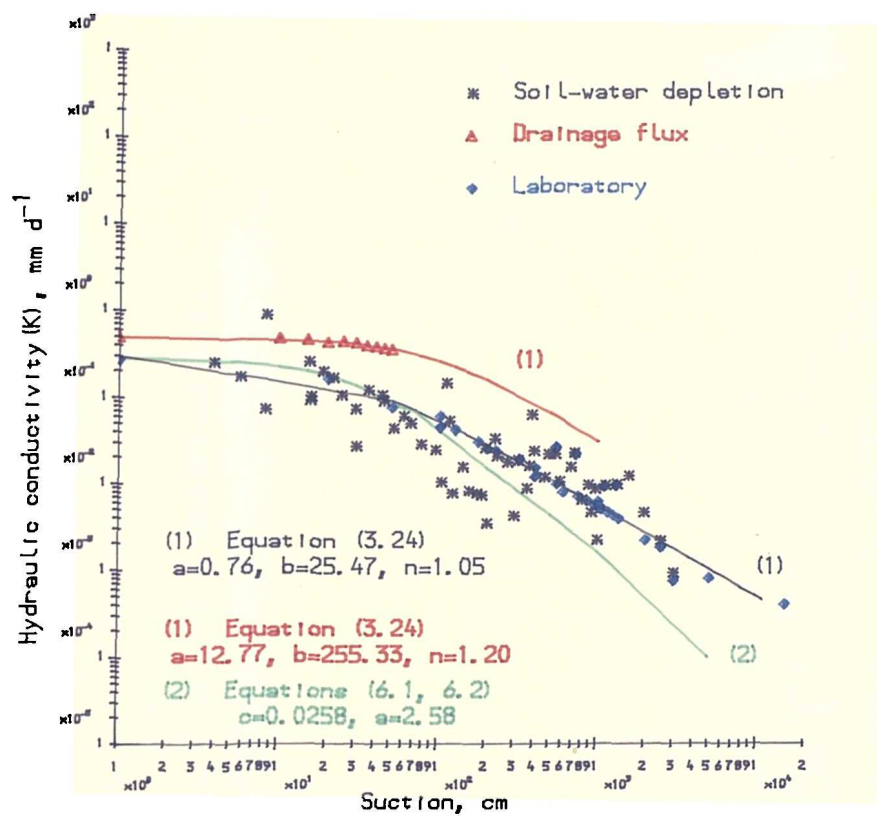


Fig. 6.2. (a) Hydraulic conductivity versus soil moisture suction for WT-60.

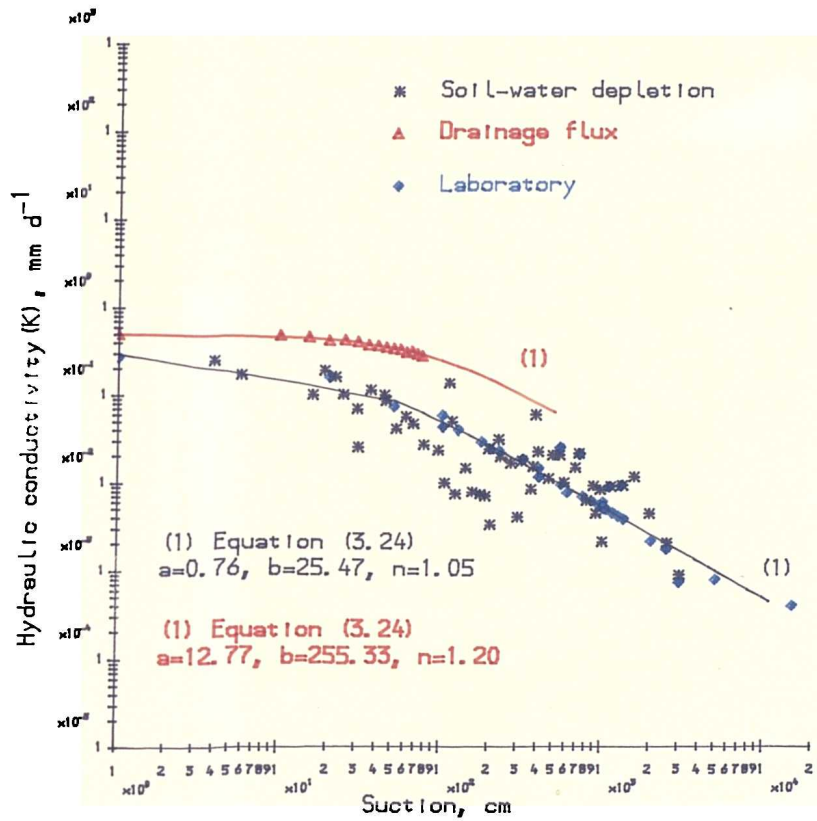


Fig. 6.2. (b) Hydraulic conductivity versus soil moisture suction for WT-90.

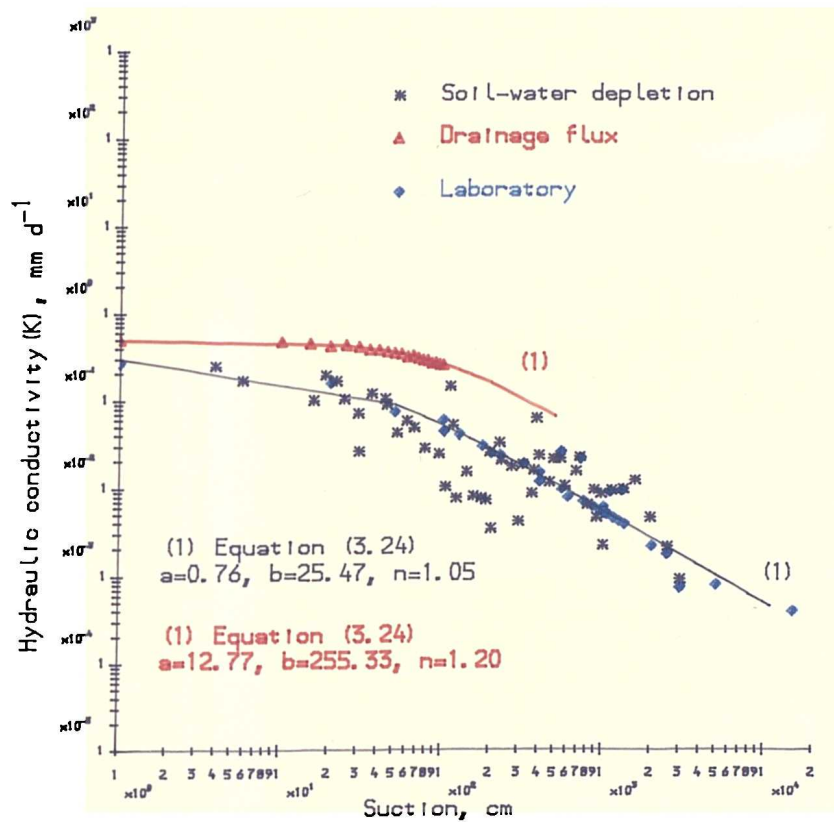


Fig. 6.2. (c) Hydraulic conductivity versus soil moisture suction for WT-120.

6.1.5 Soil Moisture Suction

Soil moisture suction values (cm water) as a function of time are shown in Figs. 6.3a, b and c for water tables 60, 90 and 120 cm deep, respectively, during the bean experiment. It was observed that the suctions were changing very slowly. This could be due to water draining very slowly to the water table. Tensiometers at 5 and 15 cm depth failed to read after 70 and 85 days from sowing with water table at 60 cm depth. A similar trend was also observed in the lysimeter with the water table at 90 cm depth. But tensiometers failed to read after 65, 70 and 95 days from sowing in the lysimeter with the water table at 120 cm depth. This could be due to the higher root water uptake from the upper profiles. Tensiometer readings near the water table fluctuated in all lysimeters except the water table at 60 cm depth, possibly because of profile drainage to the water table.

But tensiometer readings in the barley experiment behaved differently for all water table treatments. All tensiometers in lysimeter with the water table at 60 cm depth failed to give readings after 54 days from sowing. Only one tensiometer, just 15 cm above water table, was working in the other two lysimeters until harvest. The behaviour of tensiometers under barley can be seen in Figs. 6.4a, b and c, respectively, for different water table treatments. There was no fluctuation in readings near the water table, possibly because of equilibrium water profile establishment before starting the experiment.

In the lettuce experiment, tensiometers were working in all the lysimeters up to harvest. Only one tensiometer, at 5 cm depth in lysimeter with the water table at 120 cm depth, failed at 51 days from sowing. The behaviour of tensiometers under lettuce can be seen in Figs. 6.5a, b and c, respectively, for different water table treatments. There was no fluctuation in readings near the water table, possibly because of equilibrium water profile establishment before starting the experiment.

Tensiometers could be read to about 750 cm water suction which can be seen in Figs. 6.3 to 6.4. After that tensiometers failed to read because of air-entry through the tensiometer cup. A summary of tensiometer failure with respect to sowing time and depth for the respective crops is presented in Tables 6.4 (bean), 6.5 (barley) and 6.6 (lettuce).

Table 6.4 — Summary of time at which tensiometers failed (days from sowing) at different depths for different water table treatments under beans.

Crop	Bean, 1988		
Depth below soil surface cm	Depth to water table from soil surface		
	60 cm	90 cm	120 cm
	Days from sowing		
5	70	70	65
15	85	80	70
30	-	-	95
45	-	-	-
60		-	-
75		-	-
90			-
105			-

When the tensiometers failed, resistances of the nylon resistance blocks were recorded. Soil moisture suctions were inferred from the combined resistance calibration (Fig. 6.5) and soil moisture characteristic (Fig. 6.1).

Diurnal variation of tensiometer readings are also shown in Fig. 6.7 for lysimeter with water table 60 cm deep under bean. Very little variation was observed at shallow depths, especially 5 and 15 cm. Similar results were observed in lysimeters with the water tables 90 and 120 cm deep under different crops. Irwin and Randolph (1958) reported that direct temperature effects were not responsible for large diurnal variations in the tensiometers. Richards and Neal (1936) reported a considerable variation in tensiometer readings from cups at a given depth for different locations on a plot.

Table 6.5 — Summary of time at which tensiometers failed (days from sowing) at different depths for different water table treatments under barley.

Crop	Barley, 1989		
Depth below soil surface cm	Depth to water table from soil surface		
	60	90	120
	cm	cm	cm
	Days from sowing		
5	27	24	23
15	39	34	35
30	44	45	39
45	54	54	44
60		66	48
75		-	52
90			71
105			-

Table 6.6 — Summary of time at which tensiometers failed (days from sowing) at different depths for different water table treatments under lettuce.

Crop	Lettuce, 1990		
Depth below soil surface	Depth to water table from soil surface		
cm	60 cm	90 cm	120 cm
	Days from sowing		
5	-	-	51
15	-	-	-
30	-	-	-
45	-	-	-
60		-	-
75		-	-
90			-
105			-

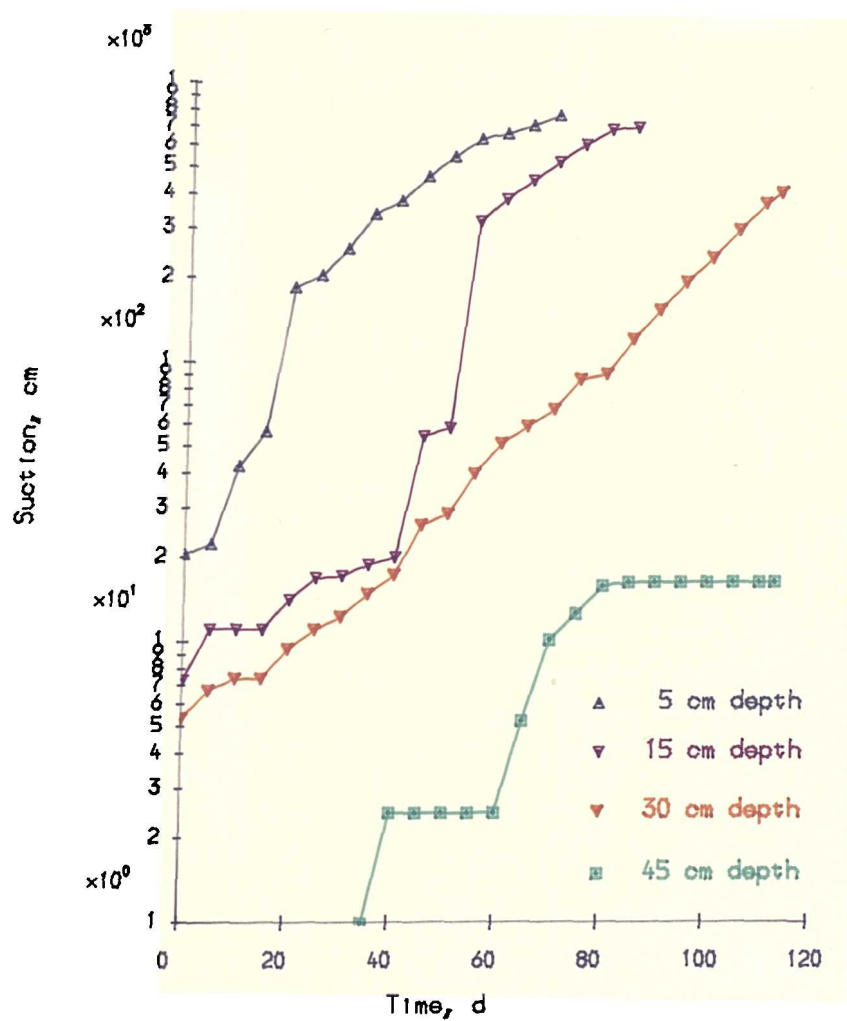


Fig. 6.3. (a) Suction from tensiometers in lysimeter WT-60 (Bean).

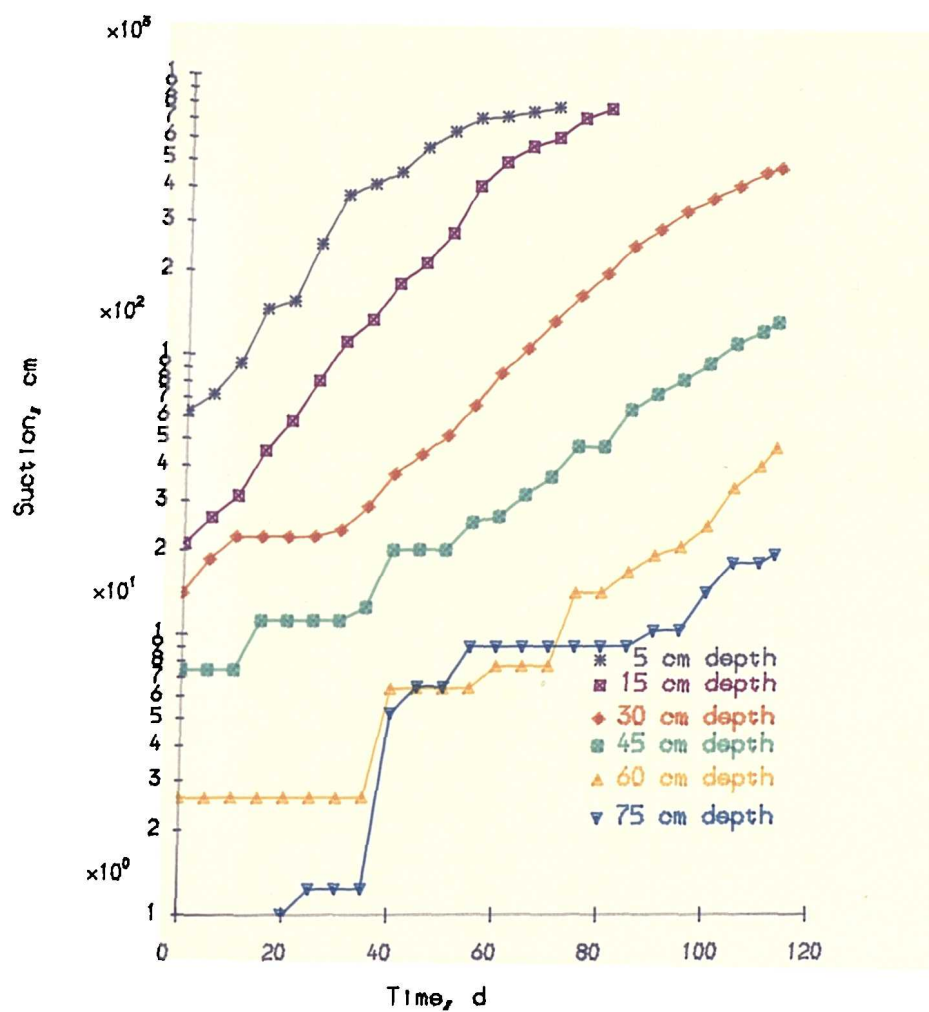


Fig. 6.3. (b) Suction from tensiometers in lysimeter WT-90 (Bean).

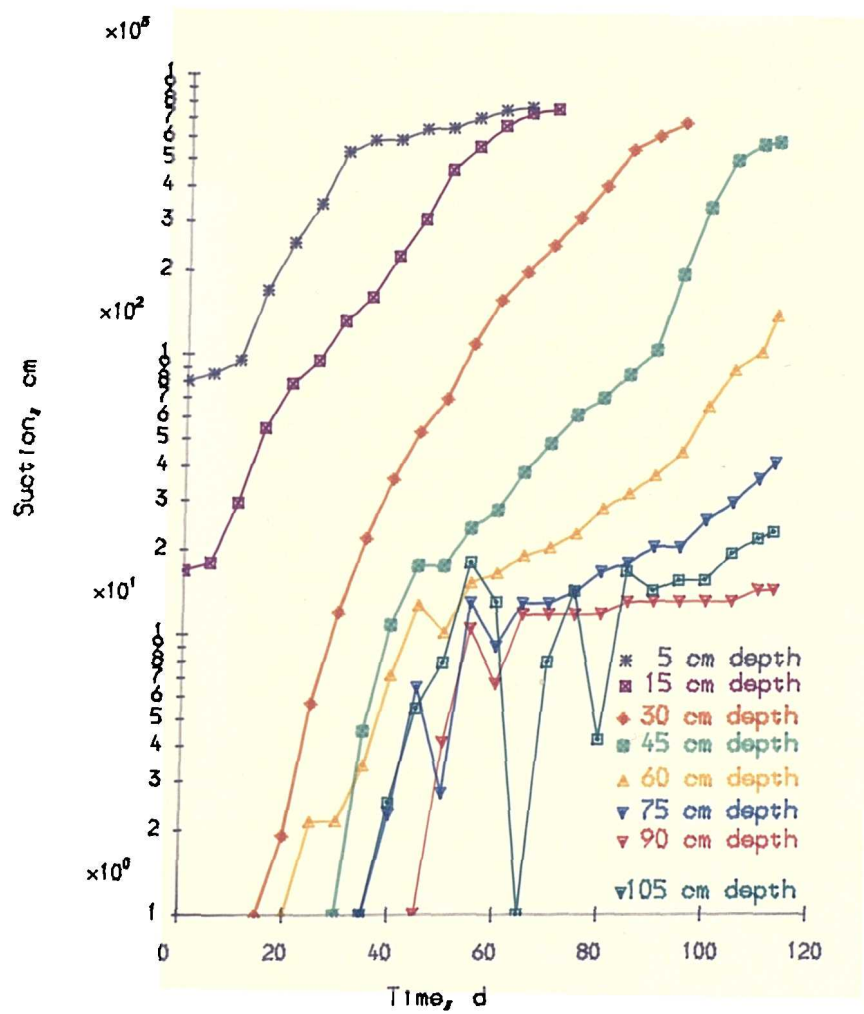


Fig. 6.3. (c) Suction from tensiometers in lysimeter WT-120 (Bean).

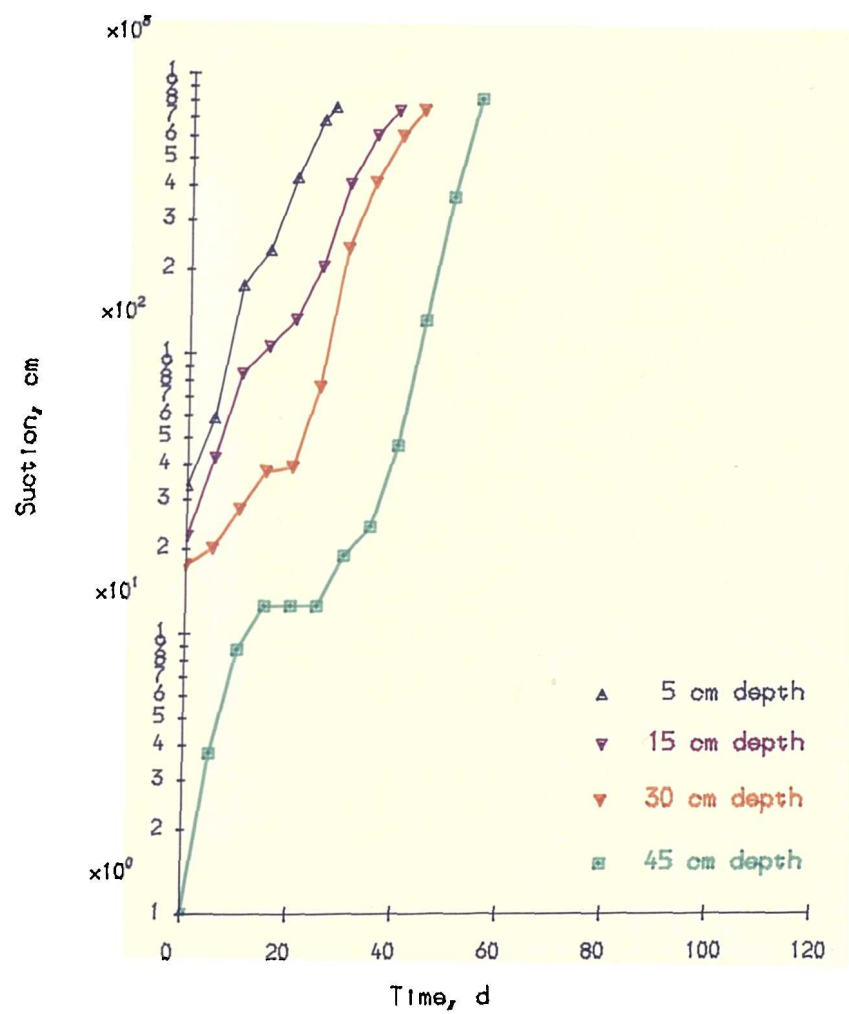


Fig. 6.4. (a) Suction from tensiometers in lysimeter WT-60 (Barley).

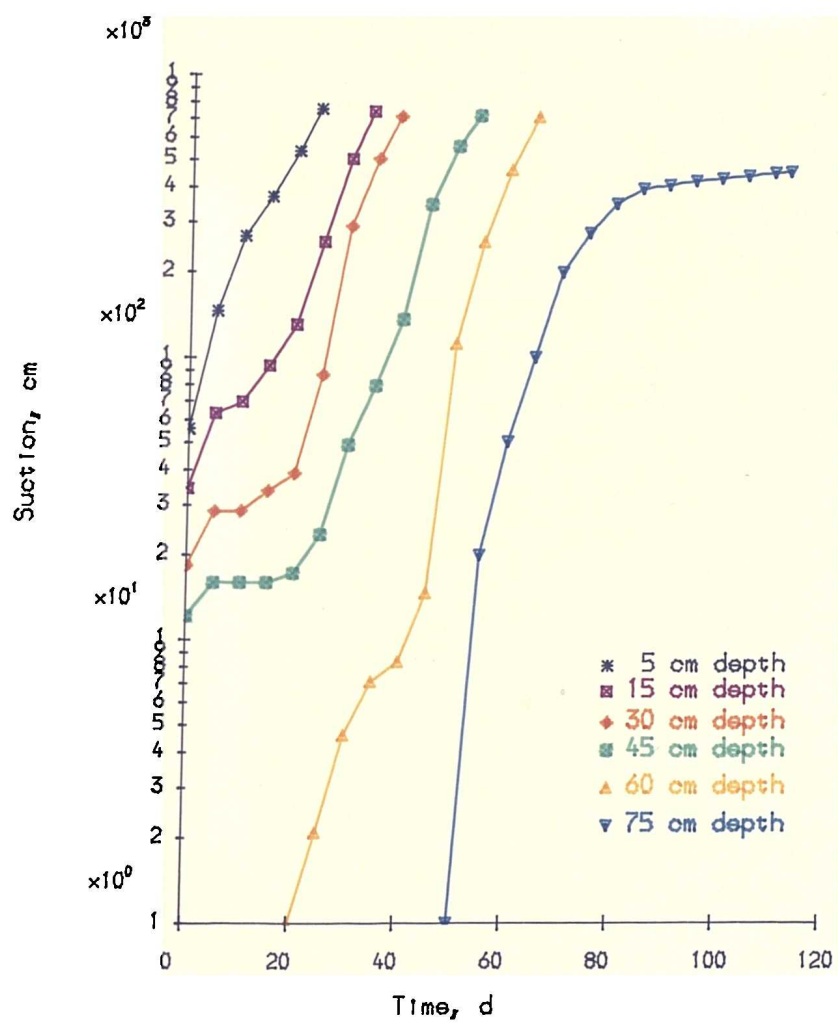


Fig. 6.4. (b) Suction from tensiometers in lysimeter WT-90 (Barley).

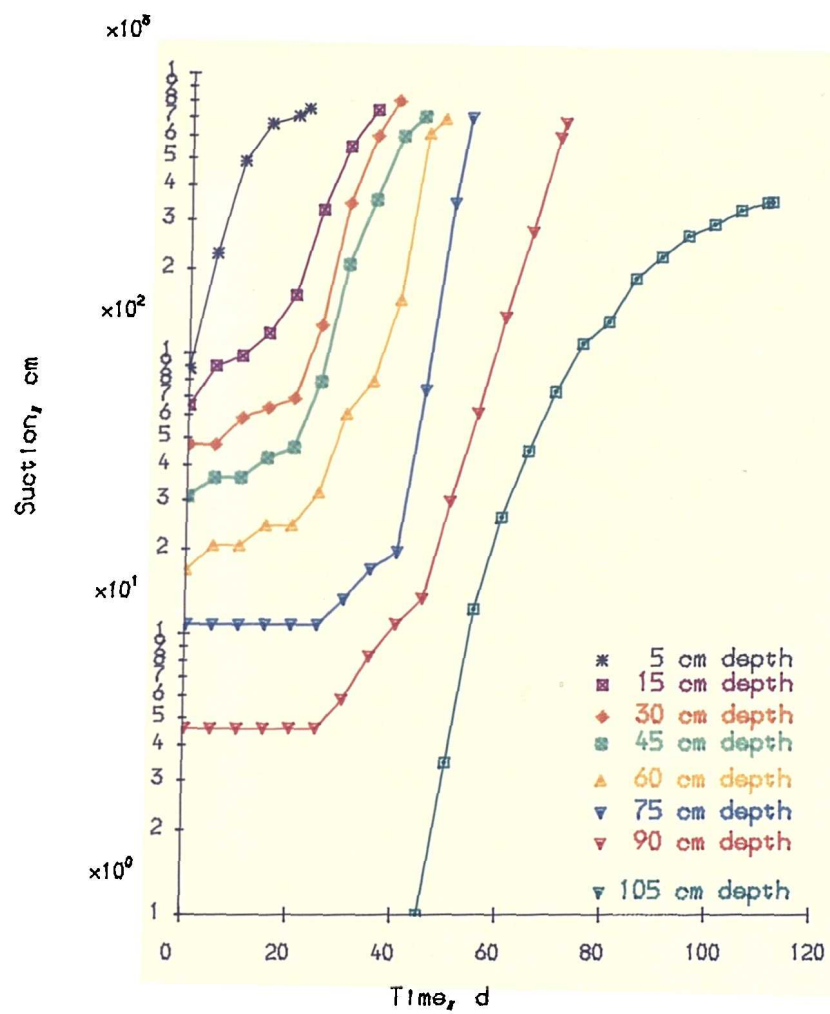


Fig. 6.4. (c) Suction from tensiometers in lysimeter WT-120 (Barley).

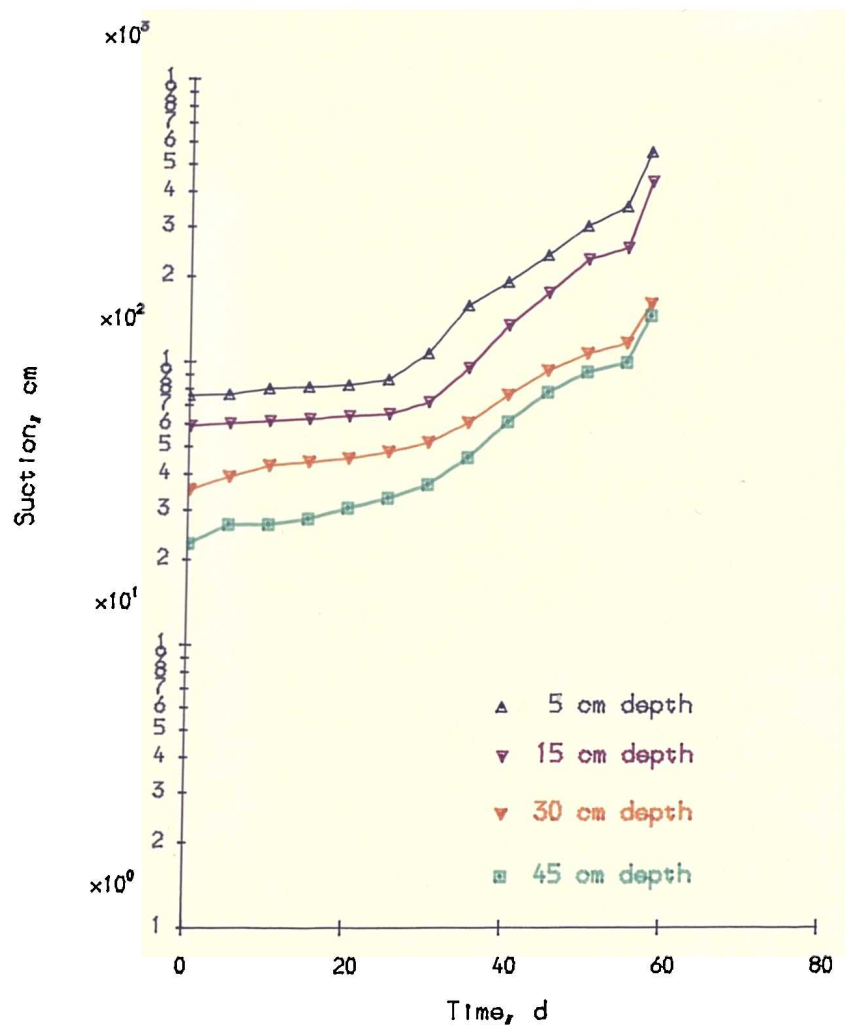


Fig. 6.5. (a) Suction from tensiometers in lysimeter WT-60 (Lettuce).

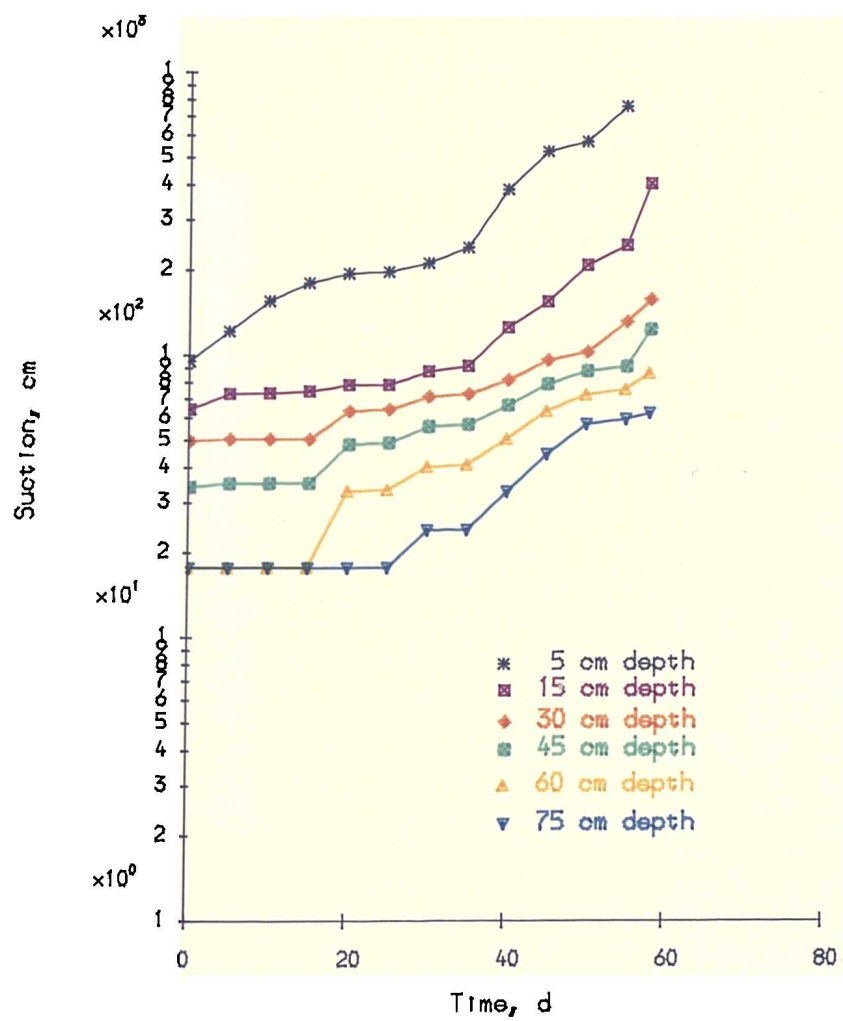


Fig. 6.5. (b) Suction from tensiometers in lysimeter WT-90 (Lettuce).

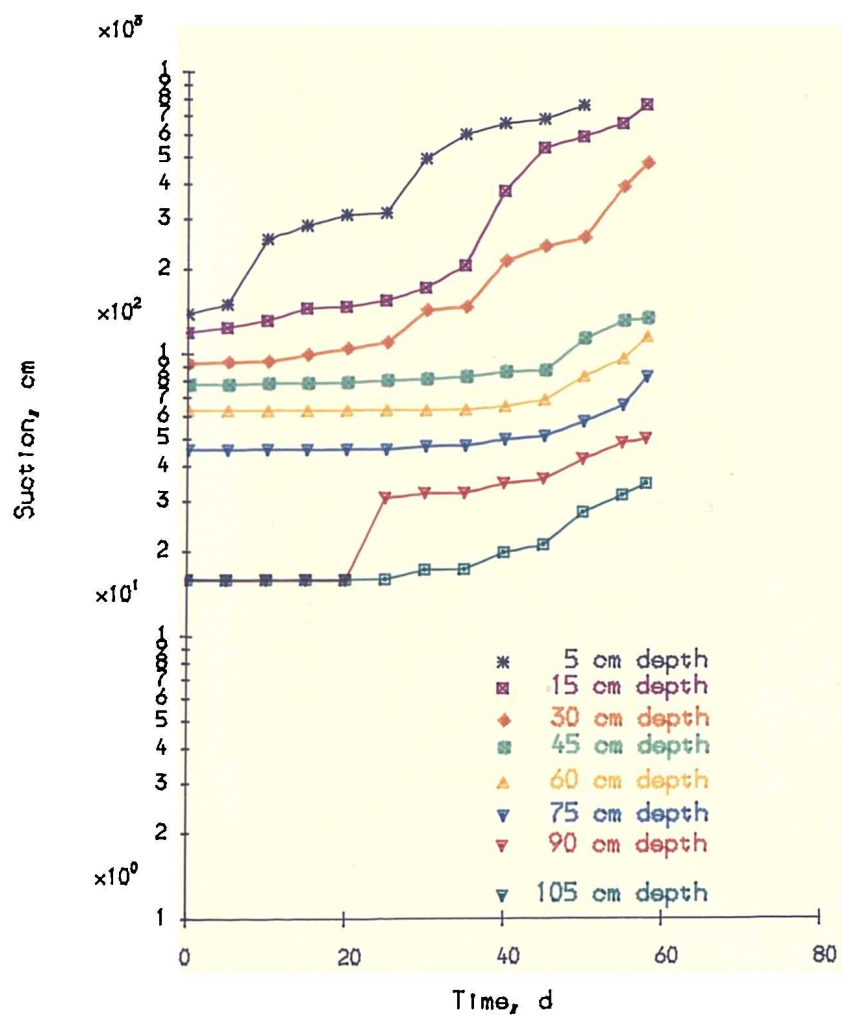


Fig. 6.5. (c) Suction from tensiometers in lysimeter WT-120 (Lettuce).

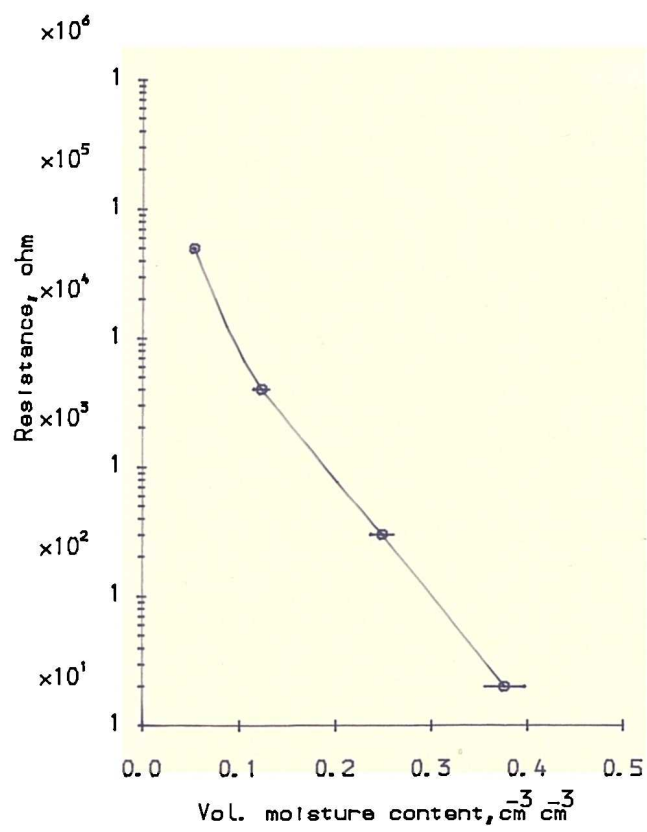


Fig. 6.6. Calibration of resistance block
(horizontal line is s.d. from mean).

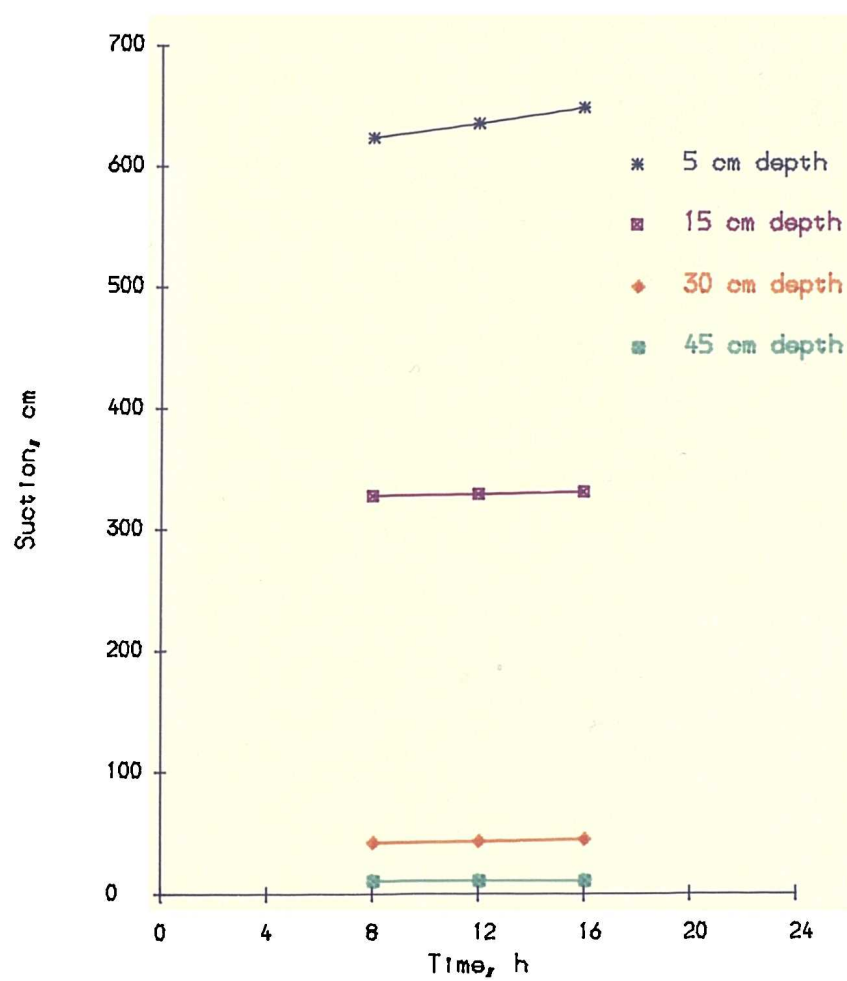


Fig. 6.7. Diurnal variation of tensiometer reading from lysimeter WT-60 (Bean).

6.2 Hydraulic Head Gradient and Plane of Zero Flux

Hydraulic head gradients at different depths were determined from tensiometer readings and plotted against time from sowing. From this, the positions of the zero flux boundary were determined for different water table treatments under different crops. Some examples are shown in Figs. 6.8a, b, c (bean); Figs. 6.9a, b, c (barley) and Fig. 6.10a, b, c (lettuce). These examples illustrate how the hydraulic head gradient at each depth changed direction from positive to negative. The position of the zero-flux boundary is identified with the depth at which the hydraulic head gradient is zero (Arya et al., 1975; Hartmann, 1984). The downward advance of the plane of zero flux is also shown in Figs. 6.8 to 6.10.

In the bean experiment, the plane of zero flux moved down to 45, 75 and 75 cm depth after 80, 105 and 105 days from sowing in lysimeters with water tables 60, 90 and 120 cm deep, respectively.

But in the barley experiment, the plane of zero flux moved down to 15 cm above water table after 30, 55 and 60 days from sowing in lysimeters with water tables 60, 90 and 120 cm deep, respectively.

In the lettuce experiment, the plane of zero flux moved down to 15 cm above the water table after 10, 20 and 25 days from sowing in lysimeters with water tables 60, 90 and 120 cm deep, respectively. The plane of zero flux shifted rapidly towards the water table because of the long time available for draining the soil profile compared to the barley experiment.

The movement of the zero-flux plane as a function of time is presented in Tables 6.7 (bean); 6.8 (barley) and 6.9 (lettuce).

Location of the plane of the zero flux enables us to determine upward or downward flux in a soil profile in the presence or absence of water table.

Table 6.7 — Summary of time at which zero-flux plane moved for different water table treatments under beans.

Crop	Bean, 1988		
Zero-flux depth below soil surface cm	Depth to water table from soil surface		
	60	90	120
	cm	cm	cm
	Days from sowing		
5	0	0	
15	45	15	0
30	45	35	35
45	80	55	65
60		105	90
75		105	90
90			-
105			-

Table 6.8 — Summary of time at which zero-flux plane moved for different water table treatments under barley.

Crop	Barley, 1989		
Zero-flux depth below soil surface cm	Depth to water table from soil surface		
	60	90	120
	cm	cm	cm
	Days from	sowing	
5	0		
15	5	0	
30	5	15	0
45	30	15	5
60		50	25
75		55	45
90			50
105			60

Table 6.9 — Summary of time at which zero-flux plane moved for different water table treatments under lettuce.

Crop	Lettuce, 1990		
Zero-flux depth below soil surface cm	Depth to water table from soil surface		
	60 cm Days from	90 cm sowing	120 cm
5			
15	0		
30	10		
45	10	0	
60		20	
75		20	0
90			25
105			25

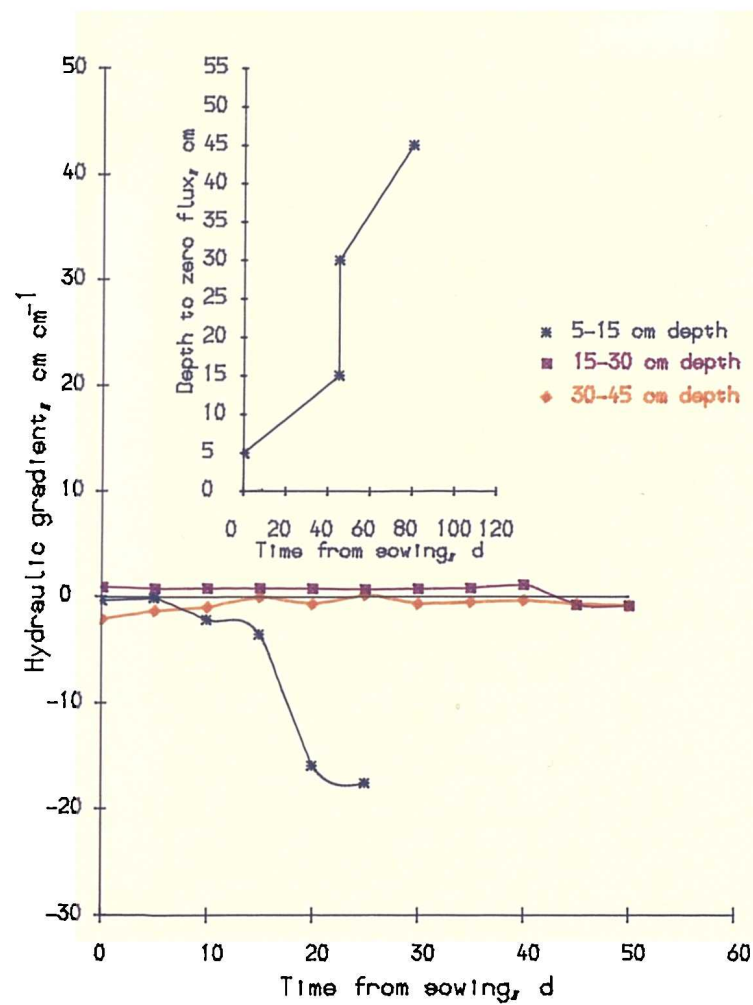


Fig. 6.8. (a) Variation of hydraulic gradient with time for WT-60 (Bean).

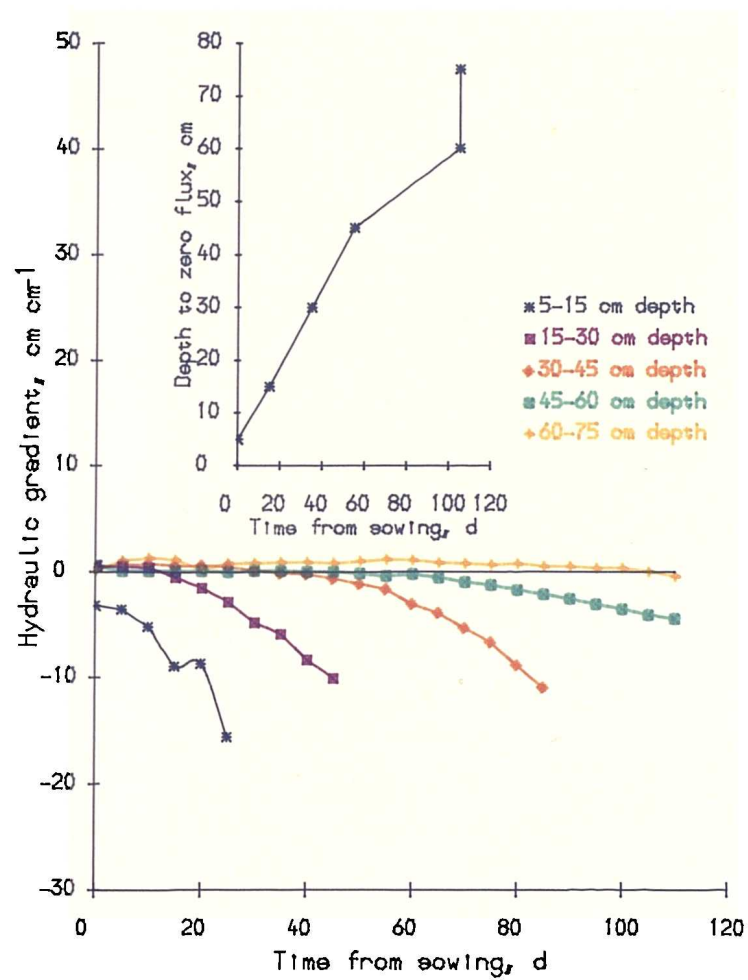


Fig. 6.8. (b) Variation of hydraulic gradient with time for WT-90 (Bean).

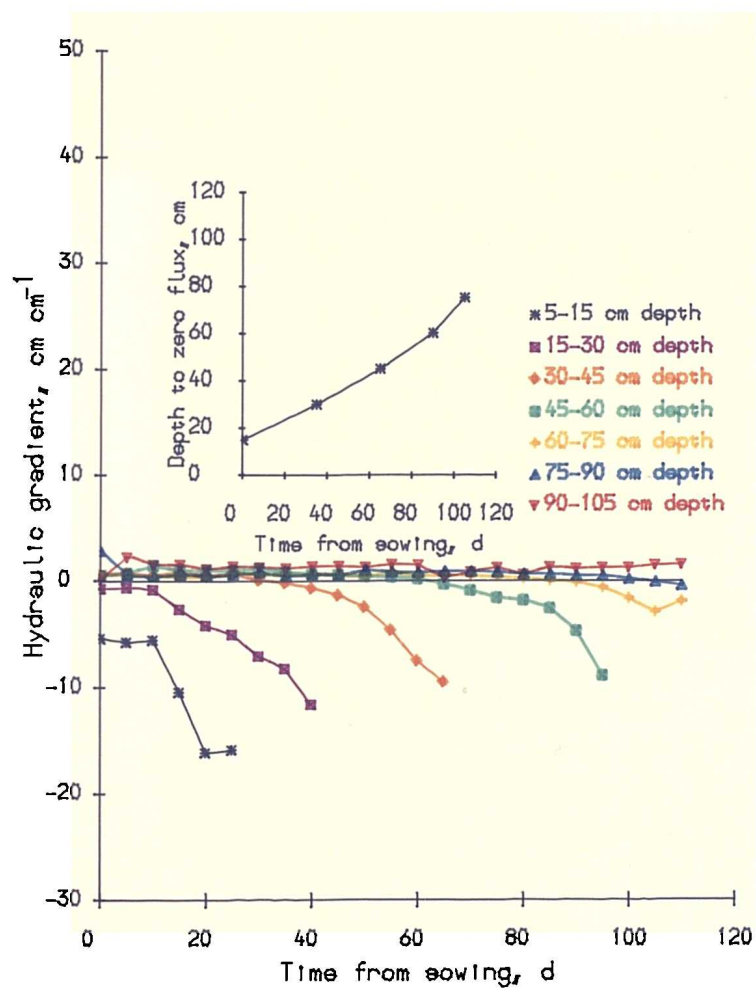


Fig. 6.8. (c) Variation of hydraulic gradient with time for WT-120 (Bean).

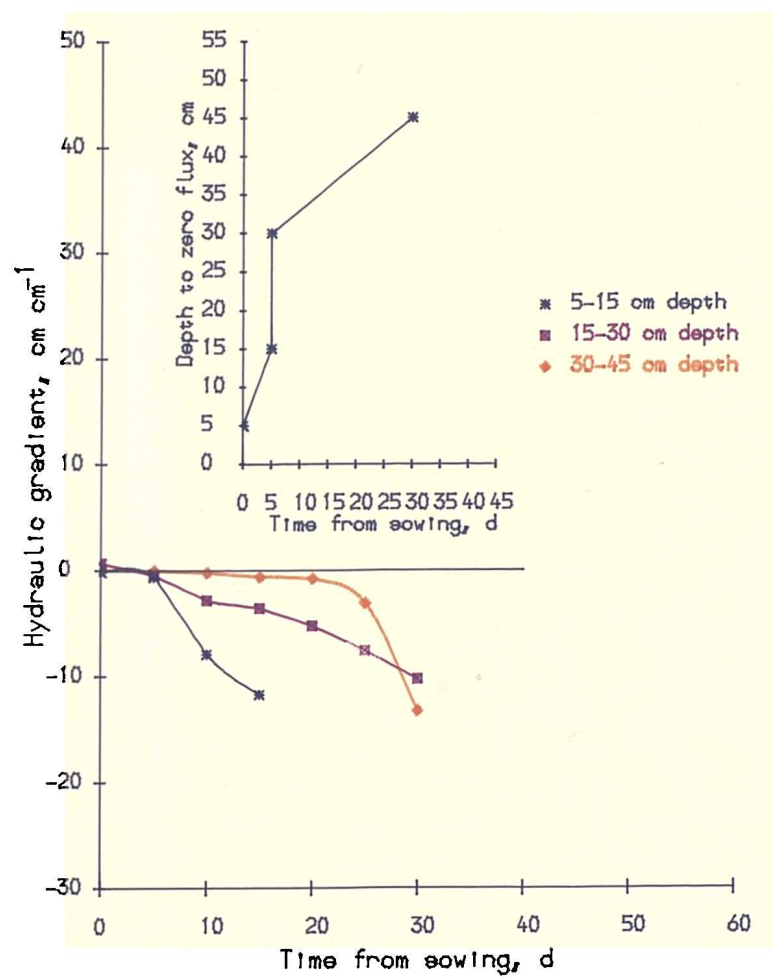


Fig. 6.9. (a) Variation of hydraulic gradient with time for WT-60 (Barley).

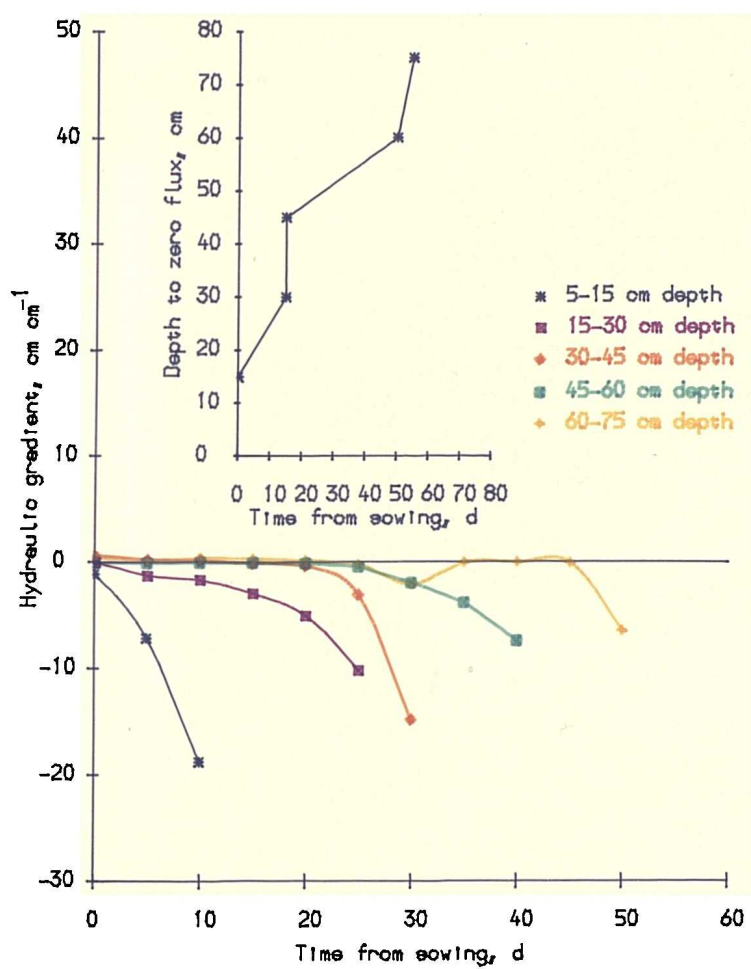


Fig. 6.9. (b) Variation of hydraulic gradient with time for WT-90 (Barley).

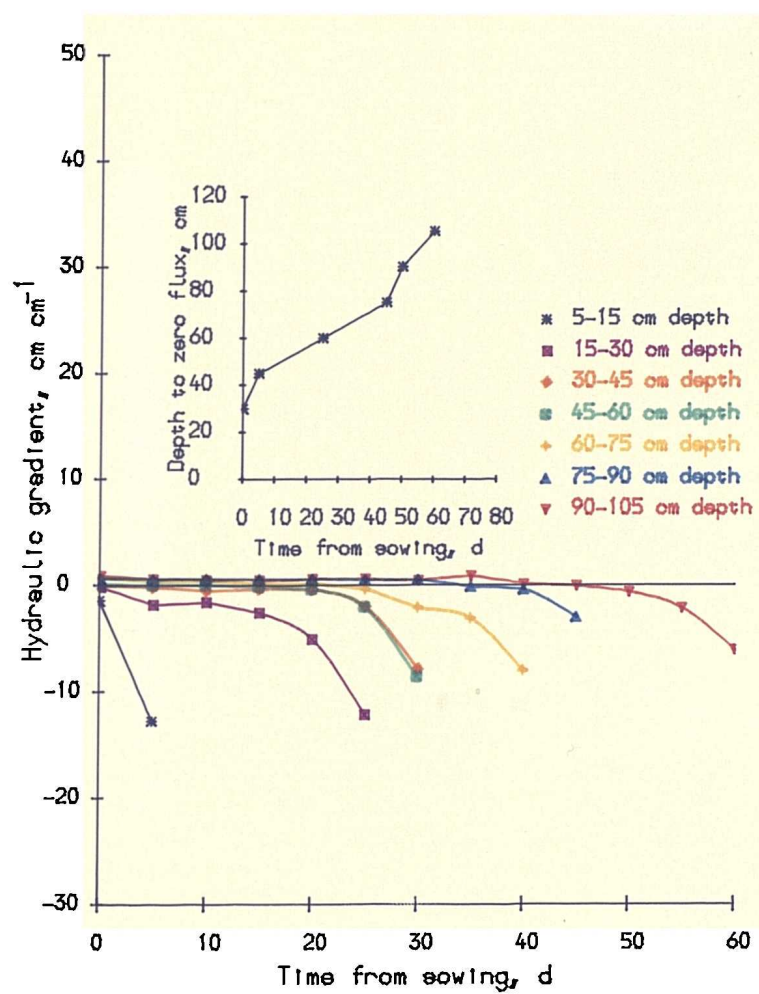


Fig. 6.9. (c) Variation of hydraulic gradient with time for WT-120 (Barley).

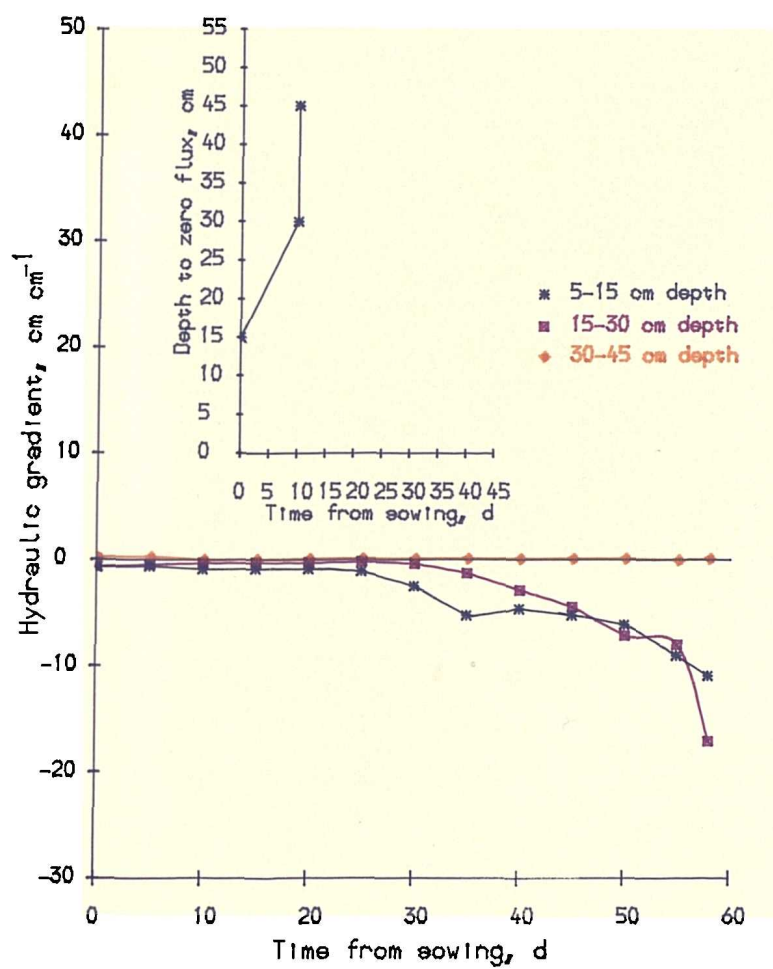


Fig. 6.10. (a) Variation of hydraulic gradient with time for WT-60 (Lettuce).

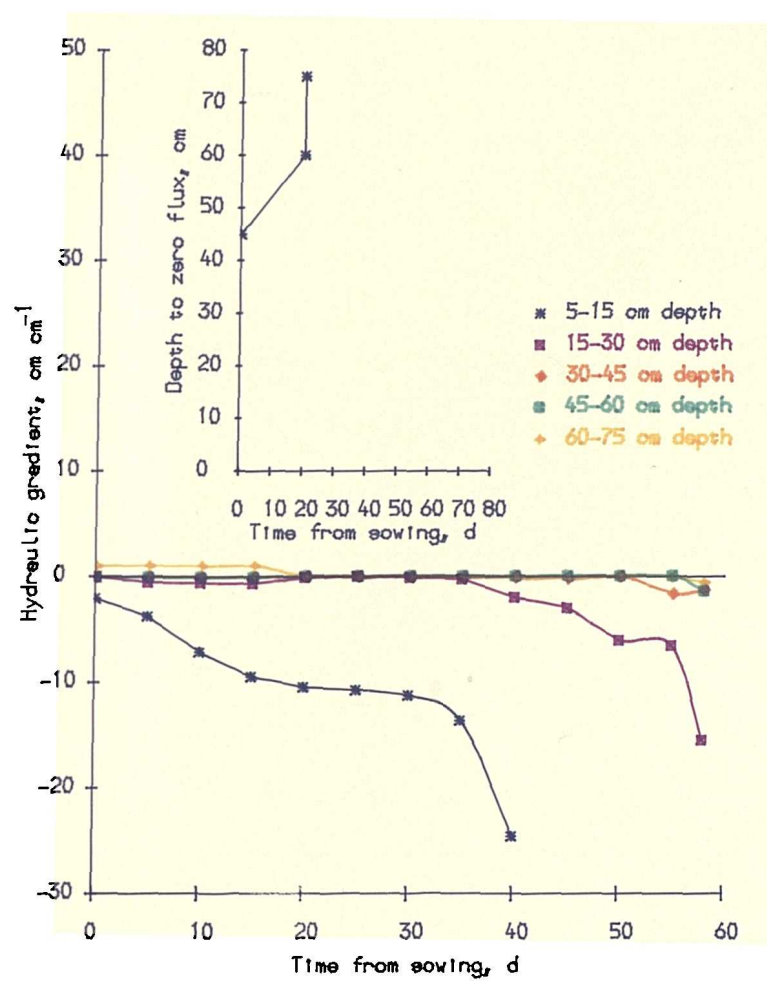


Fig. 6.10. (b) Variation of hydraulic gradient with time for WT-90 (Lettuce).

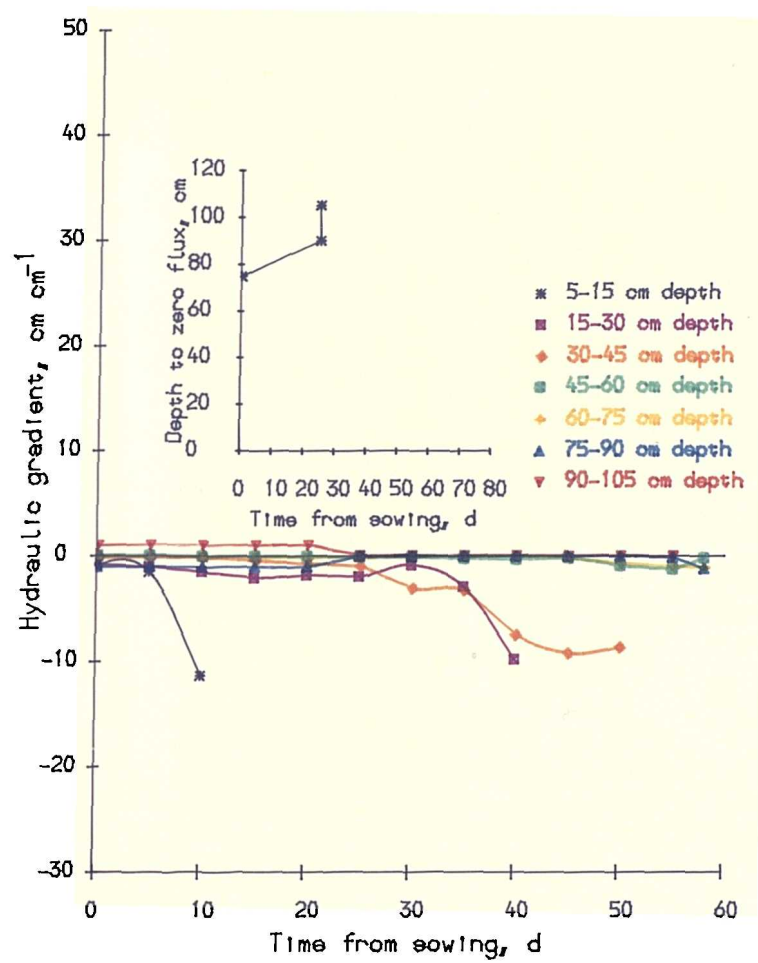


Fig. 6.10. (c) Variation of hydraulic gradient with time for WT-120 (Lettuce).

6.3 Soil Moisture Extraction

Graphs of the soil moisture extraction pattern under different crops are shown in Figs. 6.11, 6.12 and 6.13. Graphs are drawn for each depth in the profile.

The pattern of extraction by beans was the same under the different water table treatments. Initially an accelerating rate of water loss was observed from the 0-15 cm layer. Deeper layers showed a gradual water loss initially before undergoing a rapid water loss. The extraction rate is dependent on the location of the plane of zero flux (section 6.2). In the deeper layers of the soil profile, 15 cm above water table, there is little or no change in slope in the water content-time curves.

But moisture extraction patterns by barley differed from those by beans. Progress of extraction to the deeper layers was more rapid. There was no change of water content at depth 15 cm above the water table up to 50 and 60 days of growth in water tables 90 and 120 cm deep, respectively. Plants were extracting moisture from deeper layers gradually in the lysimeters with water tables 90 and 120 cm deep. But extraction rates were accelerated from deeper layers when shallow layers were exhausted. After an elapse of time, the extraction rate was rapid at 45 cm depth in the lysimeter with the water table at 60 cm depth.

The moisture extraction by lettuce was only confined to the top 0-5 cm depth in all the lysimeters. The change of moisture in the lower layers was caused by the upward flux to the upper layer to satisfy the crop water demand. The upper layer (0-5 cm) showed rapid moisture extraction while deeper layers had only a slow change rate due to upward flux. The moisture content in the top layer was above the wilting point in all the lysimeters up to harvest.

The point at which the rate of water extraction starts to increase at each depth, represents the arrival of the drying front associated with root water extraction, and this information may be used to distinguish drainage from evaporation losses of water from the soil. Water losses from all depth intervals are most strongly influenced by the growth stages (sowing, vegetative, flowering, maturity etc.) of the plants from sowing. This is also reported by Arya et al. (1975).

The depth of soil to which an accelerated rate of soil drying is observed can be considered as an "effective rooting depth" and by tracing the course of drying for

successive depths in the profile information can be obtained about the development of rooting. The same concept was reported by McGowan (1973).

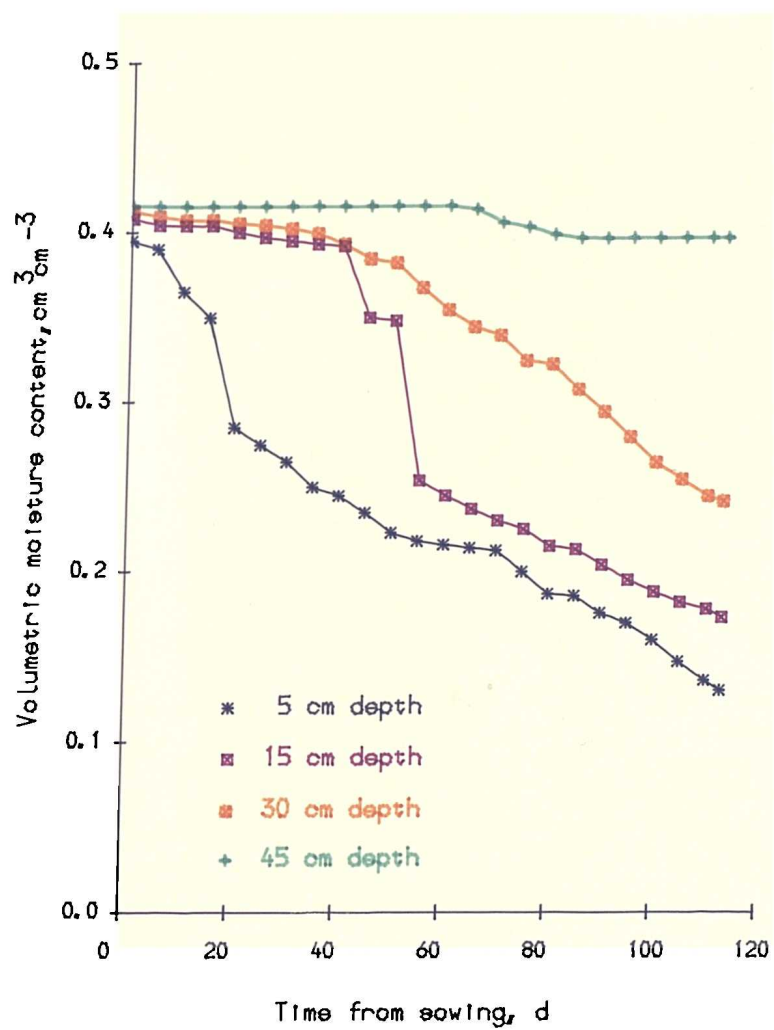


Fig. 6.11. (a) Water content versus time for WT-60 (Bean).

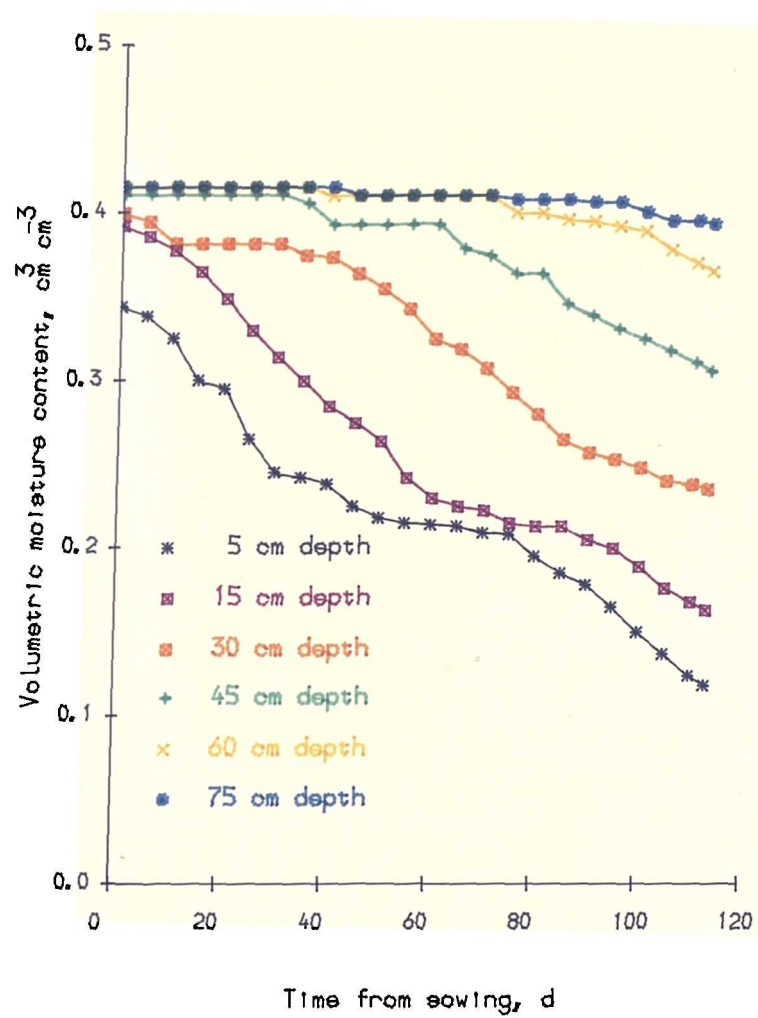


Fig. 6.11. (b) Water content versus time for WT-90 (Bean).

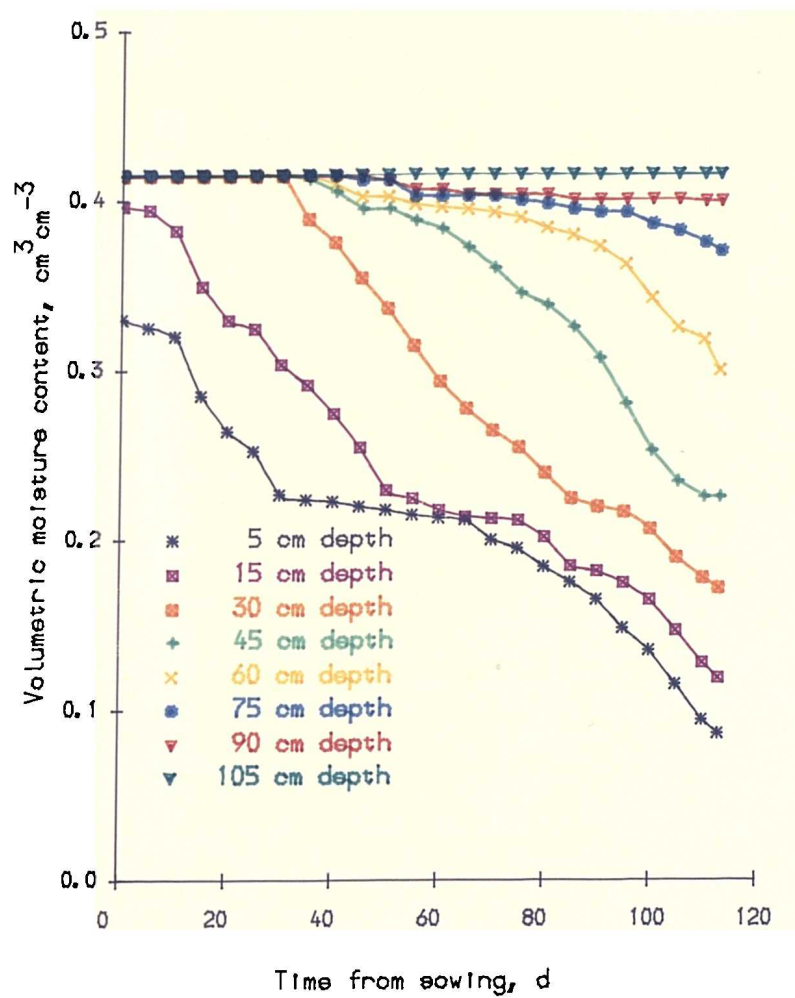


Fig. 6.11. (c) Water content versus time for WT-120 (Bean).

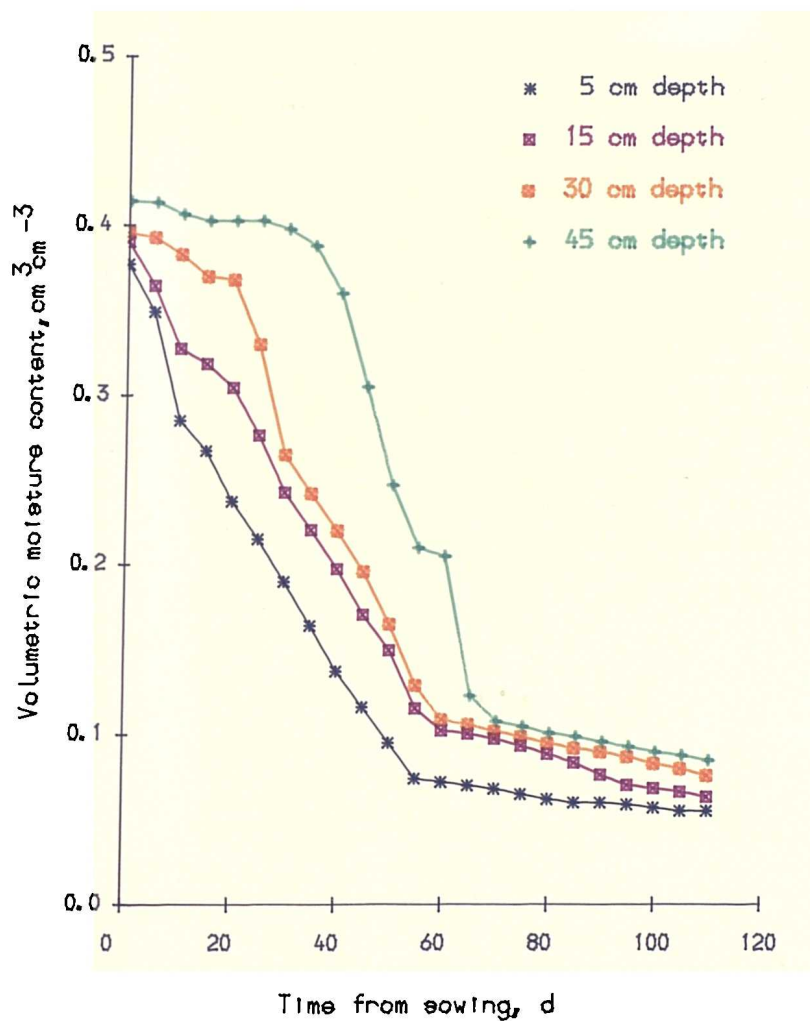


Fig. 6.12. (a) Water content versus time for WT-60 (Barley).

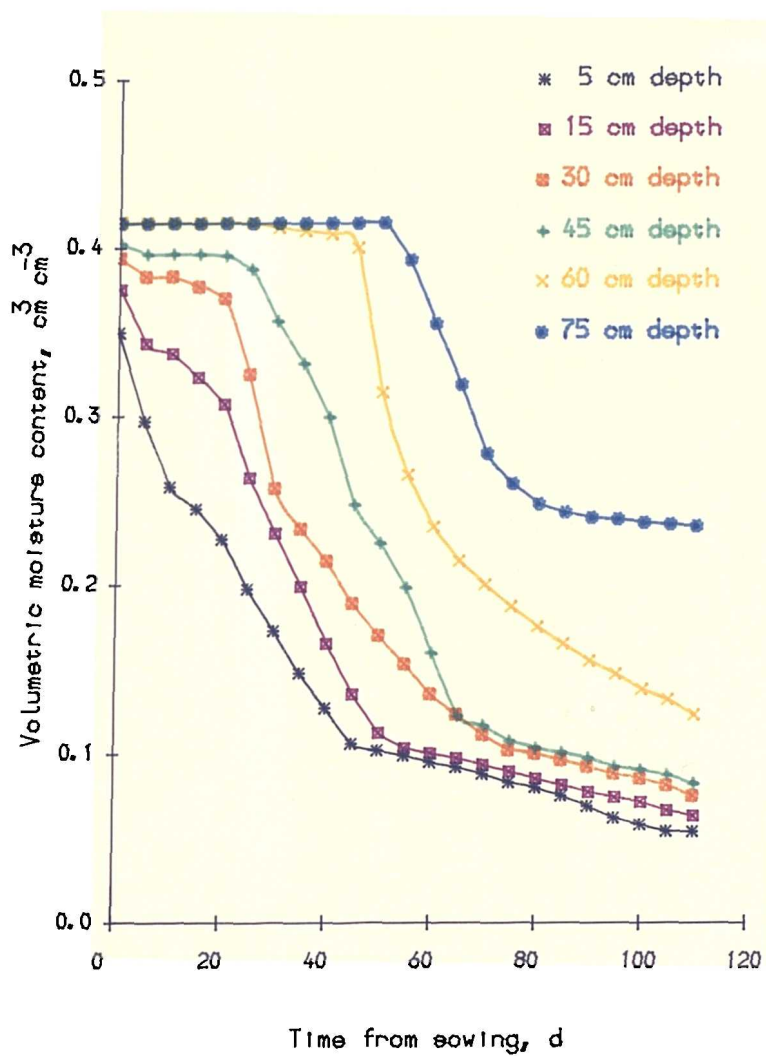


Fig. 6.12. (b) Water content versus time for WT-90 (Barley).

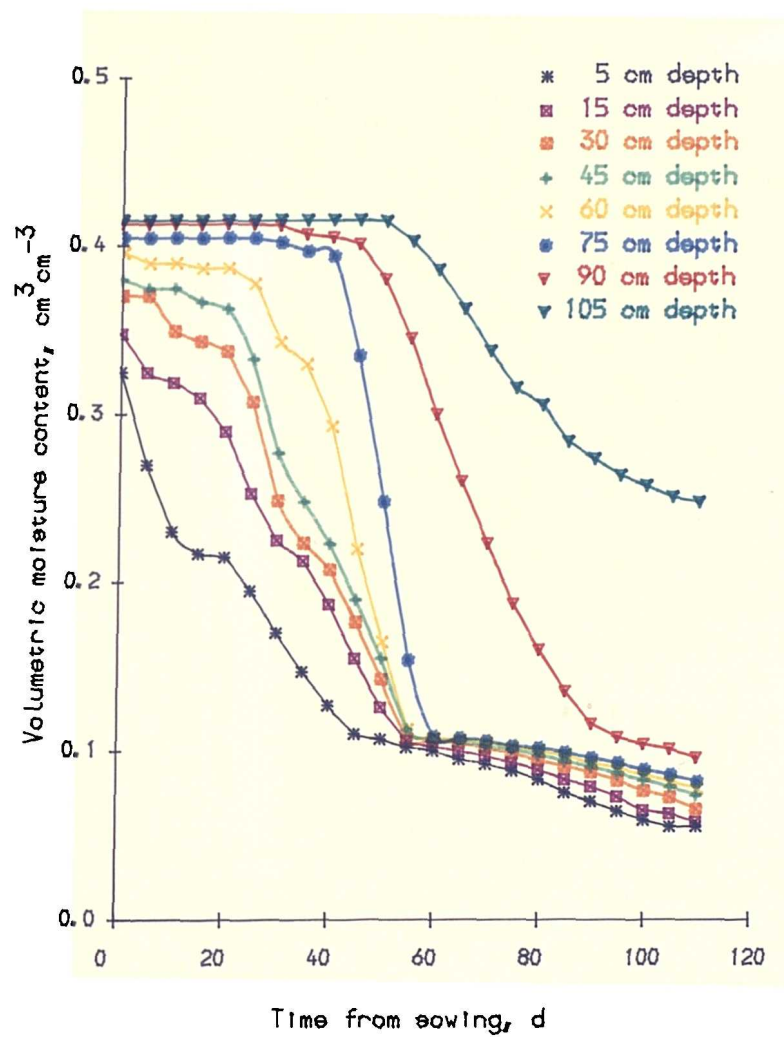


Fig. 6.12. (c) Water content versus time for WT-120 (Barley).

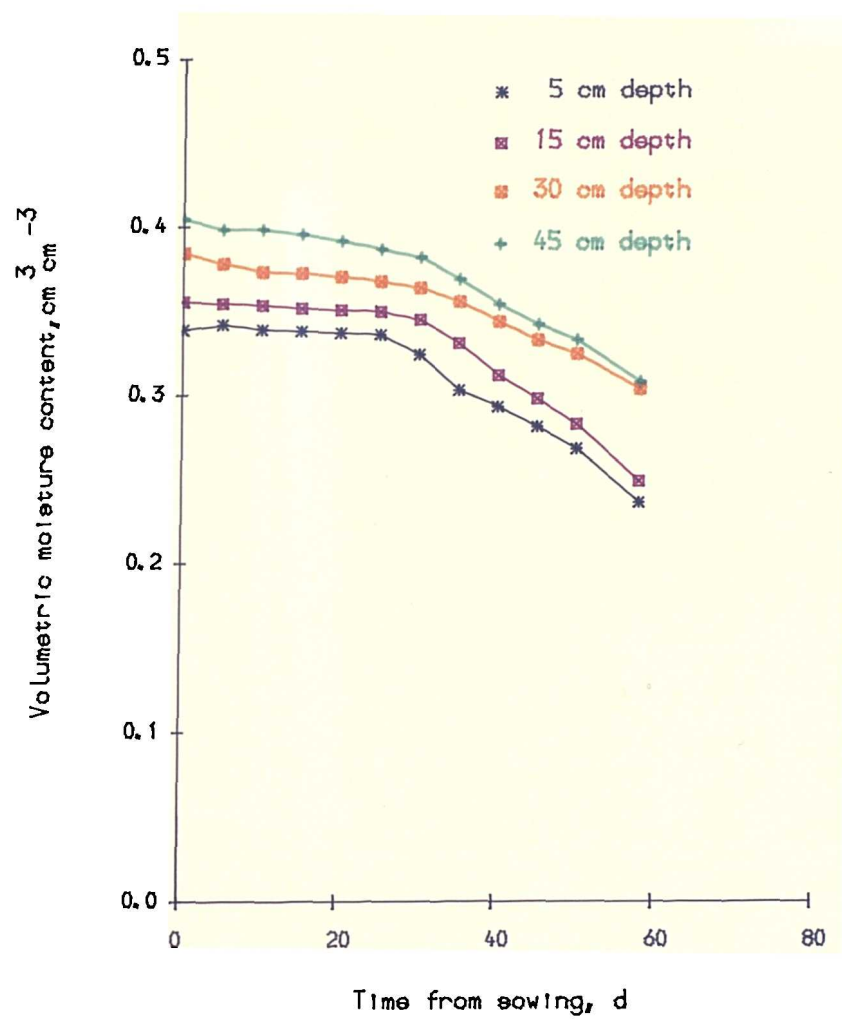


Fig. 6.13. (a) Water content versus time for WT-60 (Lettuce).

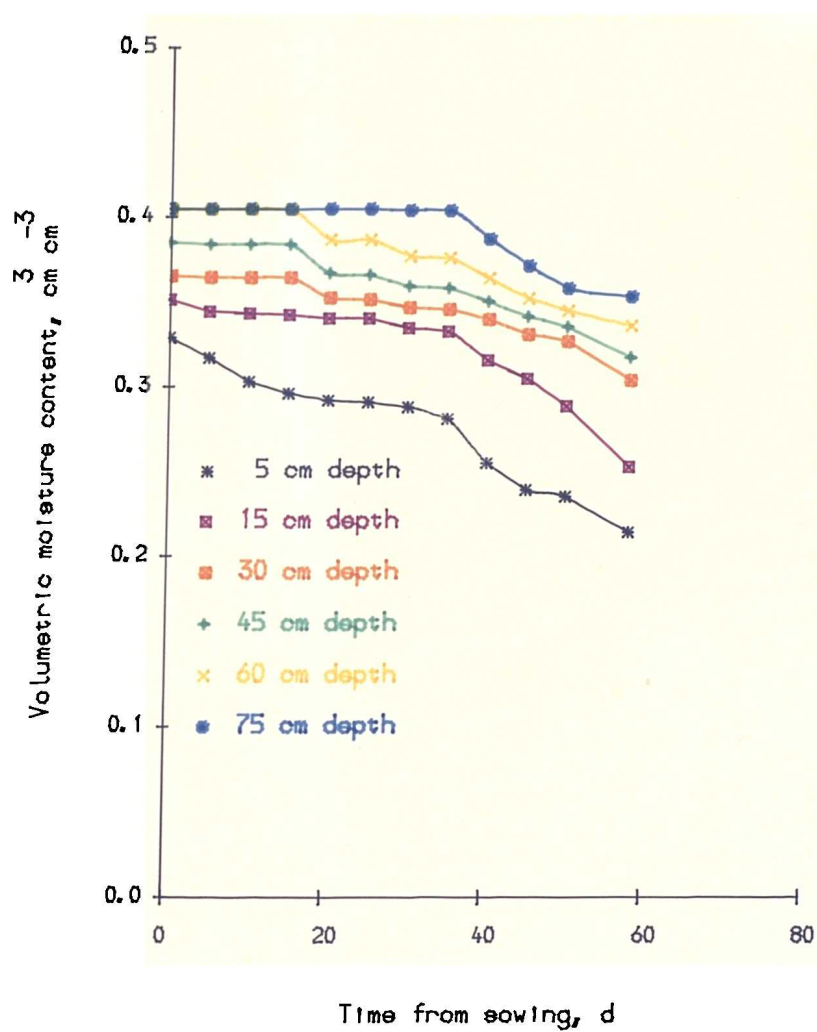


Fig. 6.13. (b) Water content versus time for WT-90 (Lettuce).

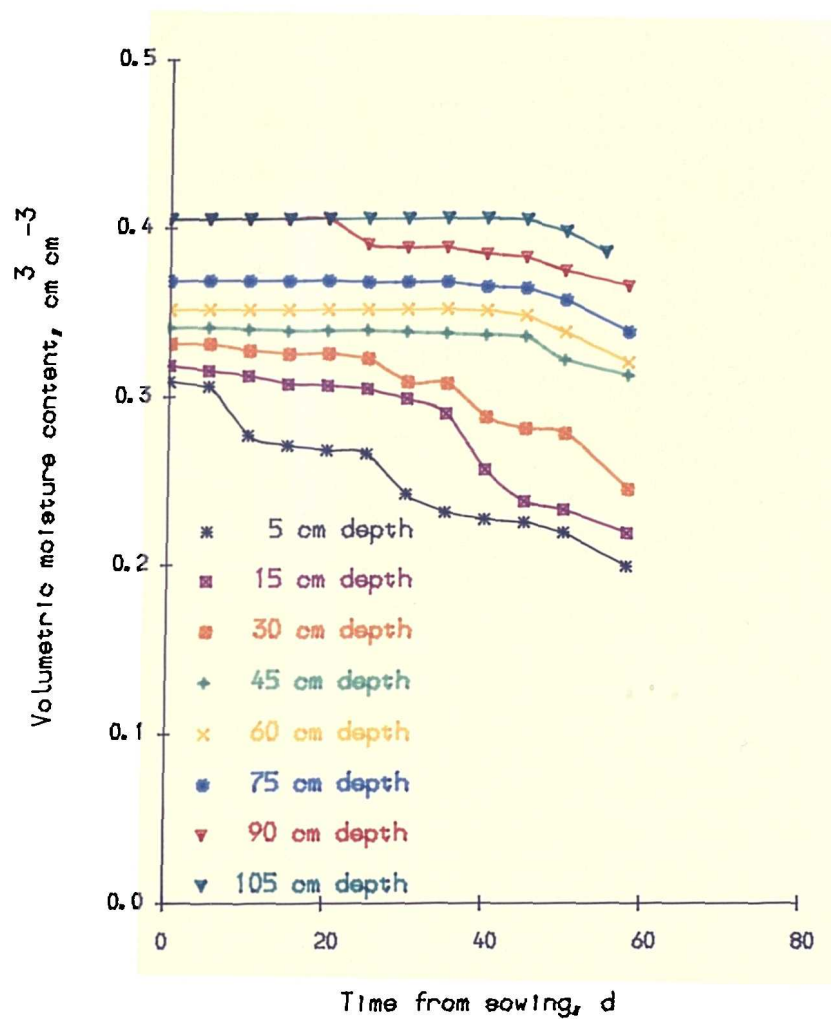


Fig. 6.13. (c) Water content versus time for WT-120 (Lettuce).

6.4 Soil Water Flux

Examples of soil water flux as a function of time are shown in Figs. 6.14a, b, c (bean); Figs. 6.16a, b, c (barley) and Figs. 6.18a, b, c (lettuce). Fluxes are measured as a function of depth using Equation (3.27) above the water table, and determined from the inflow from the Mariotte siphon at the water table. At the beginning of growing period i.e. seedling to emergence, fluxes were not significant. Therefore, fluxes for bean and barley were measured from the 20th day of sowing and for lettuce from the 15th day after sowing.

In the bean experiment, there was drainage to the water table almost throughout the growing period (Figs. 6.14a, b, c). In the lysimeter with water table at 60 cm, upward flux was mainly from the top 15 cm layer up to 45 days from sowing. Upward flux from the 15-30 cm layer started when the plane of zero flux moved down to 30 cm depth (Table 6.7 and Fig. 6.14a). The sharp decrease in soil water flux was caused by rapid decrease in soil moisture content. Soil water flux was mainly from top 15 cm layer up to 40 days of sowing in the lysimeter with the water table at 90 cm. Then the upward flux from the 5 cm layer decreased but started to increase from 30 and 45 cm depth. There was no upward flux from 60 and 75 cm depth up to 105 days from sowing (Fig. 6.14b). The upward flux moved deeper with the decrease of soil moisture content. The changes of hydraulic conductivity as a function of depth due to soil moisture changes in beans is shown in Figs. 6.15a, b, c. A similar trend was observed in the lysimeter with the water table at 120 cm (Fig. 6.14c and Fig. 6.15c). There was no upward flux from 90 and 105 cm depth; rather there was downward flow.

In the barley experiment, drainage was observed in lysimeters with water tables at 90 and 120 cm up to 55 and 60 days from sowing, respectively (Figs. 6.16b, c). There was a very small rate of drainage in the lysimeter with water table at 60 cm depth up to 30 days from sowing (Fig. 6.16a). Upward flux was diminishing from shallow depths and was increasing in deeper layers. In the lysimeter with a water table at 60 cm, upward flux was almost zero at 15 cm depth above the water table (Fig. 6.16a). But in the other two lysimeters, upward flux from 15 cm depth above the water table was initiated after 55 and 60 days from sowing, respectively and was almost constant up to harvest (Figs. 6.16b, c). This is due to rapid extraction

of soil moisture. Hydraulic conductivity as a function of depth due to soil moisture changes in barley is shown in Figs. 6.17a, b, c. The experiment was started when soil profiles had almost saturated hydraulic conductivity at different depths (Figs. 6.17a, b, c). The upper layers were exhausted in terms of available water due to water uptake by roots.

In the lettuce experiment, drainage was observed up to 9, 19 and 24 days from sowing in lysimeters with water tables 60, 90 and 120 cm deep, respectively (Table 6.9 and Figs. 6.18a, b, c). After that, an upward flux was observed in all the lysimeters. Higher fluxes were observed at 15 cm above the water table in the lysimeter with water table at 60 cm compared to the other two lysimeters. The changes of hydraulic conductivity as a function of depth due to soil moisture changes in lettuce is shown in Figs. 6.19a, b, c.

The sharp decrease in soil water flux was caused primarily by the hydraulic conductivity's dramatic change with depth (Reicosky et al., 1972). The transmitting ability of the profile is limited by the hydraulic conductivity of the soil in relation to the suction in presence of water table (Marshall and Holmes, 1988; Hillel, 1980). The upward flux is not only controlled by the crop water demand, but is rather a simultaneous function of crop water demand and the profile's transmitting property.

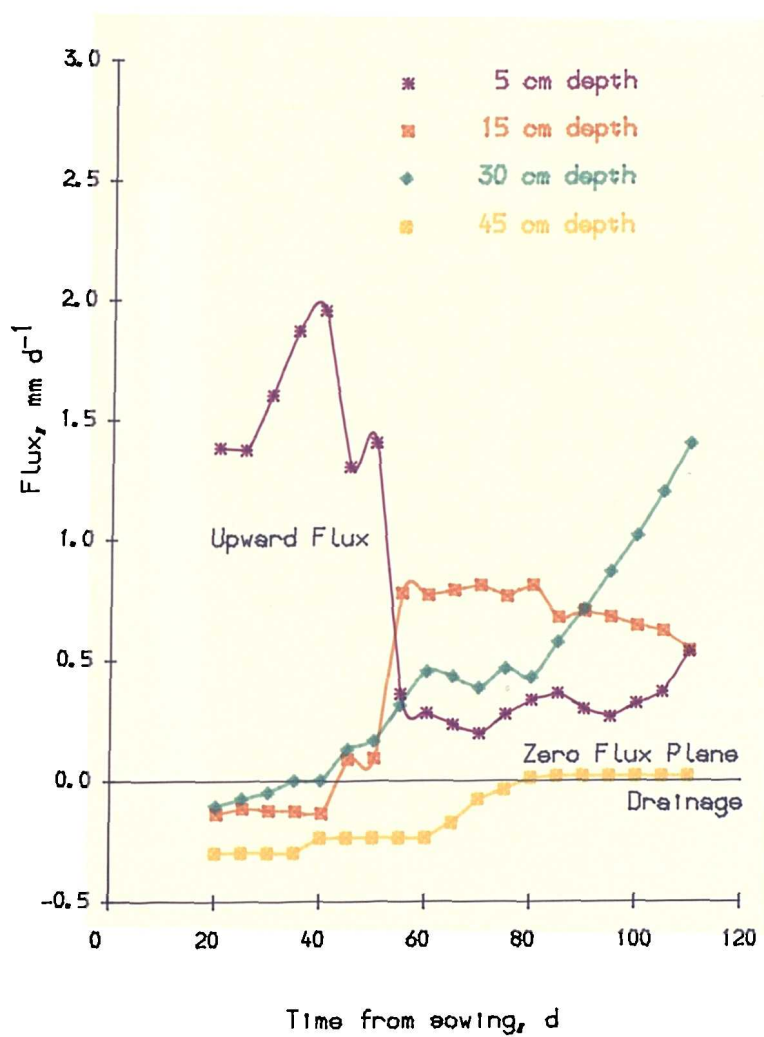


Fig. 6.14. (a) Measured flux versus time for WT-60 (Bean).

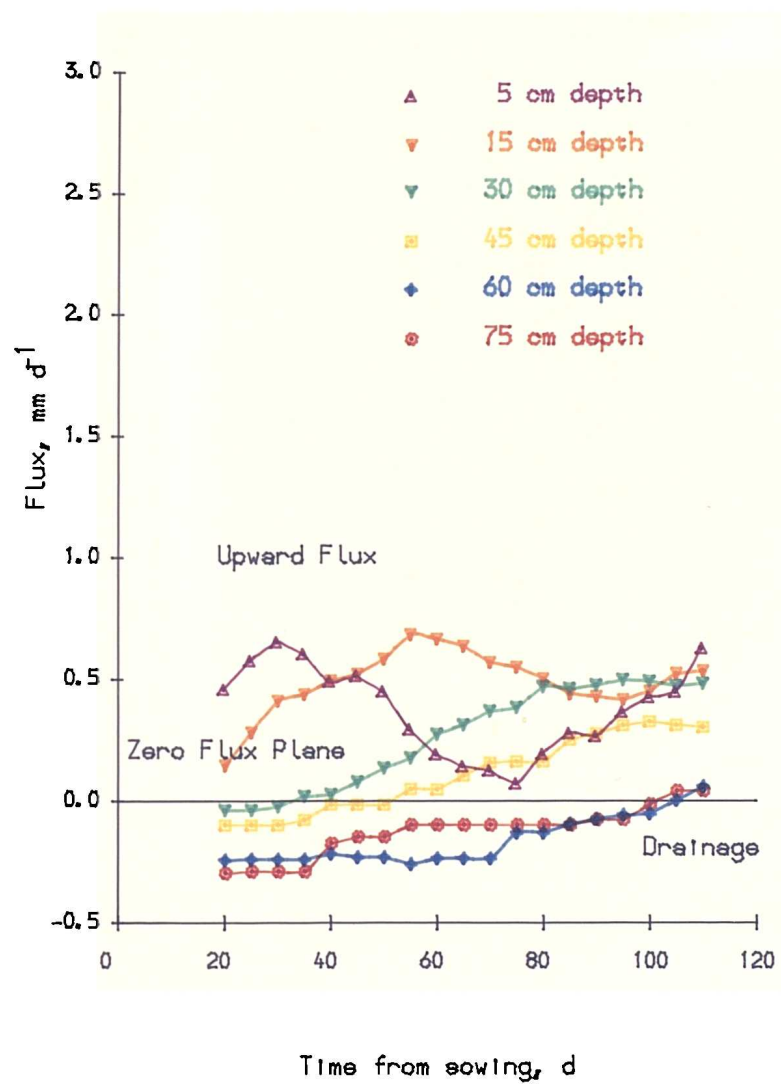


Fig. 6.14. (b) Measured flux versus time for WT-90 (Bean).

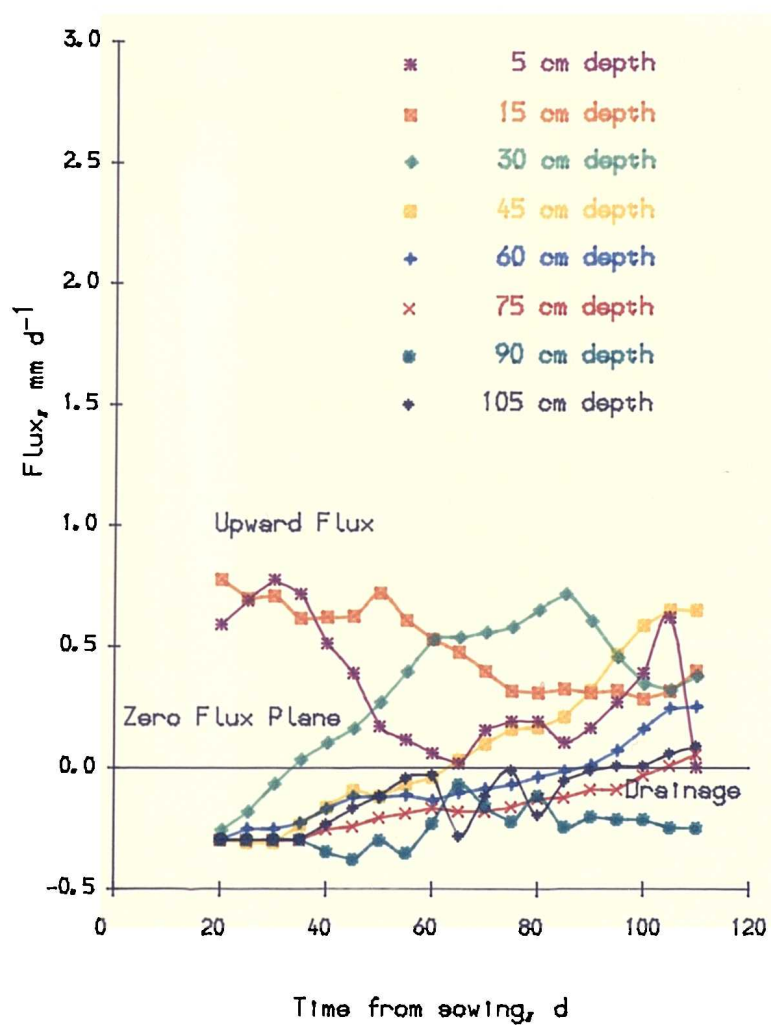


Fig. 6.14. (c) Measured flux versus time for WT-120 (Bean).

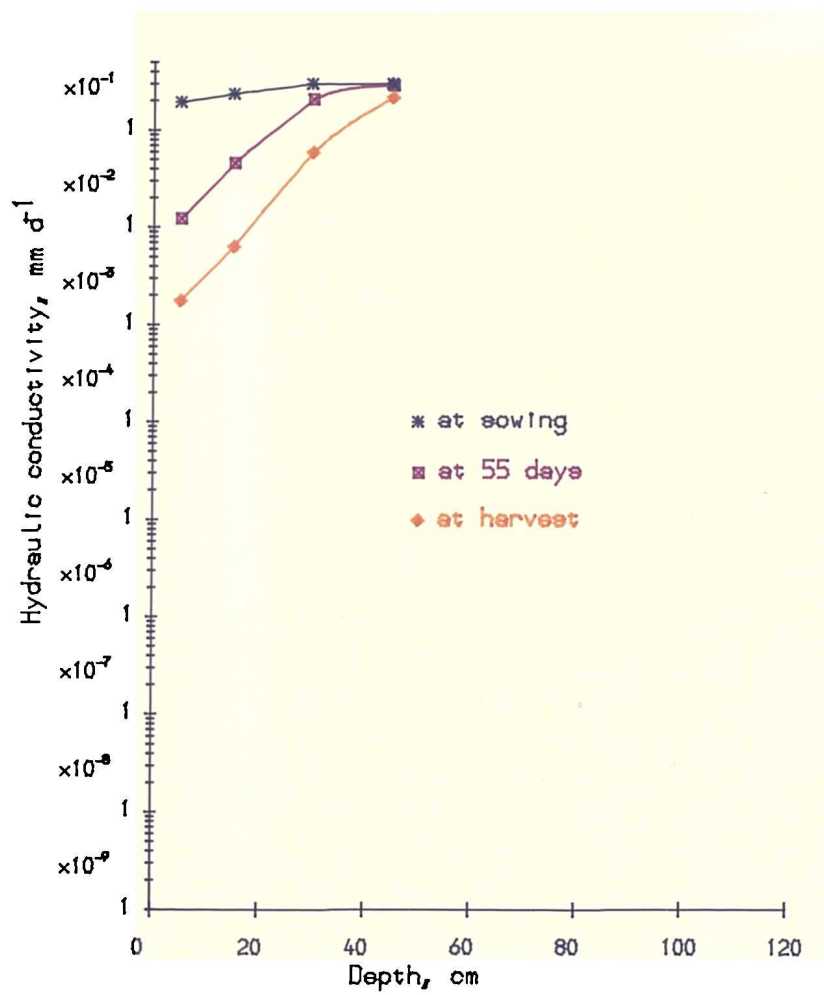


Fig. 6.15. (a) Hydraulic conductivity as a function of depth for WT-60 (Bean).

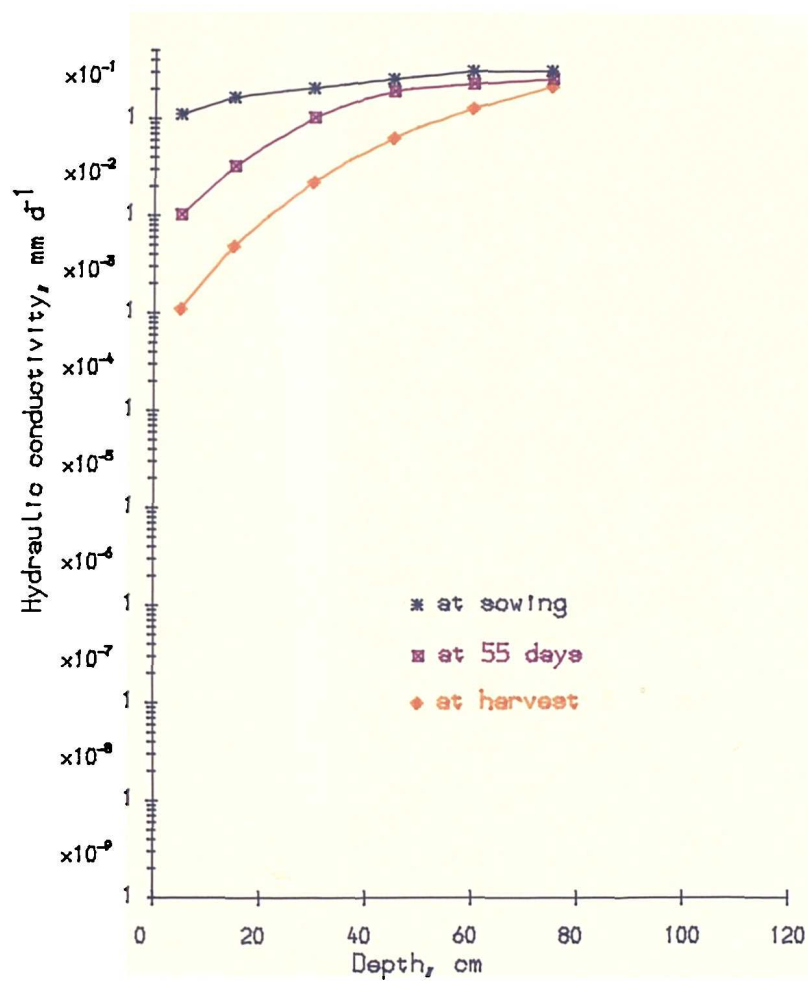


Fig. 6.15. (b) Hydraulic conductivity as a function of depth for WT-90 (Bean).

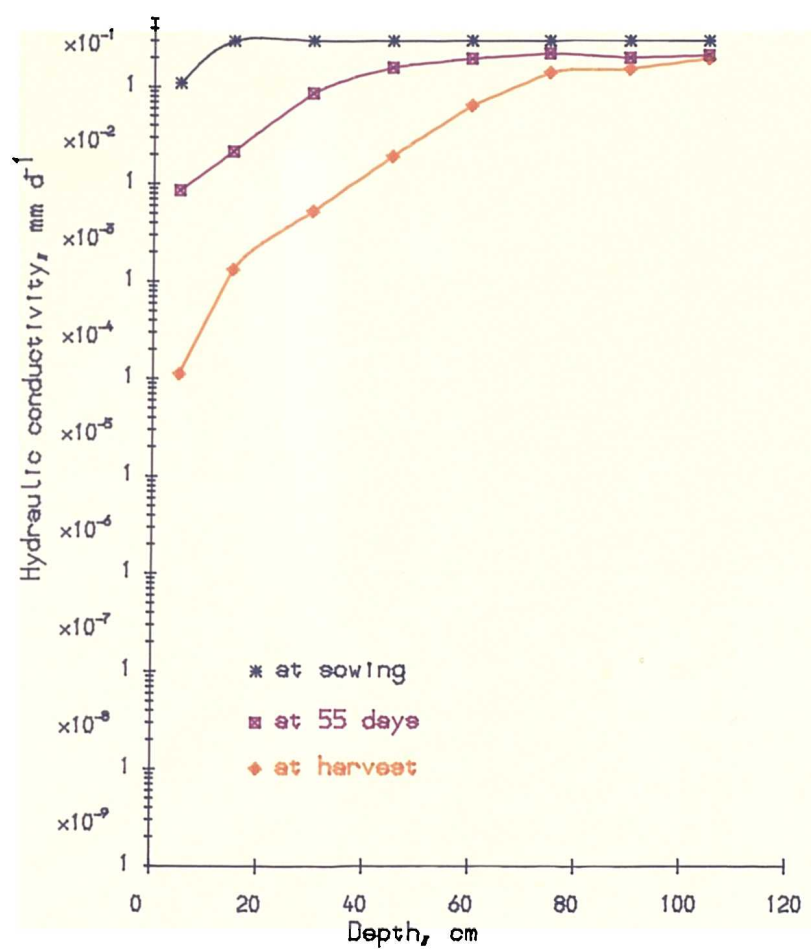


Fig. 6.15. (c) Hydraulic conductivity as a function of depth for WT-120 (Bean).

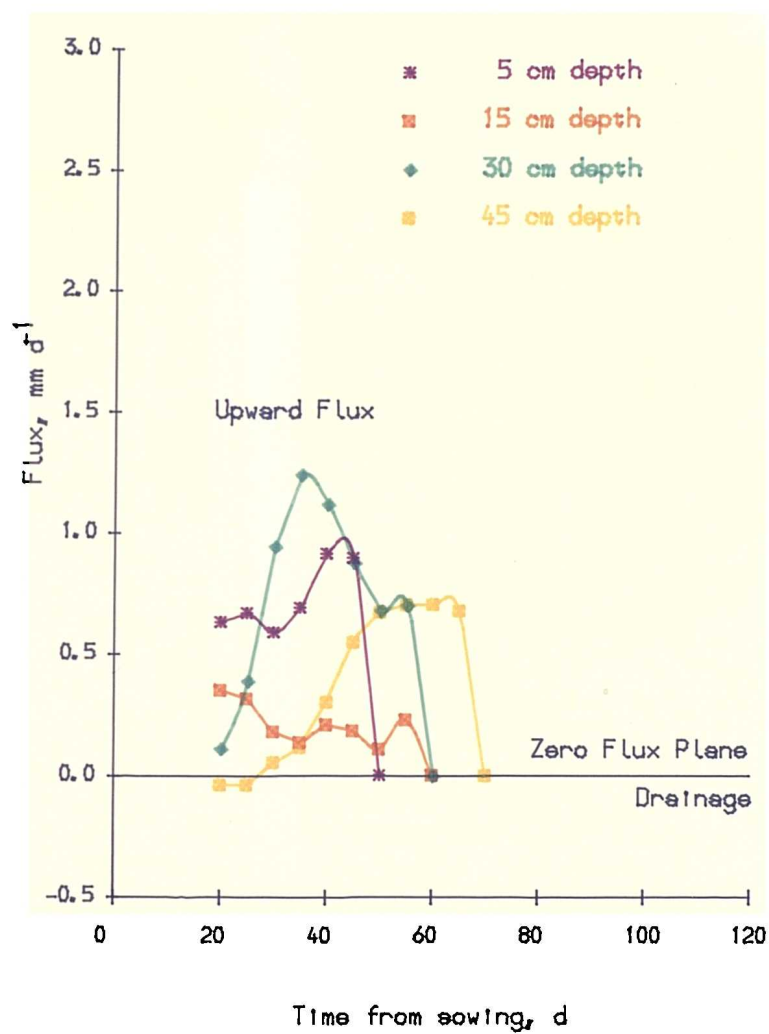


Fig. 6.16. (a) Measured flux versus time for WT-60 (Barley).

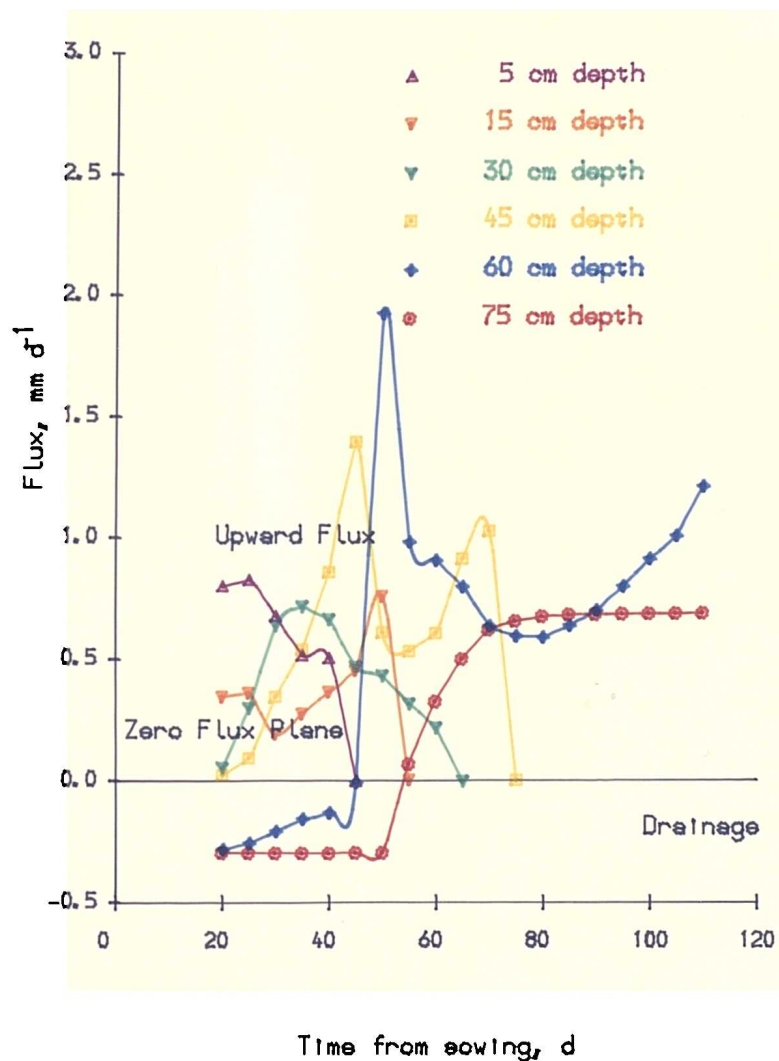


Fig. 6.16. (b) Measured flux versus time for WT-90 (Barley).

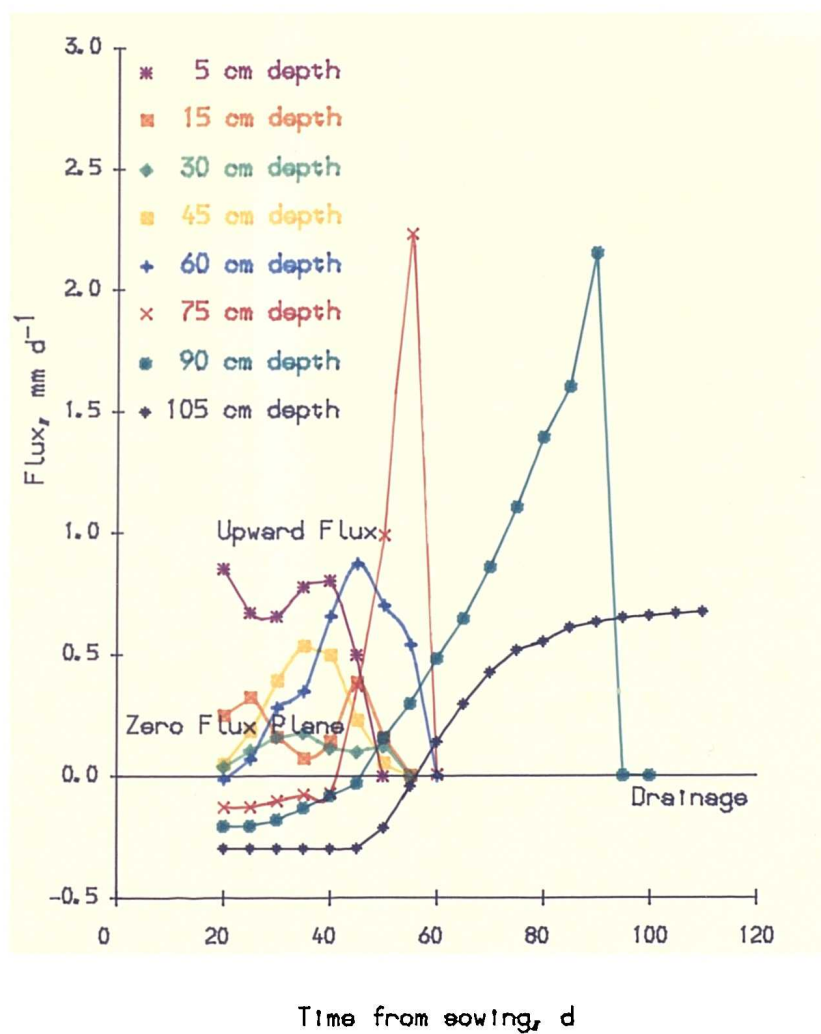


Fig. 6.16. (c) Measured flux vs time for WT-120 (Barley).

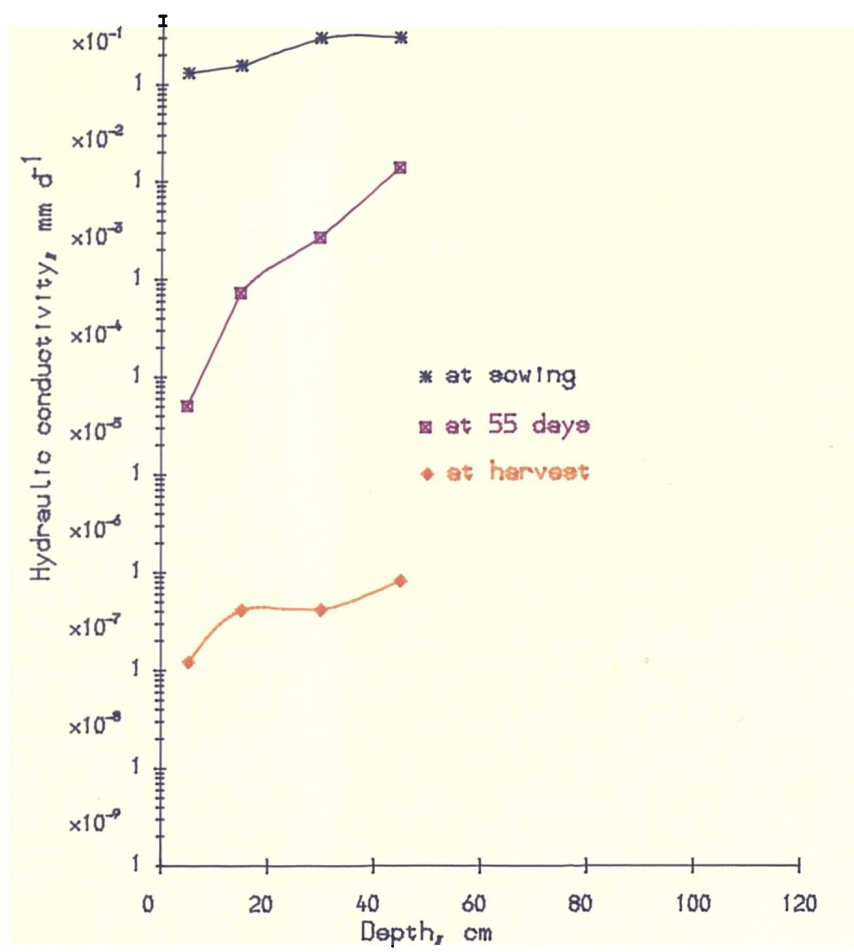


Fig. 6.17. (a) Hydraulic conductivity as a function of depth for WT-60 (Barley).

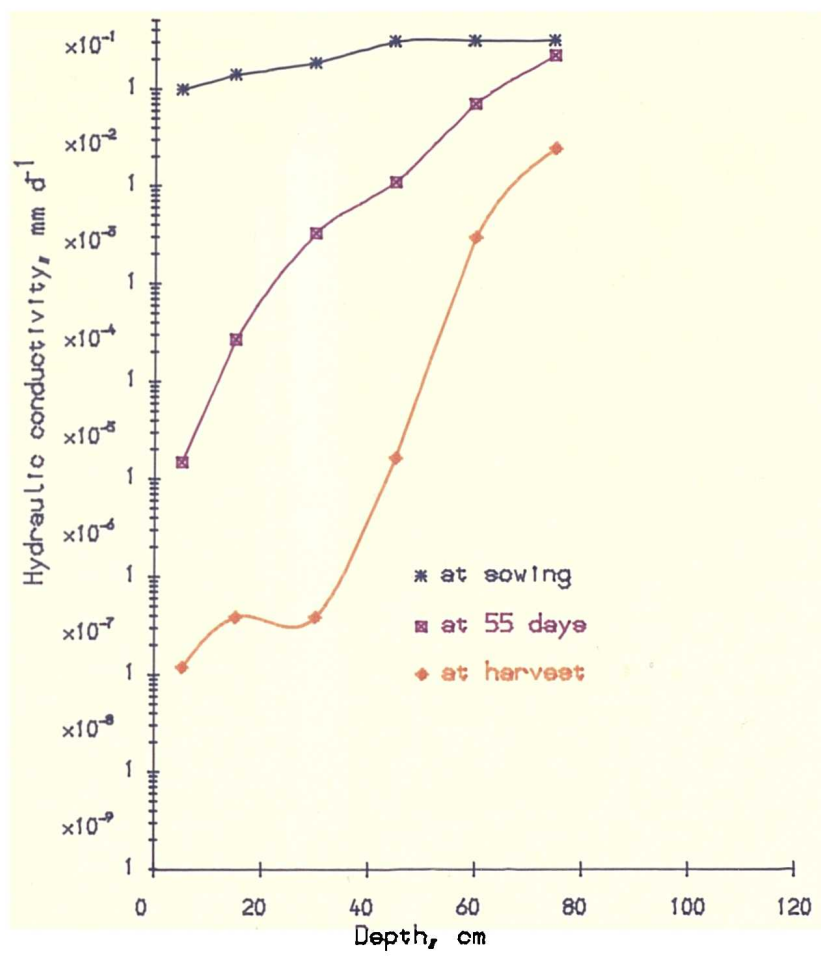


Fig. 6.17. (b) Hydraulic conductivity as a function of depth for WT-90 (Barley).

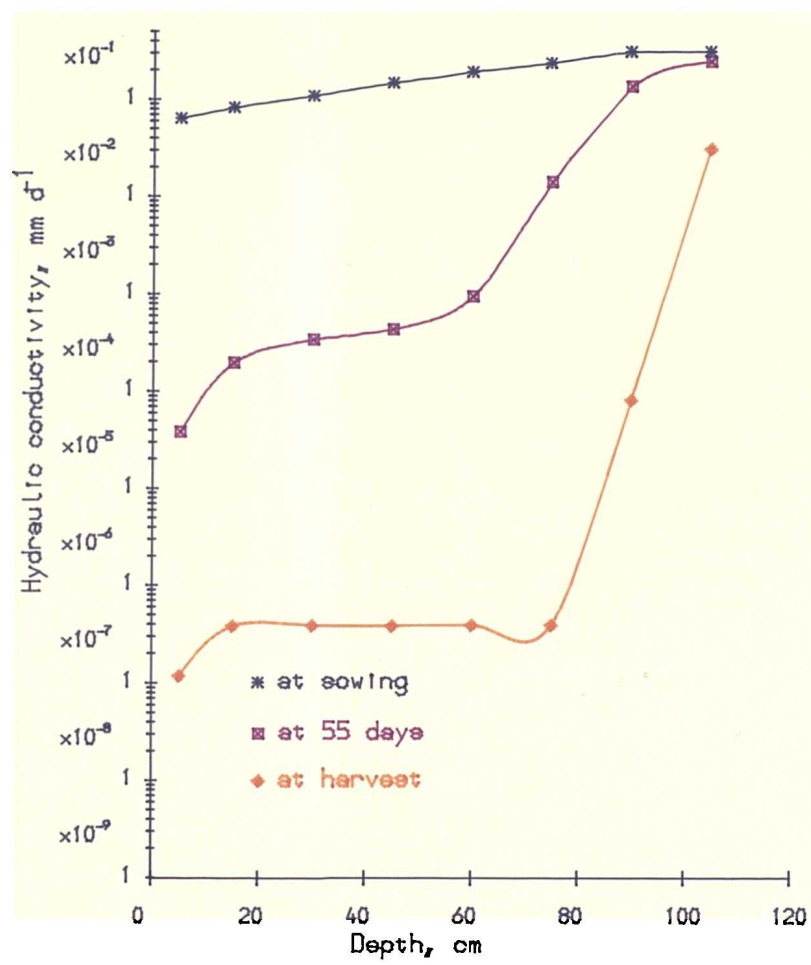


Fig. 6.17. (c) Hydraulic conductivity as a function of depth for WT-120 (Barley).

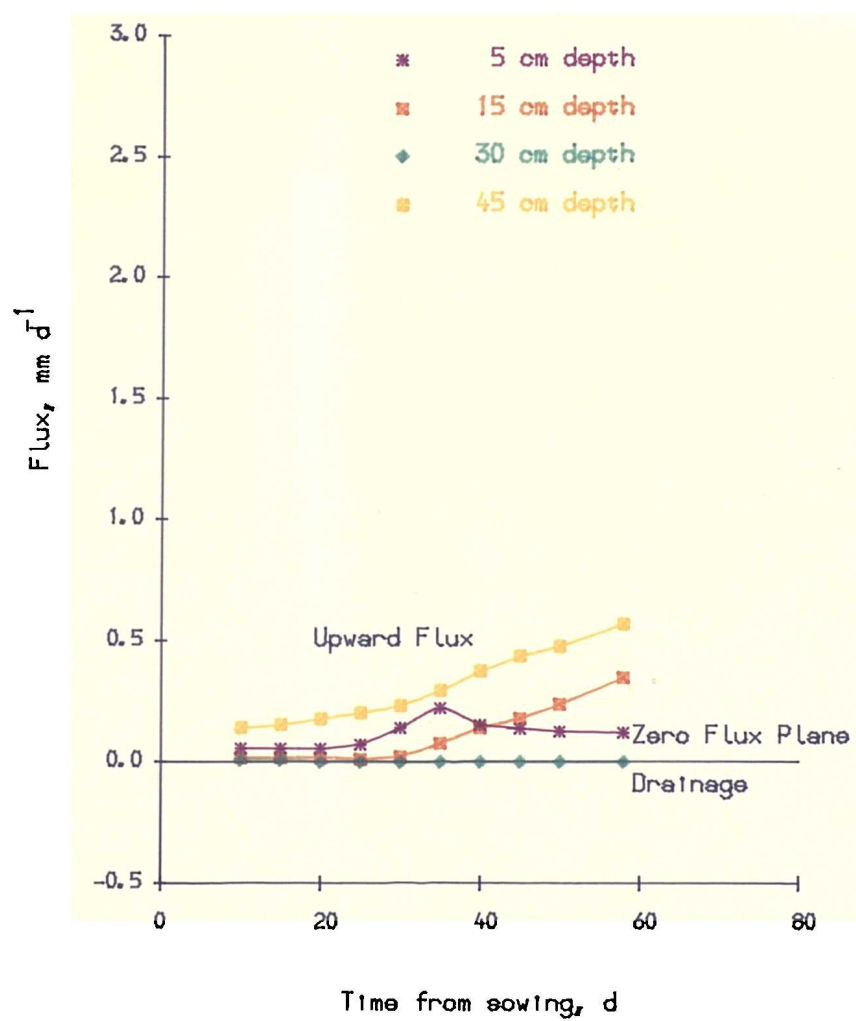


Fig. 6.18. (a) Measured flux versus time for WT-60 (Lettuce).

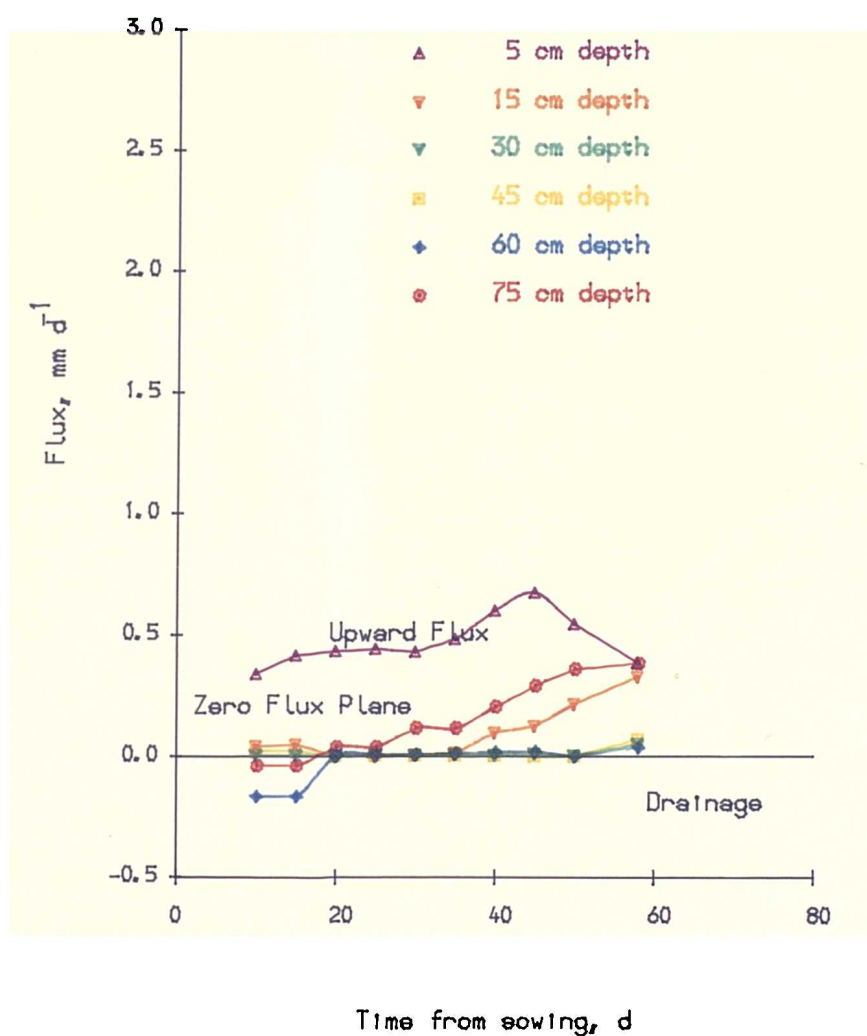


Fig. 6.18. (b) Measured flux versus time for WT-90 (Lettuce).

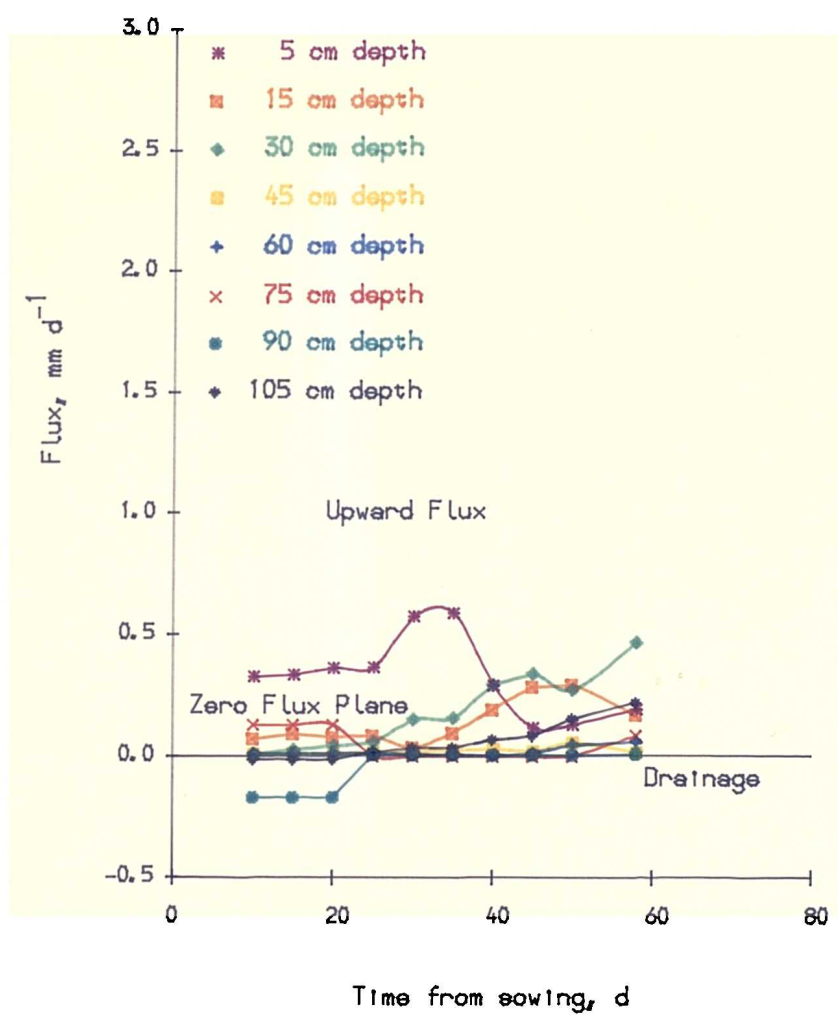


Fig. 6.18. (c) Measured flux vs time for WT-120 (Lettuce).

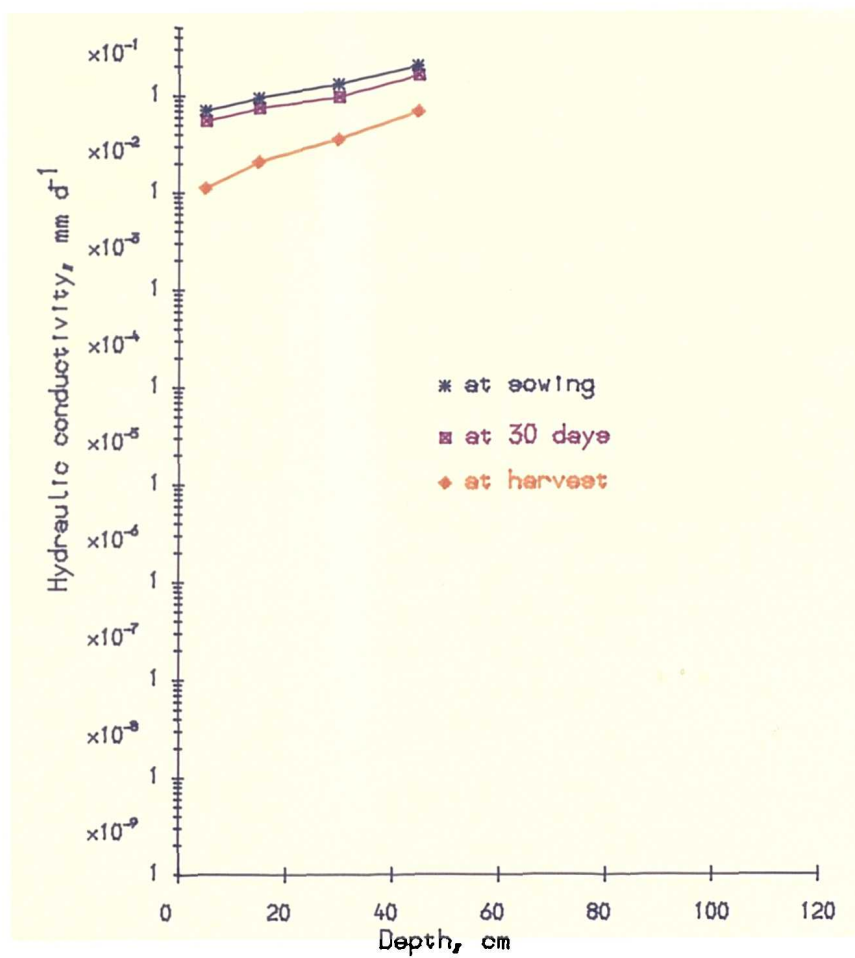


Fig. 6.19. (a) Hydraulic conductivity as a function of depth for WT-60 (Lettuce).

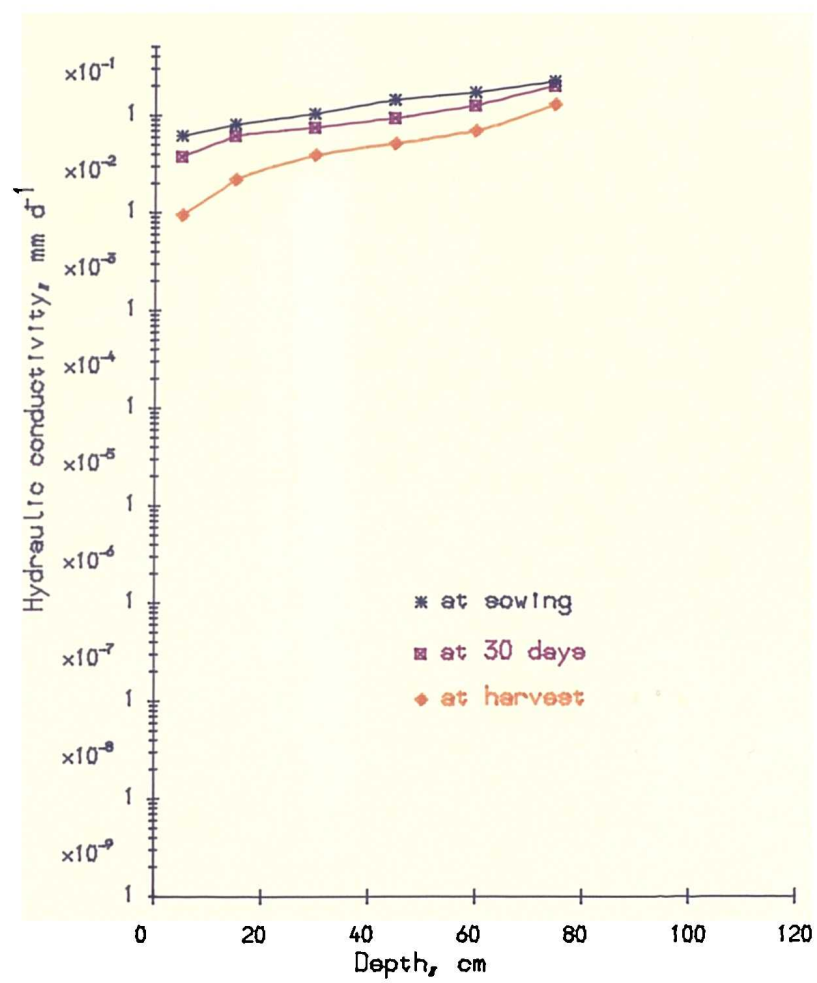


Fig. 6.19. (b) Hydraulic conductivity as a function of depth for WT-90 (Lettuce).

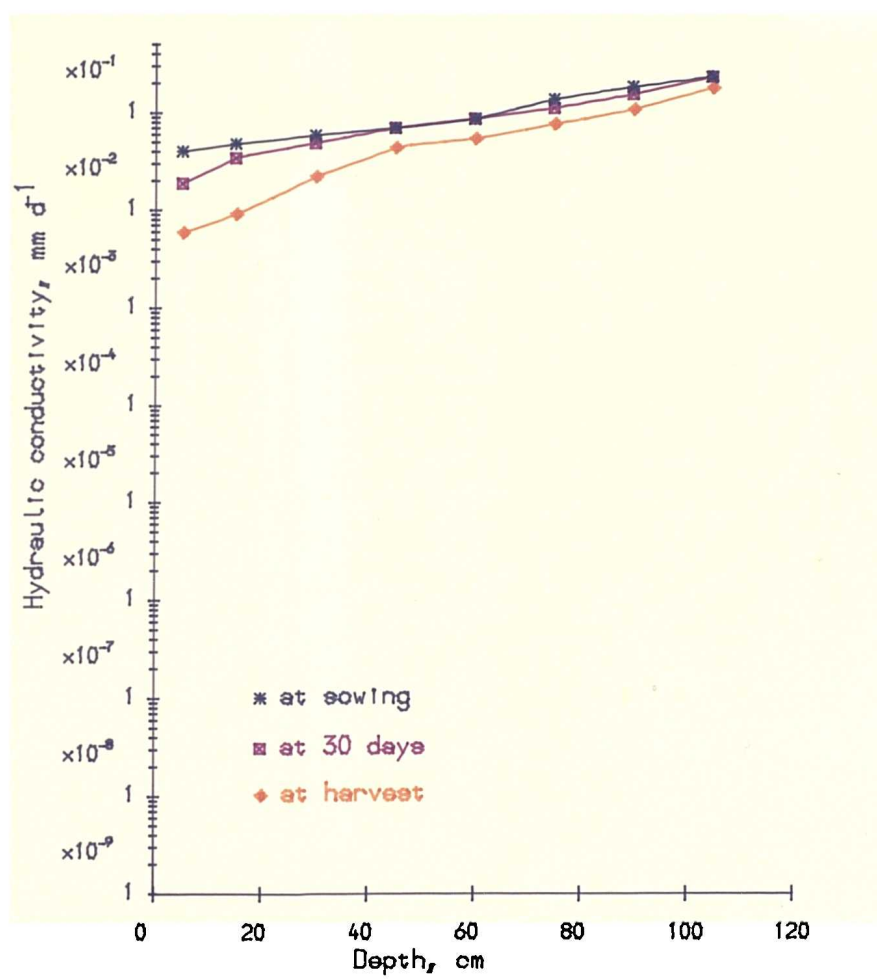


Fig. 6.19. (c) Hydraulic conductivity as a function of depth for WT-120 (Lettuce).

6.5 Capillary Rise from Water Table

There was no capillary rise in lysimeters with water tables 90 and 120 cm deep under bean. The reason was the location of the plane of zero flux. In these two lysimeters, the planes of zero flux were above the water table (Table 6.7 and Figs. 6.8b, c). Very small amounts of capillary rise occurred in the lysimeter with water table at 60 cm. Total measured amount of water contributed from the water table was 2.5 mm (Table 6.10). This is ascertained from the movement of the zero-flux plane towards water table (Fig 6.8a, and Table 6.7). Although the plane of zero-flux moved down to 45 cm depth on 80 days after sowing, an upward flux occurred on 100 days after sowing and continued until harvest.

Table 6.10 — Components of the water balance equation (mm) for different water tables after harvest of bean (1988).

Water table depth below soil surface cm	Evapo- transpiration (<i>E</i>)		Soil water depletion (ΔW)		Upward flux (<i>C</i>)	
	meas- ured	simu- lated	meas- ured	simu- lated	meas- ured	simu- lated
60	55.2	54.5	52.7	53.8	2.5	0.7
90	63.2	67.7	63.2	67.1	-	0.6
120	84.0	90.4	84.0	90.4	-	-

Capillary rise from the water table contributed to the total evapotranspiration from all water table depths in barley (Table 6.11). Capillary rise started from the day the plane of zero flux moved down to 15 cm depth above the water table (Table 6.8). Measured capillary rise from the water table in different lysimeters is shown graphically (Fig. 6.20).

Table 6.11 — Components of the water balance equation (mm) for different water tables after harvest of barley (1989).

Water table depth below soil surface cm	Evapo- transpiration (E)		Soil water depletion (ΔW)		Upward flux (C)	
	meas- ured	simu- lated	meas- ured	simu- lated	meas- ured	simu- lated
60	166.4	172.1	121.9	129.0	45.0	43.1
90	222.0	229.1	185.5	193.7	36.5	35.4
120	277.3	286.3	245.8	256.6	31.5	29.7

Capillary rise from the water table contributed to the evaporative demand of lettuce from all water table depths (Table 6.12). Capillary rise started from the day the plane of zero flux moved down to 15 cm above the water table (Fig. 6.10 and Table 6.9). Measured capillary rise from the water table in different lysimeters is shown graphically (Fig. 6.21). The capillary contribution increased slowly in the lysimeter with the water table at 60 cm. But, in the other two lysimeters, a larger capillary contribution was observed at the beginning (Fig. 6.21), which then declined. The decrease of the capillary contribution from the water table is associated with the atmospheric demand (Fig. 6.28).

Soil water does not attain equilibrium even in the absence of vegetation, since the soil surface is subjected to solar radiation and the evaporative demand of the ambient atmosphere (Hillel, 1980). If soil is of stable structure, the water table is stationary, and the atmospheric evaporativity also remains constant, then in time, a steady-state flow situation may develop from water table to atmosphere via the soil (Hillel, 1980). Initial profile water equilibrium at the beginning of experiment promotes steady-state capillary rise through evaporation from soil surface and increasing suction at shallow depth. For the same reason, although lettuce had a

Table 6.12 — Components of the water balance equation (mm) for different water table after harvest of lettuce (1990).

Water table depth below soil surface cm	Evapo- transpiration (E)		Soil water depletion (ΔW)		Upward flux (C)	
	meas- ured	simu- lated	meas- ured	simu- lated	meas- ured	simu- lated
60	47.5	47.2	31.0	32.1	16.5	15.1
90	48.0	50.3	41.5	42.4	6.5	7.9
120	50.0	51.7	47.0	48.2	3.0	3.5

very shallow rooting system (0-5 cm), the water table contributed to its evaporative demand. In practice, capillary rise from the water table is a very complex process, because of a combination of different factors. If plane of zero flux is above the water table, then there will be no capillary upward flux from the water table. For this reason, there was no capillary rise in lysimeters with the water table at 90 and 120 cm under beans. Other factors related to capillary rise are type of crop (root distribution) and atmospheric demand. If crop water demand is satisfied from the upper layers, the drying front is confined just below the rooting system of the crop. Upward flux occurred significantly in the presence of soybean roots (Arya et al., 1975). Fig. 6.20 and Fig. 6.21 suggest that capillary rise in barley and lettuce is associated with the drying of upper layers (Fig. 6.4, Fig. 6.12; Fig. 6.5, Fig. 6.13), profile equilibrium, movement of the plane of zero flux (Fig. 6.9 and Fig. 6.10), and higher evaporative demand due to gradual growth of the crop (Fig. 6.20, Fig. 6.27; Fig. 6.21, Fig. 6.28).

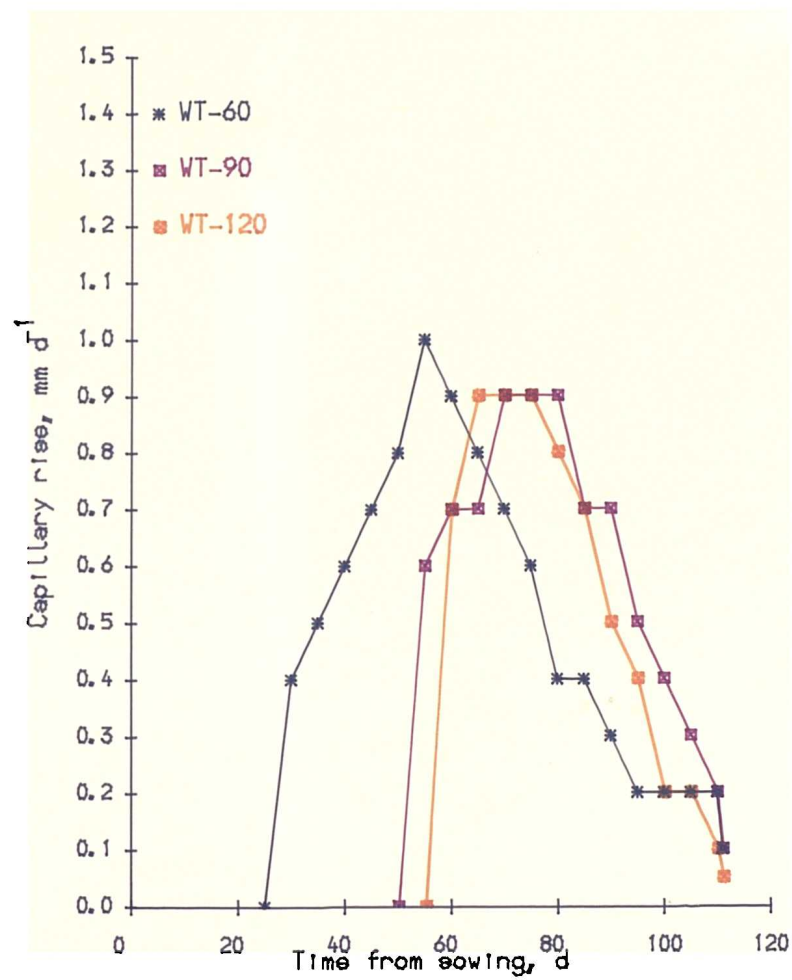


Fig. 6.20. (a) Capillary rise as a function of time (Barley).

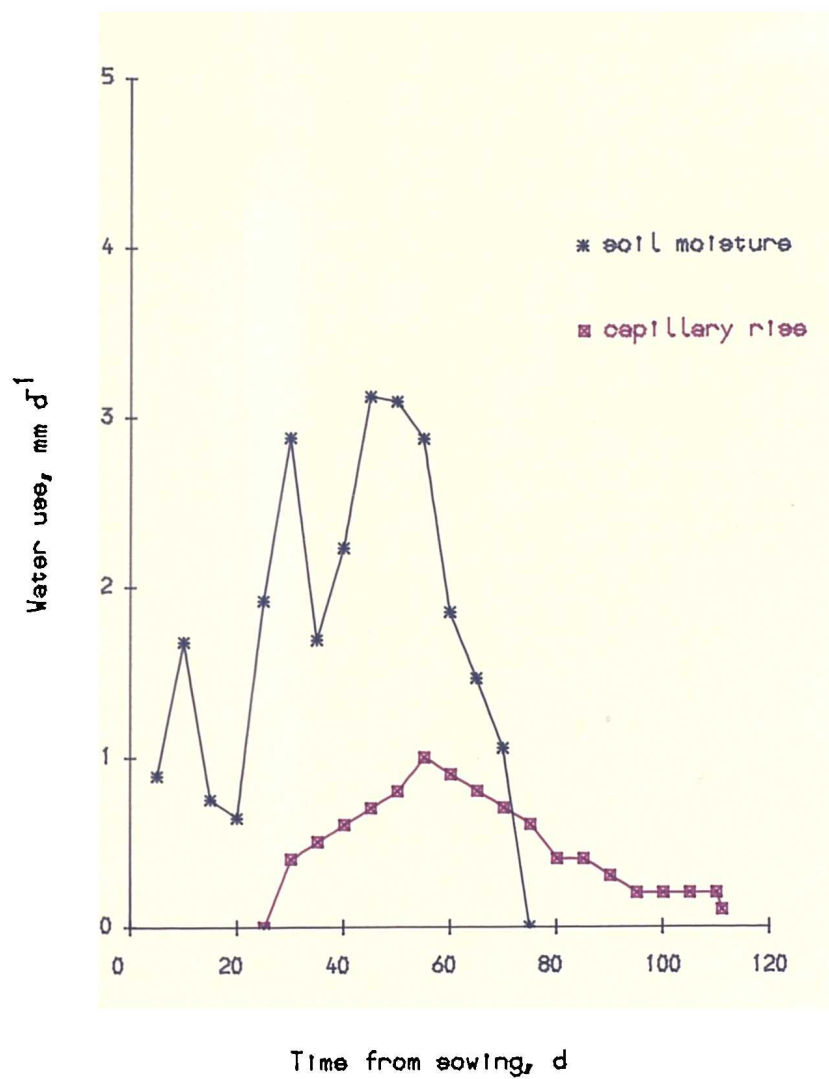


Fig. 6.20. (b) Water use from soil profile and water table against time for WT-60 (Barley).

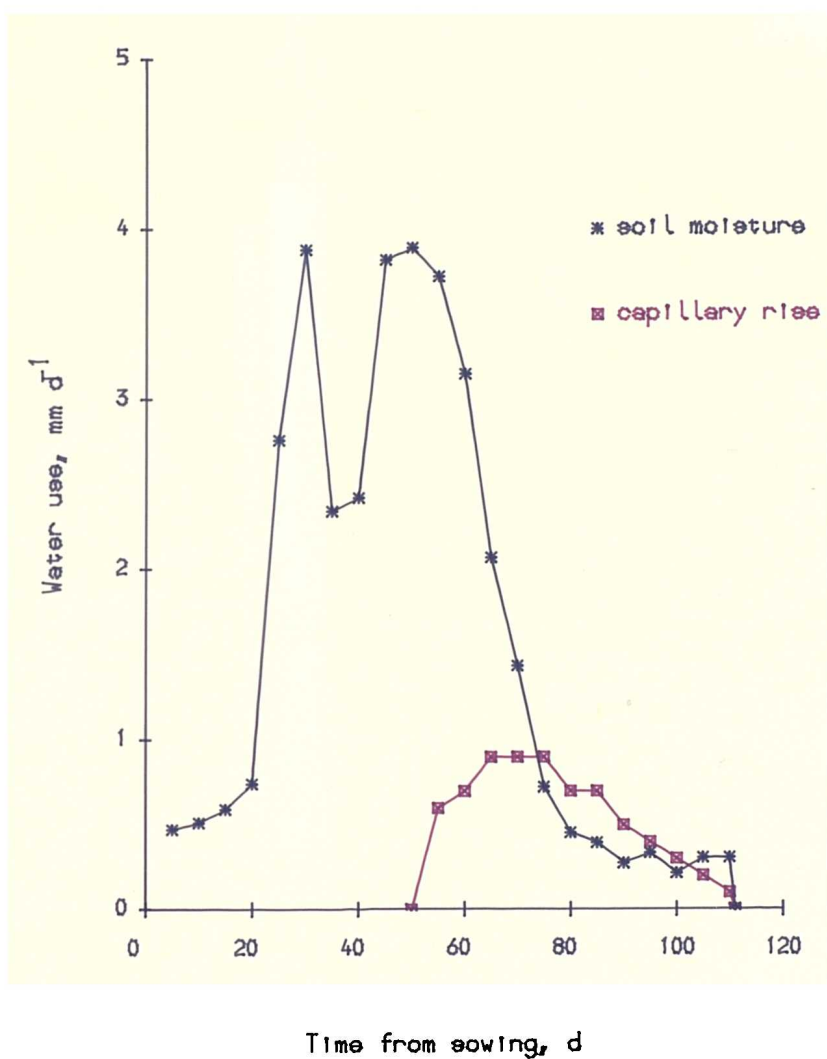


Fig. 6.20. (c) Water use from soil profile and water table against time for WT-90 (Barley).

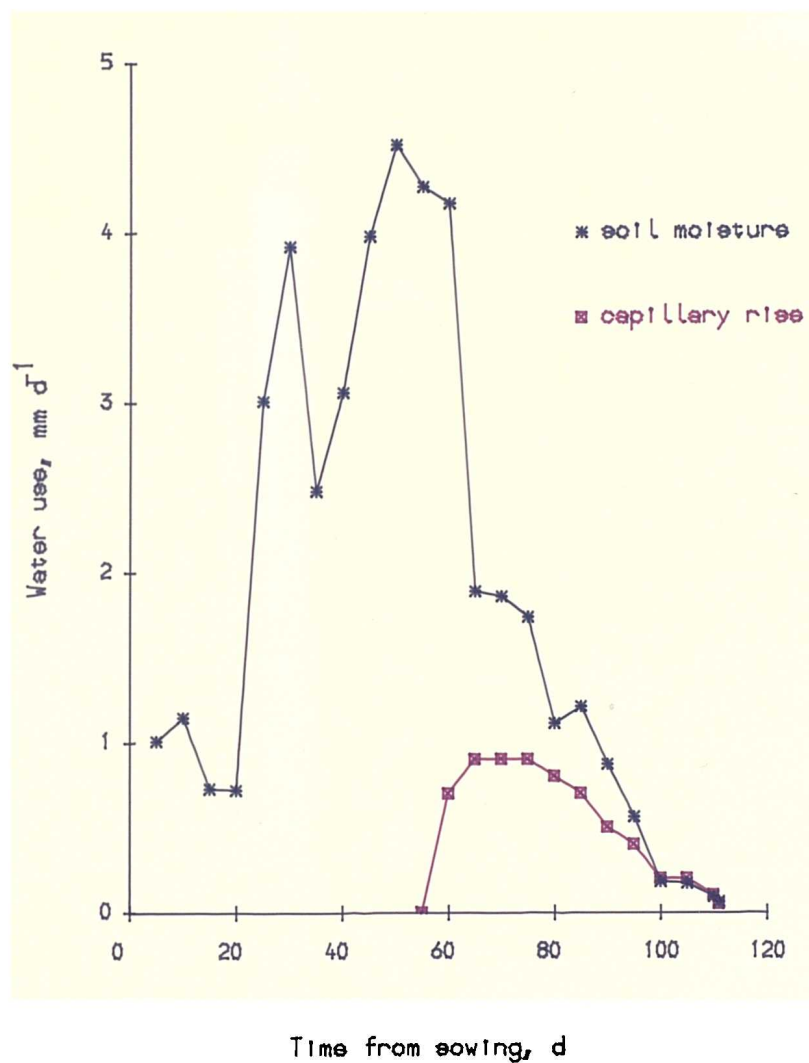


Fig. 6.20. (d) Water use from soil profile and water table against time for WT-120 (Barley).

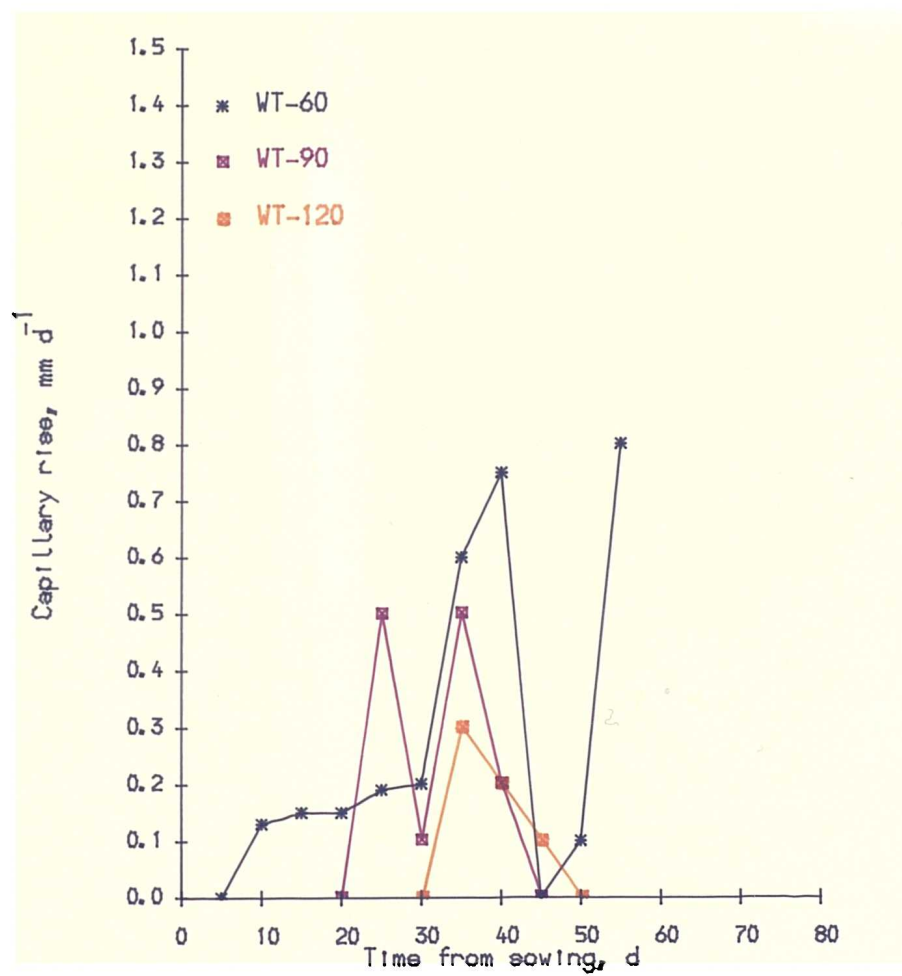


Fig. 6.21. (a) Capillary rise as a function of time (Lettuce).

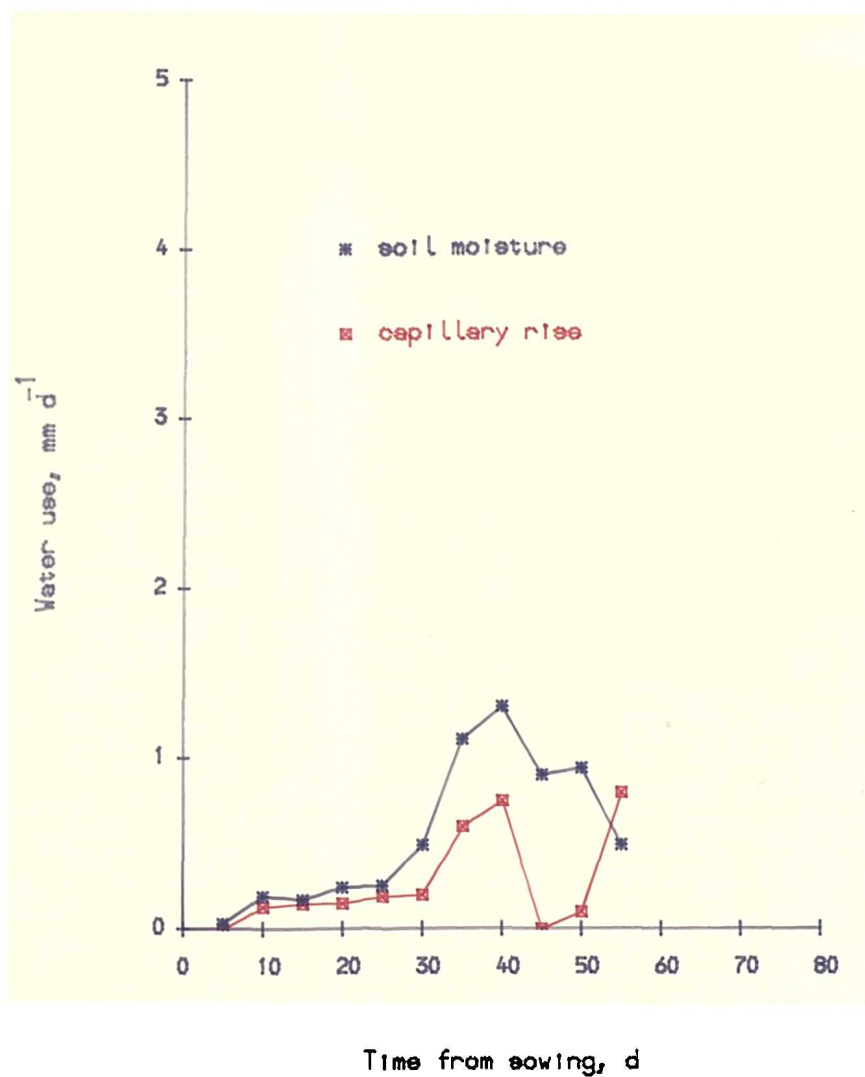


Fig. 6.21. (b) Water use from soil profile and water table against time for WT-60 (Lettuce).

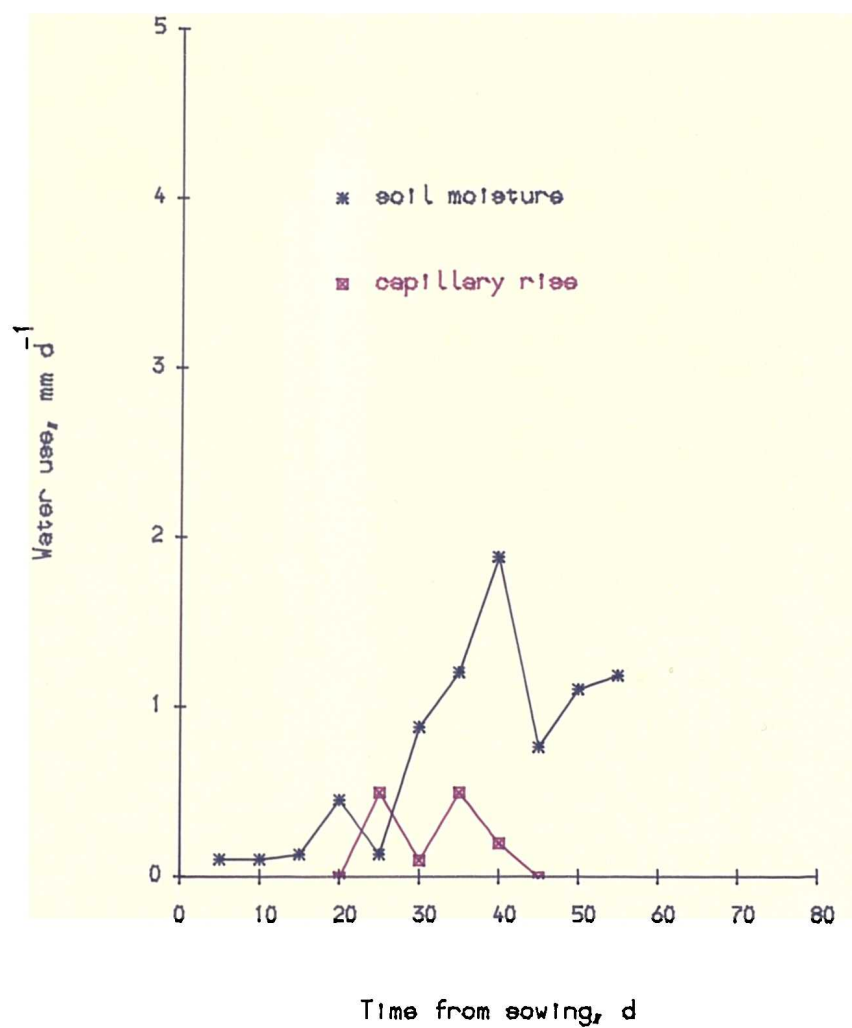


Fig. 6.21. (c) Water use from soil profile and water table against time for WT-90 (Lettuce).

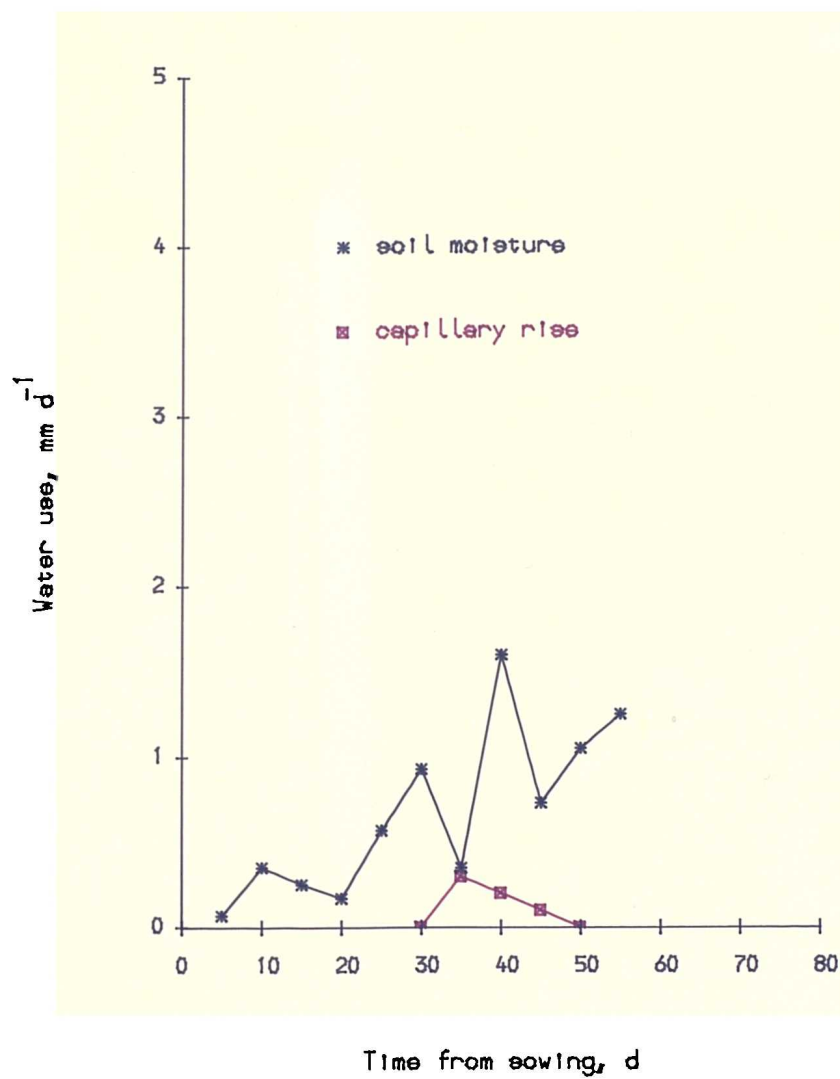


Fig. 6.21. (d) Water use from soil profile and water table against time for WT-120 (Lettuce).

6.6 Root Water Uptake

Root water uptake (sink term) was measured using Equations (3.24), (3.27), (3.28) and Figs. 6.1a, b, c. Root water uptake as a function of time at different depths is shown in Figs. 6.22a, b, c for bean, Figs. 6.23a, b, c for barley and Figs. 6.24a for lettuce. At the beginning of the growing period i.e. seedling to emergence, the sink terms were not significant. Therefore, the sink terms for bean and barley were measured from the 20th day after sowing and for lettuce from the 15th day after sowing.

In the early part of the bean experiment, the sink was confined to a 5 cm depth up to 50 days of sowing in the lysimeter with the water table at 60 cm. As time passed, the sink moved down to 15 cm depth and the maximum sink was observed at 55 days after sowing. Later in the experiment, the sink was confined up to 15 cm depth (Fig. 6.22a). The sink moved to 15 and 30 cm depths after 55 and 80 days, respectively in the lysimeter with the water table at 90 cm and declined to about zero near harvest time (Fig. 6.22b). The sink was confined to 5 cm depth in the lysimeter with the water table at 120 cm up to 40 days from sowing (Fig. 6.22c). After that, the sink started to go deeper as time passed. Lastly the sink moved down to 45 cm depth. Sink activity at 5 cm depth was almost constant throughout the experiment and tended to zero at harvest.

In the barley experiment, the sink moved down into deeper layers faster compared to beans. In all the lysimeters, maximum sink activity was found to be between 55-60 days after sowing. Sink activity was exhausted at all depths (Fig. 6.23a) within 65 days in the lysimeter with water table at 60 cm. After that, the sink at 45 cm depth was dependent on capillary rise from the water table (Fig. 6.20). Capillary rise was almost constant from the 80th day to harvest. A similar trend was observed in the lysimeter with the water table at 90 cm (Fig. 23b). The period of maximum sink activity in the lysimeter with the water table at 120 cm was the same as the other two (Fig. 6.23c).

The sink term in the lettuce was confined to the top layer (0-5 cm). The sink did not go deeper (Fig. 6.24) because the roots only penetrated to 5 cm.

These results indicate that in the later part of the experiment maximum water

absorption was occurring in the capillary fringe just above the water table, especially in barley. The maximum sink value increased with time, and tended to increase in depth with time. A similar result also reported by Reicosky et al. (1972). Changes in the suction patterns with the crop growth reflect changing distribution of roots in the soil profile (Fig. 6.3 and Fig. 6.5). Water use patterns also explained the phenomenon (Figs. 6.20 b, c, d; Figs. 6.21 b, c, d). These changes have affected water losses from the different soil layers. It is to be noted that the total uptake for the profile is given by the sum of the uptake from individual layers. Water losses from all depths are most strongly influenced by the age of the plants (Arya et al., 1975). Water uptake was initially confined to surface layers. When the upper layers get dry, the root system penetrates deeper into the soil in search of water. So the zone of maximum root activity moves downward and water uptake from the upper layers becomes less important. This has also been reported by several authors (Taylor and Klepper, 1971; Allmaras et al., 1975; Gregory et al., 1978; Gregory, 1988).

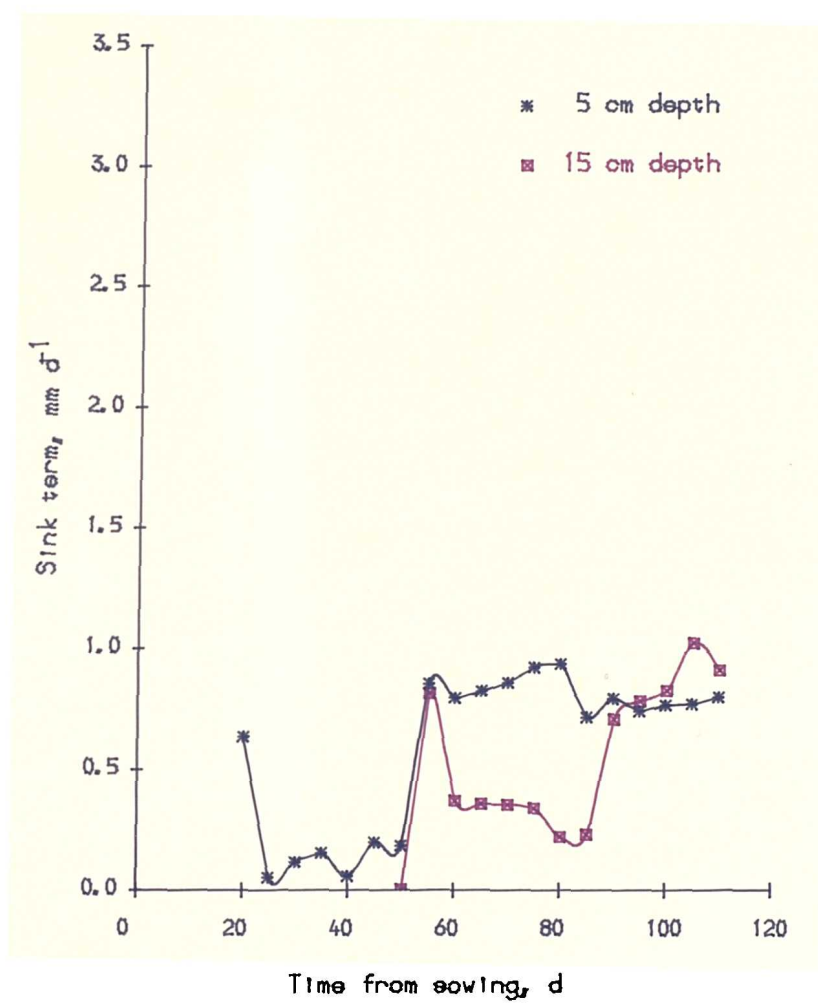


Fig. 6.22. (a) Measured sink term versus time for WT-60 (Bean).

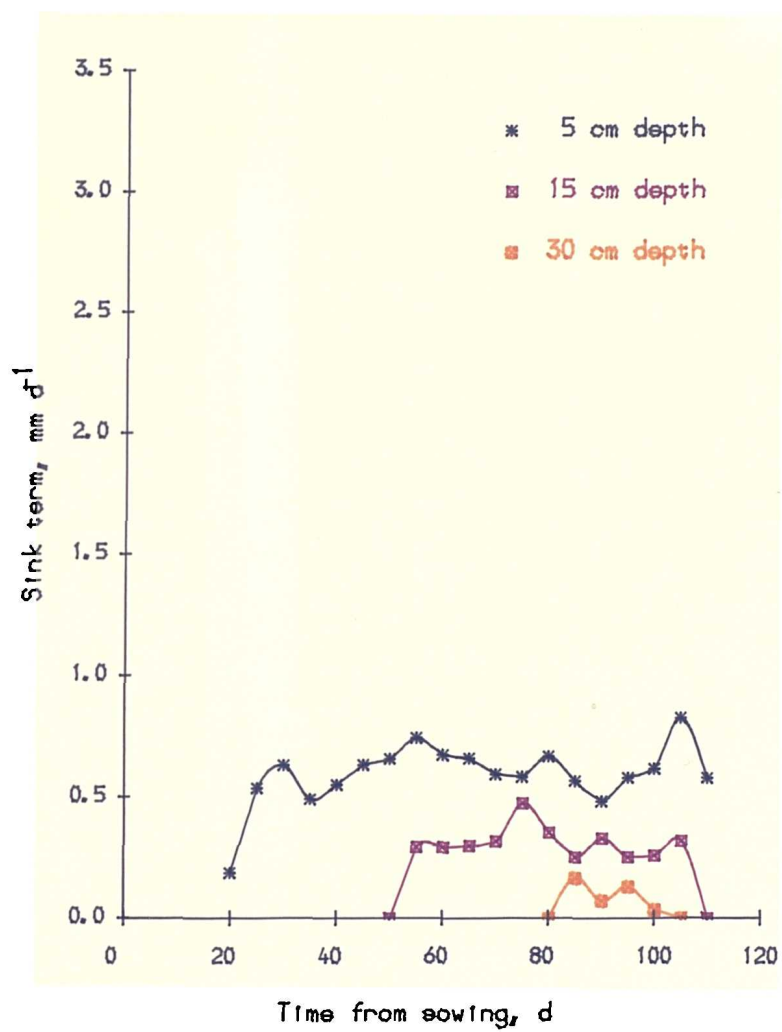


Fig. 6.22. (b) Measured sink term versus time for WT-90 (Bean).

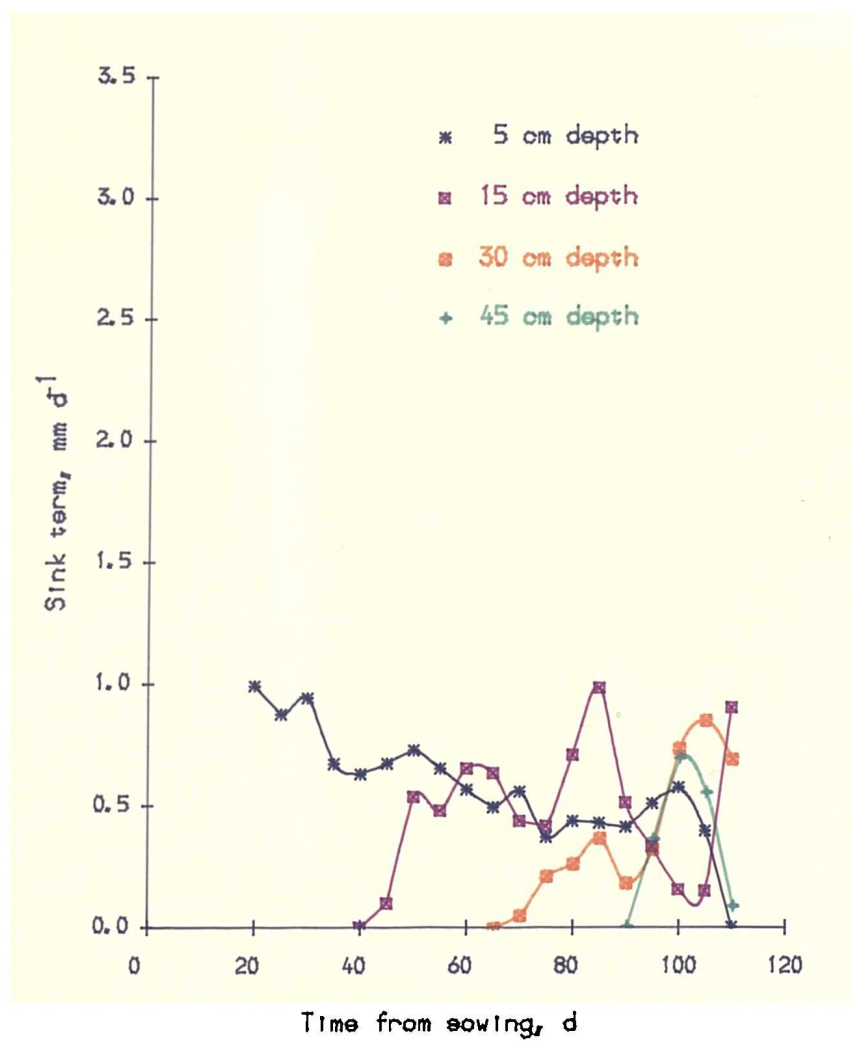


Fig. 6.22. (c) Measured sink term versus time for WT-120 (Bean).

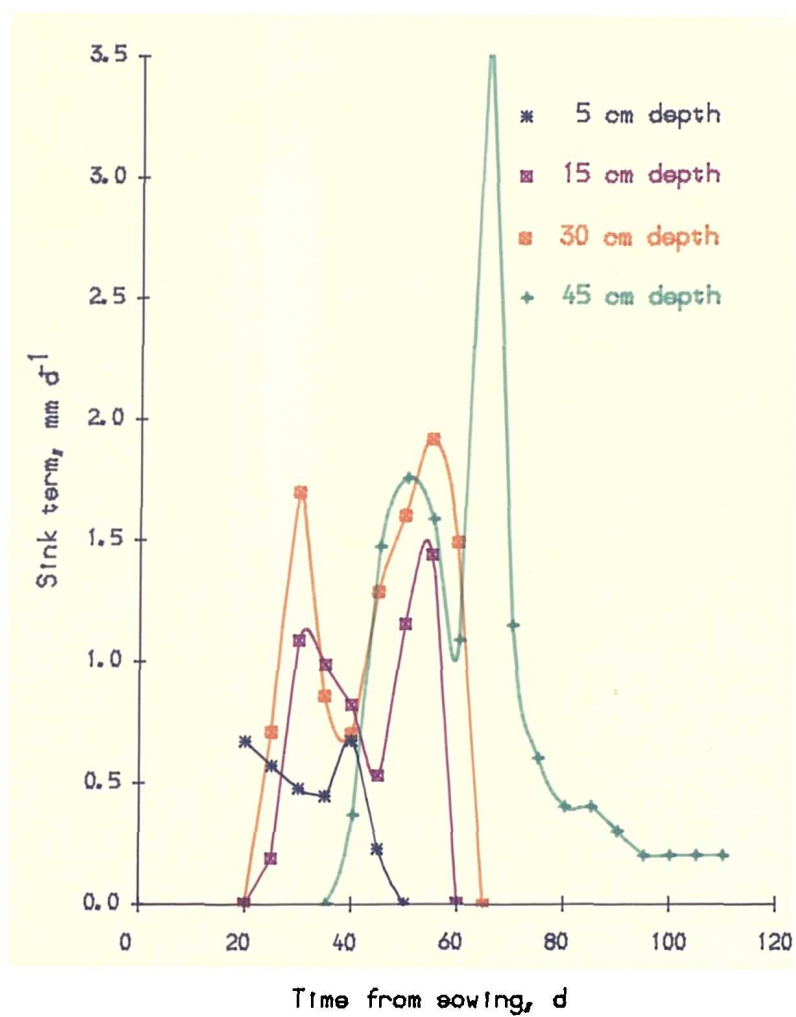


Fig. 6.23. (a) Measured sink term versus time for WT-60 (Barley).

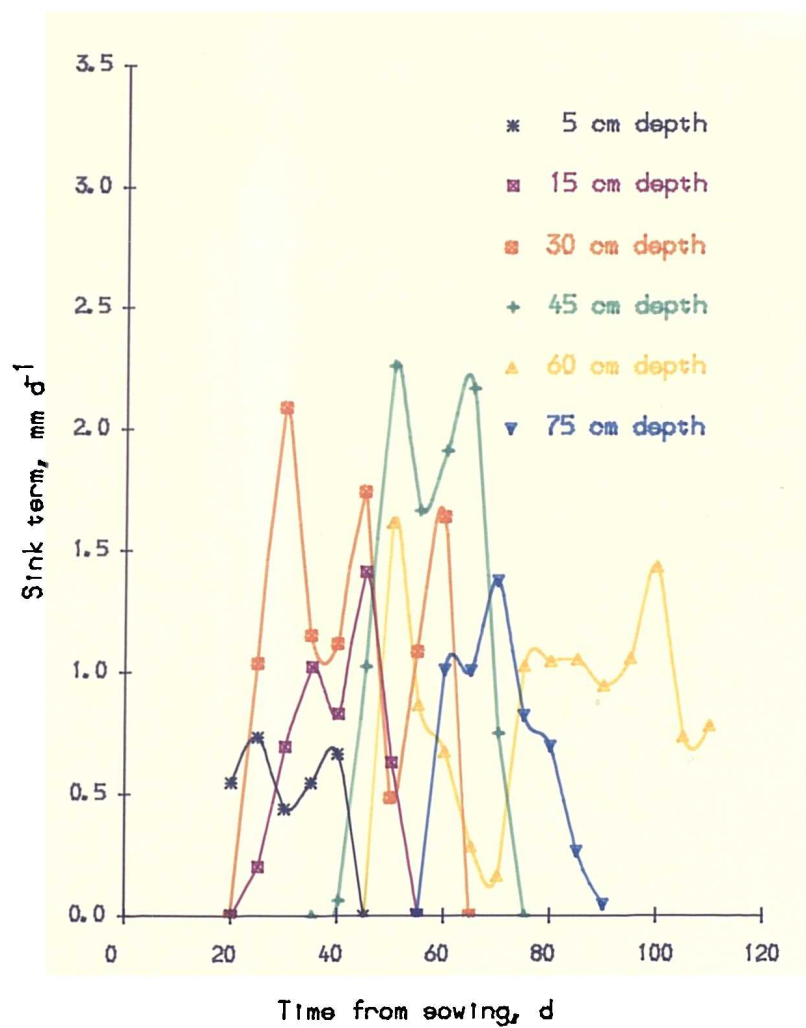


Fig. 6.23. (b) Measured sink term versus time for WT-90 (Barley).

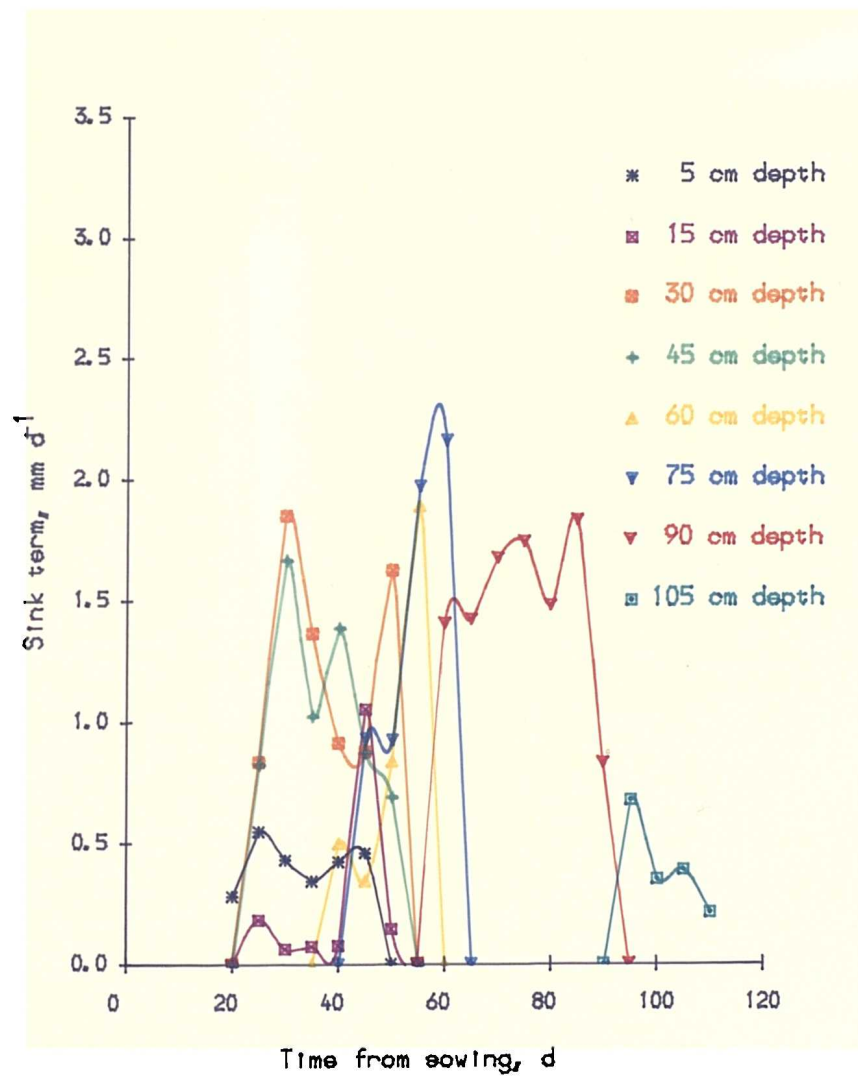


Fig. 6.23. (c) Measured sink term versus time for WT-120 (Barley).

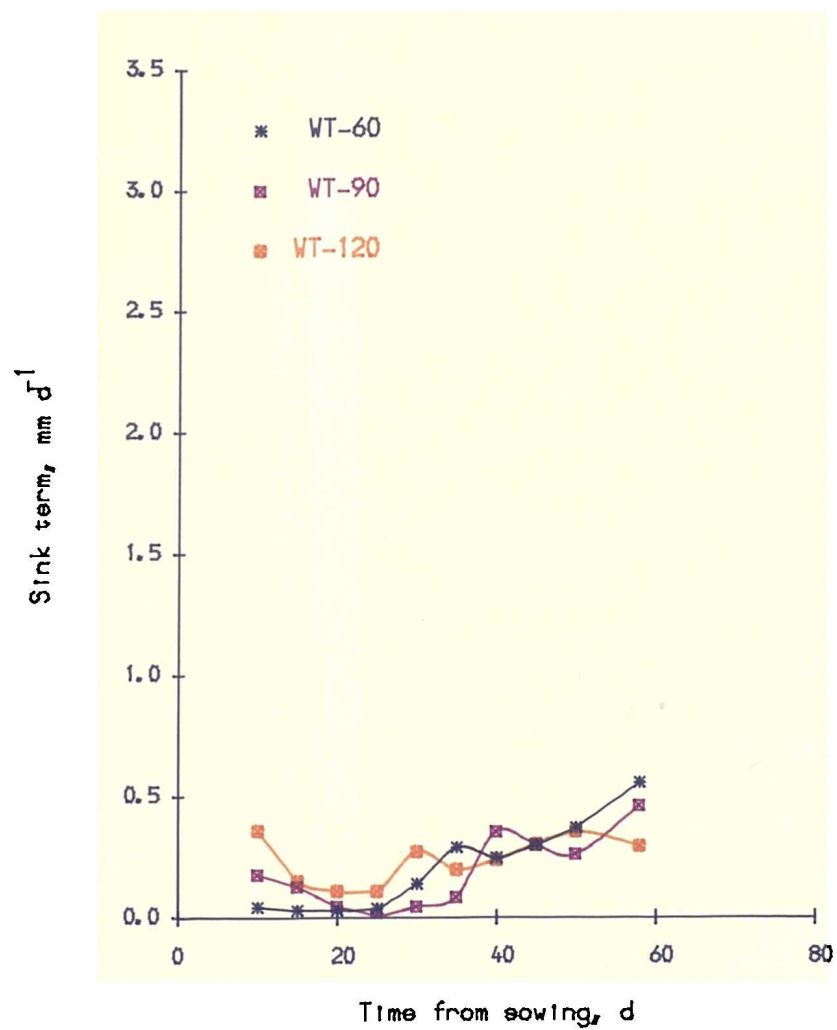


Fig. 6.24. Measured sink term versus time for lettuce at 5 cm depth.

6.6.1 Sink Term and Suction

The variation in the sink term with suction at 5 cm depth is shown for beans (Fig. 6.25a), barley (Fig. 6.25b) and lettuce (Fig. 6.25c). The general shape of the sink term as a function of suction, hypothesized by Feddes and Zaradny (1978), is shown in Fig. 6.25d. Feddes and Zaradny (1978) used this as an input to their model.

It is assumed that under conditions wetter than at anaerobiosis point (ψ_1) and drier than wilting point (ψ_3), the sink term is zero. Suction at anaerobiosis is found in the range of 55-100 cm of water for three different crops. After elapse of time, the sink term is limited by the soil moisture suction, referred as the limiting point (ψ_2).

The suction (ψ_2) at which soil moisture begins to limit the plant growth is difficult to define but found in the range 3500-5000 cm of water for bean and barley. Feddes et al. (1978) have taken a constant limiting value (1000 cm of water) in their model of water uptake by roots. The value of ψ_2 in fact is not a constant but it varies with demand of the type of crop and atmosphere. Under conditions of high evaporative demand, a drop in the root water uptake generally occurs at lower ψ values than under conditions of low demand (Yang and de Jong, 1972).

At the beginning of the growing period, the sink terms were not significant (as mentioned in section 6.6). Ritchie (1972) mentioned that at the early stage of crop growth, the evaporation rate from the entire field surface is dominated by the soil evaporation rate. These explain the similarities of general hypothesis of Feddes and Zaradny, 1978 (Fig. 6.25d) at the beginning of growing period. But as the plant cover increases, the sink term dominates. But it is observed that the sink term does not attain suddenly the maximum value at the anaerobiosis point (ψ_1) and is not constant up to the limiting point (ψ_2) as in the hypothesis (Fig. 6.25d). The changes of the sink term between anaerobiosis (ψ_1) and limiting point (ψ_2) are not linear (Fig. 6.25a, b, c) with the increase of suction. The sink term fluctuated, depending on the demand of the plant and atmosphere. This does not agree with the general shape of the sink term hypothesis by Feddes and Zaradny (1978).

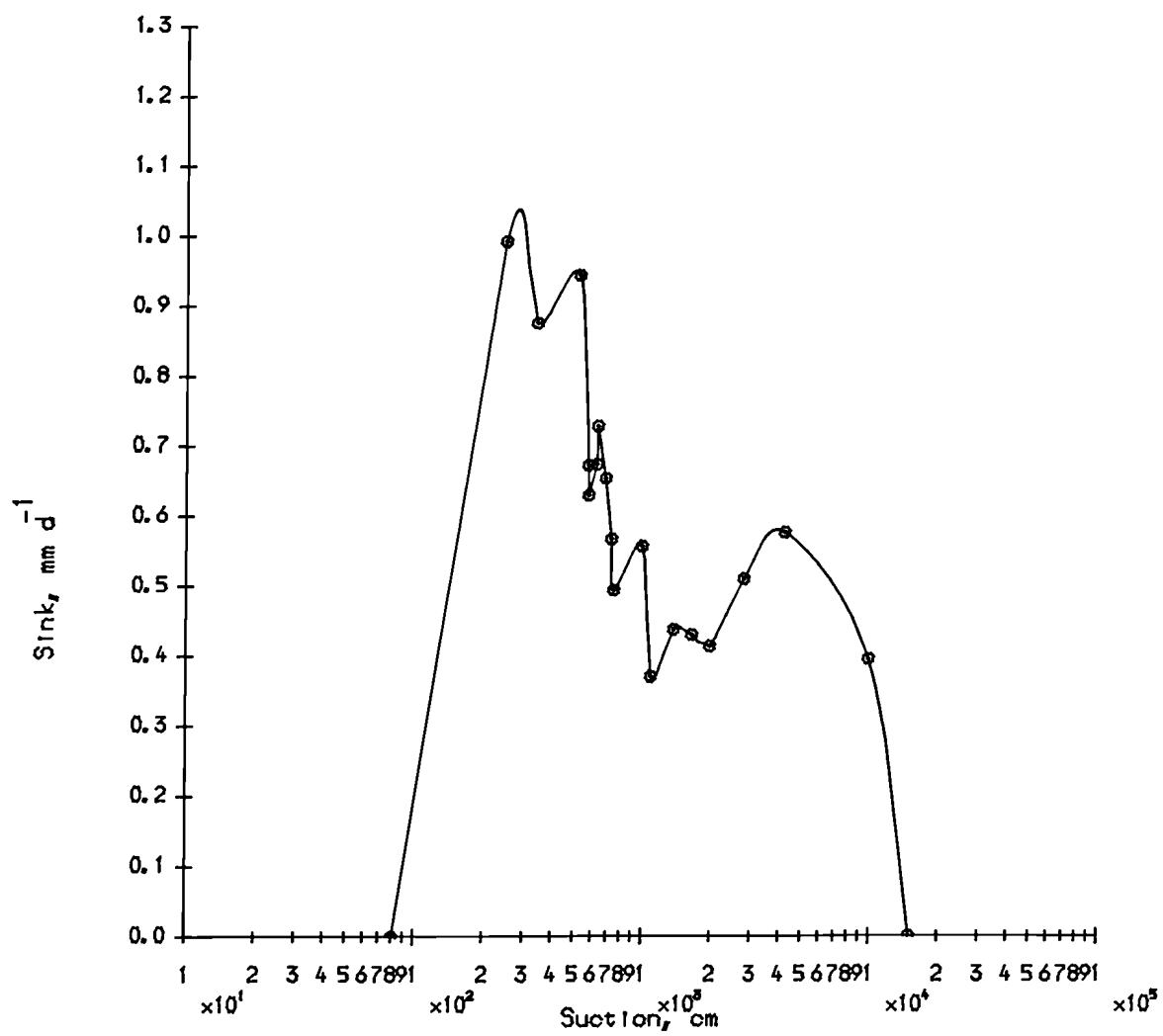


Fig. 6.25. (a) Sink term as a function of suction (Bean).

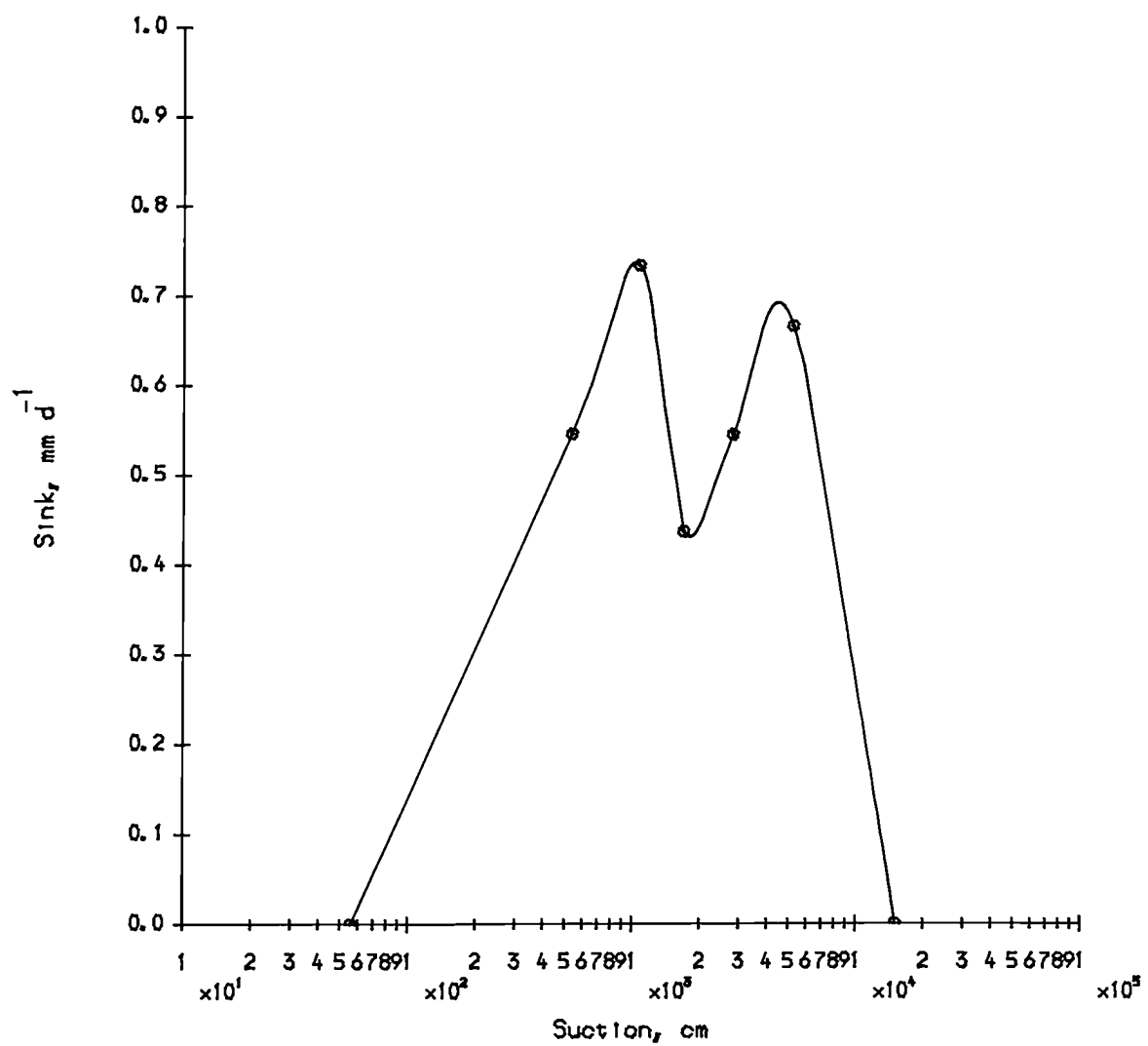


Fig. 6.25. (b) Sink term as a function of suction (Barley).

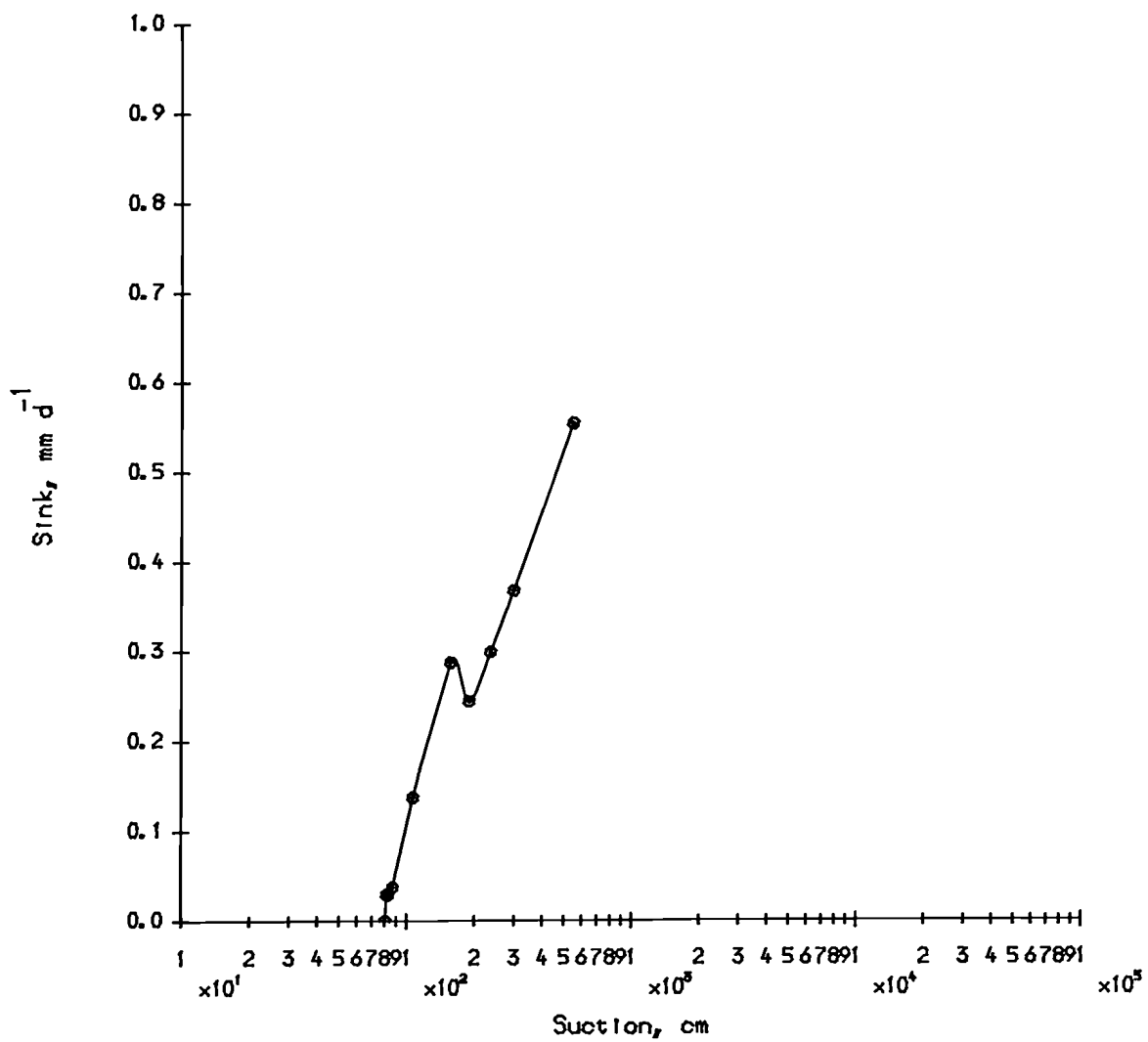


Fig. 6.25. (c) Sink term as a function of suction (Lettuce).

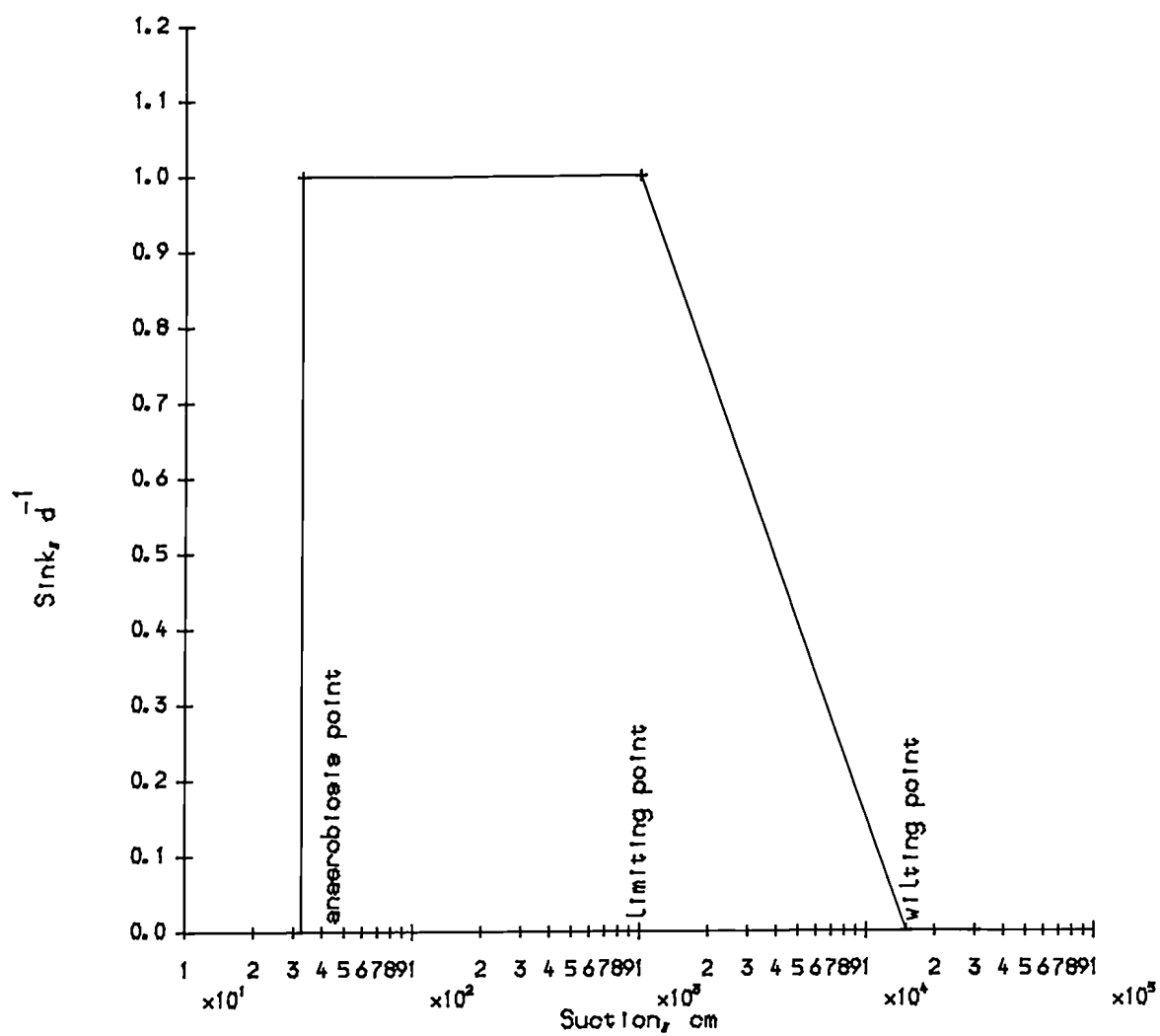


Fig. 6.25. (d) Sink term hypothesis as a function of suction (after Feddes and Zaradny, 1978).

6.6.2 Inflow Rate to Roots

Because of difficulties in measuring root distribution (non destructive) during the experiments, water uptake by plant roots was evaluated using the sink term in the continuity equation. Drying front advance has given an indication of effective rooting depth (McGowan, 1973). Matric suctions (Fig. 6.3 to Fig 6.4) and water table contributions (Fig. 6.20) have indicated downward root development. The results suggest that the root grew downward faster than water could move up through the soil. Once the roots reached the capillary fringe, they were able to extract water to supply the tops with all the water used. Root length density, measured at the end of each experiment, is shown in Table 6.13 (beans), Table 6.14 (barley) and Table 6.15 (lettuce). Root distribution in barley as a function of depth was more uniform compared to beans. Root length density in lettuce was almost the same in the different water table treatments.

Fig. 6.24 indicates that root water extraction in lettuce occurred only in the top layer. Lettuce being shallow-rooted, the water table contributed (Fig. 6.21) to crop water use by transmitting water through the soil between the water table and the root zone. Initial profile moisture equilibrium and plane of zero flux 15 cm above the water table played an important role for capillary rise from the water table. A small potential gradient development with higher hydraulic conductivity of the profile promoted capillary fringe activity from the water table to 5.0 cm depth below the soil surface. Thus the capillary rise from the water table contributed to the evaporative demand of the crop by replenishing the soil moisture store so that there was a gradual change in the soil moisture profile, not a steep drying front as in barley (Figs. 6.12a, b, c).

Table 6.13 — Root length density (R_l) and inflow to roots (I_r) in each lysimeter for bean (Mean \pm s.d.,n=3).

Depth cm	Depth to water table from soil surface					
	60 cm		90 cm		120 cm	
	(R_l^*)	(I_r^\dagger)	(R_l^*)	(I_r^\dagger)	(R_l^*)	(I_r^\dagger)
0-15	2.01 ± 0.88	0.19	1.32 ± 0.34	0.30	1.56 ± 0.48	0.26
15-30	0.07 ± 0.06	6.26	0.07 ± 0.008	2.75	0.17 ± 0.08	1.97
30-45	-		0.04 ± 0.009	1.70	0.42 ± 0.22	0.54
45-60	-		0.01 ± 0.001		0.15 ± 0.04	1.88
60-75			-		-	
75-90			-		-	
90-105					-	
105-120					-	

With the measured root length density and computed sink term, inflow rate to the roots was calculated as a function of depth. A very small proportion of roots at the tip was absorbing maximum water in case of bean (Table 6.13) above zero flux plane. The average inflow rate to roots were 3.23×10^{-2} , 1.58×10^{-2} and $1.16 \times 10^{-2} \text{ cm}^3(\text{water}) \text{ cm}^{-1}(\text{root}) \text{ d}^{-1}$ in lysimeters with water tables 60, 90 and 120 cm deep, respectively.

* $\text{cm}(\text{root})\text{cm}^{-3}(\text{soil})$.

† $10^2 \text{ cm}^3(\text{water}) \text{ cm}^{-1}(\text{root})\text{d}^{-1}$.

Table 6.14 — Root length density (R_l) and inflow to roots (I_r) in each lysimeter for barley (Mean \pm s.d., n=3).

Depth	Depth to water		table		from soil		surface
	60		90		120		
cm	cm		cm		cm		
	(R_l^*)	(I_r^\dagger)	(R_l^*)	(I_r^\dagger)	(R_l^*)	(I_r^\dagger)	
0-15	1.90 \pm 0.024	0.15	3.11 \pm 0.067	0.13	2.40 \pm 0.048	0.11	
15-30	0.56 \pm 0.012	1.01	0.70 \pm 0.014	0.68	0.91 \pm 0.033	0.26	
30-45	0.51 \pm 0.016	1.60	0.41 \pm 0.043	1.90	0.38 \pm 0.017	1.99	
45-60	0.36 \pm 0.025	1.67	0.32 \pm 0.037	2.23	0.26 \pm 0.017	3.63	
60-75			0.30 \pm 0.024	2.0	0.24 \pm 0.012	4.25	
75-90			0.26 \pm 0.016	1.92	0.18 \pm 0.008	5.86	
90-105					0.16 \pm 0.012	5.17	
105-120					0.11 \pm 0.008	2.46	

* $cm(root)cm^{-3}(soil)$.

† $10^2 cm^3(water)cm^{-1}(root)d^{-1}$.

Table 6.15 — Root length density (R_l) and inflow to roots (I_r) in each lysimeter for lettuce (Mean \pm s.d., n=3).

Depth	Depth	to water	table	from	soil	surface
	60		90		120	
	cm		cm		cm	
cm	(R_l^*)	(I_r^\dagger)	(R_l^*)	(I_r^\dagger)	(R_l^*)	(I_r^\dagger)
0- 5	0.31 \pm 0.005	10.65	0.32 \pm 0.006	8.37	0.34 \pm 11.07	0.11

In barley, 10.8, 5.1 and 2.4% of roots were absorbing water from capillary fringe in lysimeters with water tables 60, 90 and 120 cm deep, respectively. Inflow rate to roots are given in Table 6.14. The average inflow rate to roots were 1.1×10^{-2} , 1.5×10^{-2} and $3.0 \times 10^{-2} \text{ cm}^3(\text{water}) \text{ cm}^{-1}(\text{root}) \text{ d}^{-1}$ in lysimeters with water tables 60, 90 and 120 cm deep, respectively.

Inflow rates to roots were 0.107, 0.084 and 0.111 $\text{cm}^3(\text{water})\text{cm}^{-1}(\text{root})\text{d}^{-1}$ in lysimeters with water tables 60, 90 and 120 cm deep, respectively in lettuce (Table 6.15).

Values from 10^{-1} to $10^{-3} \text{ cm}^3(\text{water}) \text{ cm}^{-1}(\text{root}) \text{ d}^{-1}$ are common in many studies (Gregory, 1988).

* $\text{cm}(\text{root})\text{cm}^{-3}(\text{soil})$.

† $10^2 \text{ cm}^3(\text{water})\text{cm}^{-1}(\text{root})\text{d}^{-1}$.

6.7 Water Table Contribution, Yield and Water Use of Crops

Individual components which govern the net soil water change (ΔW) over a certain time interval are given by the water balance equation:

$$\Delta W = P - E + L - R + C - D \quad (6.3)$$

where

P = precipitation,

E = actual evapotranspiration,

L = lateral inflow,

R = lateral outflow,

C = capillary rise from water table, and

D = deep percolation.

With no irrigation and controlled conditions of the lysimeters in a glasshouse,

$$E = -\Delta W + C \quad (6.4)$$

As mentioned before (section 6.5), when the zero-flux plane was above the water table, $C = 0$, so that $E = -\Delta W$. When the water table contributed to crop evapotranspiration, Equation (6.4) was applied.

A summary of different water table effects is presented in Table 6.16, Table 6.17 and Table 6.18 for bean, barley and lettuce, respectively. A statistical analysis was not possible because of only one replication for each water table treatment.

Fresh bean yield, top fresh yield, drymatter yield and water use efficiency (yield per unit quantity of water use) were found to be maximum in the lysimeter with the water table at 120 cm, possibly due to better root aeration as a result of the deep water table. It was mentioned before that the experiment could not be started with an equilibrium water profile. Plants in lysimeters with water tables at 90 and 120 cm exploited only soil water storage. But in the lysimeter with water

table at 60 cm depth, there was a very small water table contribution, only 4.5% of E (Table 6.16).

The total water use by barley (Table 6.17) was highest in the lysimeter with the water table at 120 cm. This is because of the deep profile water exploitation in addition to the water table contribution. For the same reason, the total water use in the lysimeter with the water table at 90 cm was greater than in the lysimeter with the water table at 60 cm. It is reported by several investigators (chapter2:section 2.2, 2.3) that in the presence of a water table and with irrigated conditions, the total water use is always higher with a shallow water table. Results presented here are for the water table contribution under unirrigated conditions. The water use efficiency (WUE) was highest in lysimeters with a water table at 60 and 90 cm. The water table contributed to about 27.0, 16.4 and 11.4 % of evapotranspiration of barley (Table 6.17), in lysimeters with water tables 60, 90 and 120 cm deep, respectively.

Table 6.16 — Fresh bean yield, top fresh yield, drymatter yield and proportion, water use and efficiency for different water table treatments.

Water table depth	Fresh bean yield	Top fresh yield	Dry- matter yield	Dry- matter prop- ortion	Water use effic- iency	Total water use, E (profile+ capillary)	Capillary contri- bution, \bar{C}^*	100 C/E
cm	$g\ m^{-2}$	$g\ m^{-2}$	$g\ m^{-2}$		$g\ mm^{-1}(H_2O)$	mm	mm	
60	809.2	950.7	174.2	0.183	14.7	55.2	2.5	4.5
90	640.4	653.8	126.9	0.194	10.1	63.2	-	-
120	1472.1	2709.4	442.5	0.163	16.3	90.4	-	-

In contrast top fresh yield, drymatter yield and water use efficiency in lettuce were found to be maximum in the lysimeter with a water table at 60 cm. The highest yield was obtained in that lysimeter because crop water demand was satisfied both from soil store and the shallow water table through the capillary fringe, compared to the other two lysimeters. Soil moisture suctions were lower than with water tables 90 and 120 cm deep (Fig. 6.5). Lettuce exploited more stored soil water in lysimeters with water tables 90 and 120 cm deep compared to 60 cm deep water table. Maximum water table contribution occurred in the shallow water table treatment. The water table contributed to about 34.7, 13.5 and 6.0 % of evapotranspiration (Table 6.18) in lysimeters with water tables 60, 90 and 120 cm deep, respectively.

These results confirm earlier findings (Table 2.4) but without surface water application.

* during last 13 days.

Table 6.17 — Yield of barley, top fresh yield, drymatter yield and proportion, water use and efficiency for different water table treatments.

Water table depth	Grain yield	Top fresh yield	Dry- matter yield	Dry- matter prop- ortion	Water use effic- iency	Total water use, E (profile+ capillary)	Capillary contri- bution, C	100 C/E
cm	$g\ m^{-2}$	$g\ m^{-2}$	$g\ m^{-2}$		$g\ mm^{-1}(H_2O)$	mm	mm	
60	307.1	764.9	481.6	0.629	1.8	166.4	45.0	27.0
90	401.1	821.6	583.6	0.710	1.8	222.0	36.5	16.4
120	308.2	1019.9	614.2	0.602	1.1	277.3	31.5	11.4

Table 6.18 — Fresh lettuce yield, drymatter yield and proportion, water use and efficiency for different water table treatments.

Water table depth	Fresh lettuce yield	Dry- matter yield	Dry- matter prop- ortion	Water use effic- iency	Total water use, E (profile+ capillary)	Capillary contri- bution, C	100 C/E
cm	$g\ m^{-2}$	$g\ m^{-2}$		$g\ mm^{-1}(H_2O)$	mm	mm	
60	3774	296.7	0.079	79.5	47.5	16.5	34.7
90	3129	207.3	0.066	65.2	48.0	6.5	13.5
120	2607	207.0	0.079	52.2	50.0	3.0	6.0

Measured evapotranspiration values are shown graphically as a function of

time (Figs. 6.26, 6.27 and 6.28) for bean, barley and lettuce. In bean, after establishment of the crop, evaporative demand was increasing after the elapse of time. Depending on the demand of crop and atmosphere, evapotranspiration rates were almost constant up to harvest with little variation in all lysimeters. A slightly higher evapotranspiration rate was observed in the lysimeter with a water table at 120 cm for a period of 90-113 days of sowing.

The values of evapotranspiration for the three lysimeters with barley followed a similar pattern (Fig. 6.27) i. e. they increased steadily up to the 30 days from sowing and then declined for 2 weeks. This may be due to a fall in atmospheric demand, depending on weather factors or crop environment in the glasshouse (maximum-minimum temperature record showed a fall of temperature in that period). Evapotranspiration then again increased to a peak at about mid-period from sowing and declined at the end of harvest. Peak rates were observed about the same time i. e. period between 45-65 days from sowing. Peak E values were 3.89, 4.48 and 4.87 $mm\ d^{-1}$ in lysimeters with water tables 60, 90 and 120 cm deep, respectively; the average daily E values were 1.5, 2.0 and 2.5 $mm\ d^{-1}$, respectively.

The values of evapotranspiration for the lysimeters in lettuce followed a similar pattern (Fig. 6.28) i.e. they increased steadily up to 40 days from sowing and then declined for 5 days during dull weather. This is evident from the daily free water evaporation record (Fig. 6.28). Peak rates were observed at the same time in all the lysimeters. Peak E values were 2.05, 1.08 and 1.8 $mm\ d^{-1}$ in lysimeters with water tables 60, 90 and 120 cm deep respectively; the average daily E rates were 0.83, 0.84 and 0.88 $mm\ d^{-1}$, respectively.

From Tables 6.16, 6.17, total evapotranspiration and fresh bio-mass are directly related to the water table depth under unirrigated conditions for bean and barley. But in lettuce top fresh yield is inversely related to the water table depth (Table 6.18). This higher top fresh yield above the shallow water table is due to easily available water both from the soil store and the water table.

Feddes (1968) reported the rise and fall of evapotranspiration of cabbage due to change of atmospheric demand.

It is difficult to relate yield to water table depth in bean, barley and lettuce

under no surface water application. It is not possible to calculate statistically significant differences in yield, because the treatments were not replicated.

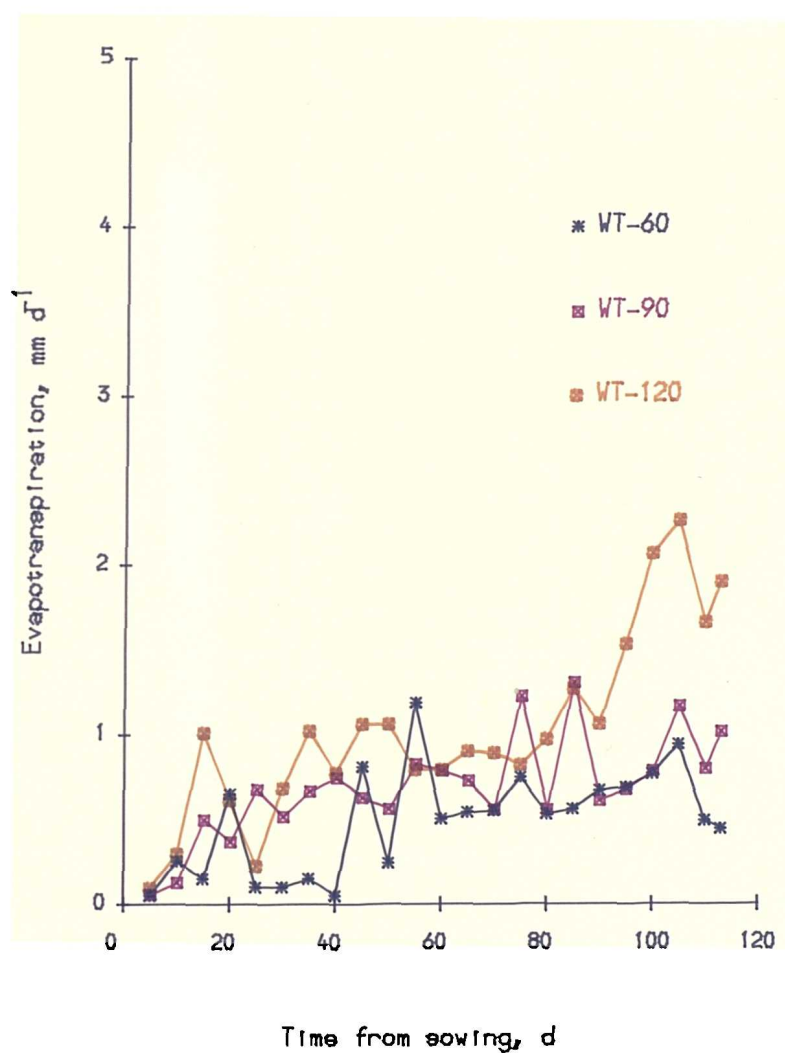
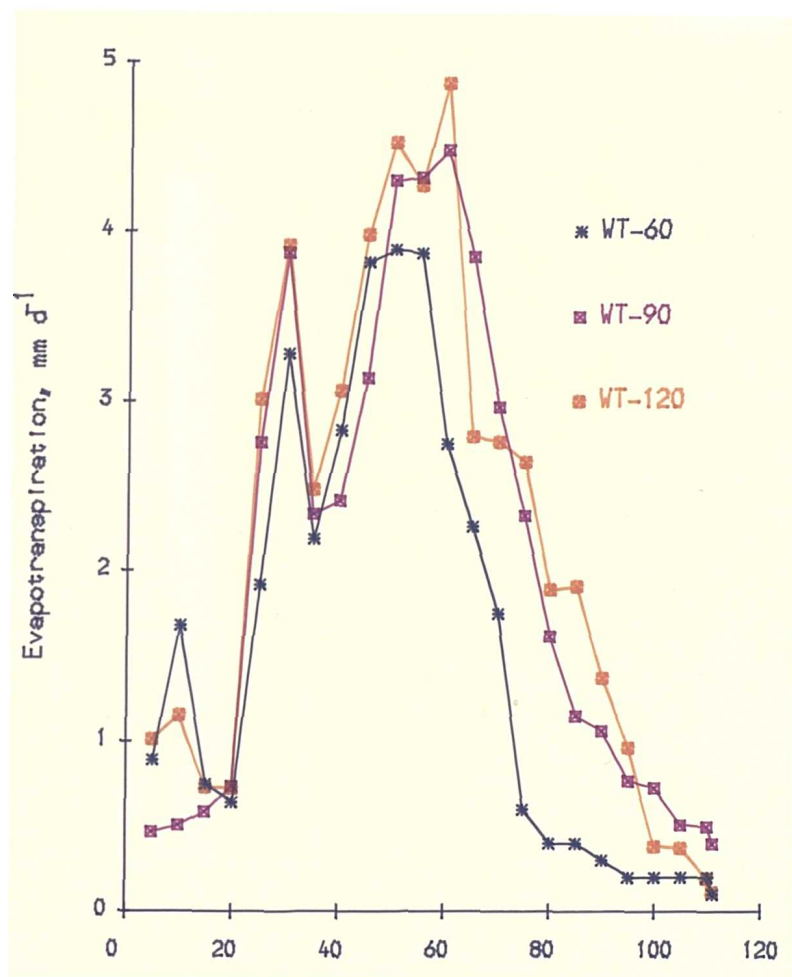


Fig. 6.26. Evapotranspiration as a function of time (Bean).



Time from sowing, d

Fig. 6.27. Evapotranspiration as a function of time (Barley).

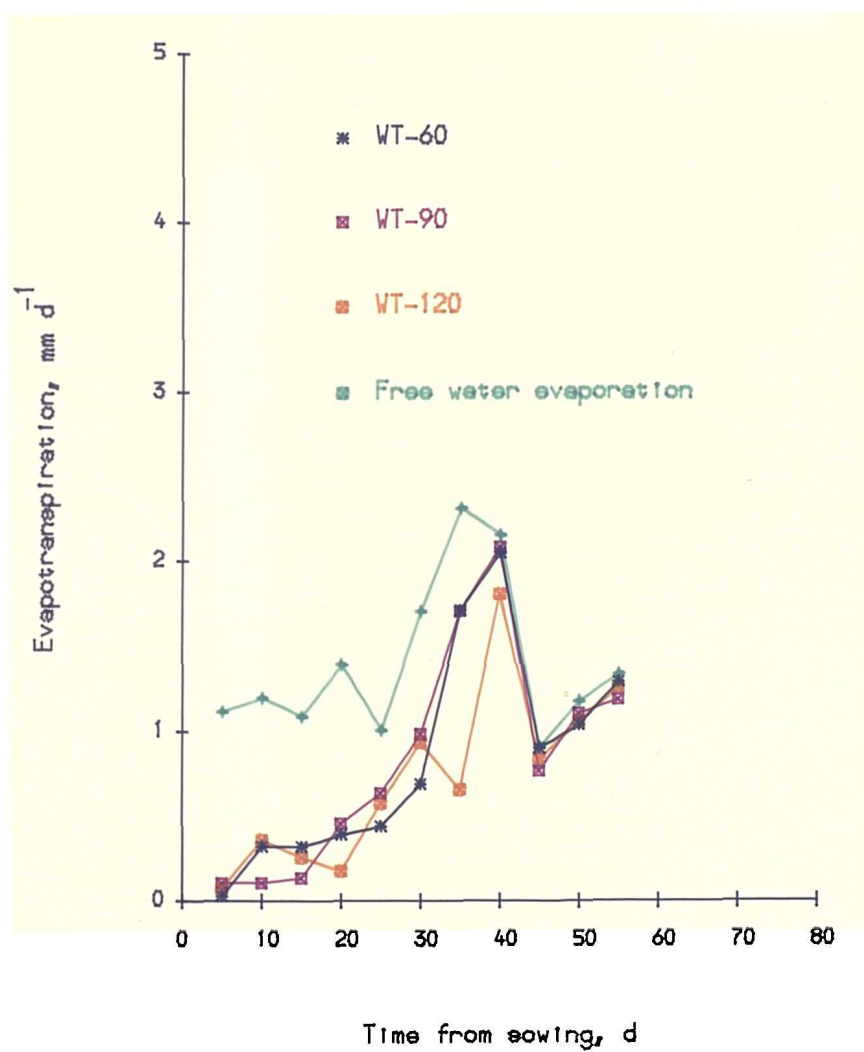


Fig. 6.28. Evapotranspiration as a function of time (Lettuce).

6.8 Separation of Evaporation and Transpiration

Using the total sink term from the profile per day (S_i) and water use per day, the evaporation rate from the soil can be partitioned from the following relation assuming that the total sink term from the profile per day represents the transpiration rate per day (T).

$$E = e + T \quad (6.5)$$

$$T = \sum_{i=1}^n S_i \quad (6.6)$$

where

e = evaporation from soil,

E = evapotranspiration,

T = transpiration by the crop, i.e. total water uptake by the plants from the profile, and

S = sink term from n layers.

From Equations (6.5) and (6.6), evaporation from soil can be represented by

$$e = E - \sum_{i=1}^n S_i$$
$$e = \Delta W + C - \sum_{i=1}^n S_i \quad [from \ Eq.(6.4)] \quad (6.7)$$

The principle of the method is given here, but no results are quoted because, when there is complete crop cover, e is approximately zero, and the attendant errors in calculating e is large.

6.9 Simulation

The simulation refers to the conditions outlined in chapter 5 (section 5.5). Besides simulation, different parameters (e. g. upward flux, sink term) were determined (section 6.4, 6.6) based on the physical constants (Fig. 6.2 b, c) measured for individual water table treatments. CAPROW was used to simulate results under the boundary conditions outlined in chapter 5 (sections 5.1 and 5.2), for lysimeters with water tables 60, 90 and 120 cm deep for three different crops.

Comparing soil moisture as a function of depth is one of the means to verify the results of the model. Comparisons of measured and simulated volumetric moisture contents as a function of depth for different crops are shown in Figs. 6.29a, b, c (bean); Figs. 6.30a, b, c (barley) and Figs. 6.31a, b, c (lettuce), respectively. Soil moisture measurements were made only at the end of an experiment to avoid disturbance of the system. There was generally excellent agreement between the measured and simulated water contents for all water table treatments under different crops. This may be due to the stable hydraulic properties of the soil. Torres and Hanks (1989) reported good agreement between the measured and simulated water content profiles at the end of 52 days. They mentioned that the agreement was best for the conditions near the water table, where a water table existed, and worst near the soil surface. Feddes et al. (1978) reported the general agreement between the measured and simulated moisture contents.

Another way of comparison could be measured and simulated upward flux. Tables 6.10, 6.11 and 6.12 show comparison of measured cumulative upward flow from the water table and simulated cumulative upward soil water flux from the effective root zone depth over the entire growth period for all the lysimeters. There was excellent agreement between measured and simulated upward flux for all water table treatments in barley and lettuce. Ragab and Amer (1986) showed good agreement between the measured and simulated upward flux in their maize experiment. They measured upward flux at a depth below the effective root zone of maize. In their experiment, water table and effective root zone depths were 68 and 45 cm, respectively.

Comparing total water use is also another way of verifying the results of the model. Equation (6.4) was used to measure the total water use. Soil water deple-

tions were measured from the measured characteristics for individual lysimeters. The water table contribution was directly measured (section 4.1.4). Simulated soil water depletion and upward fluxes were obtained as outlined in section 5.1 and 5.2. The total water use generally has shown good agreement between measured and simulated values (Tables 6.10, 6.11 and 6.12).

Simulated fluxes as a function of depth were the same as the measured ones (Figs. 6.14b, c; 6.16b, c and 6.18b, c) in the lysimeters with water tables 90 and 120 cm deep under three different crops. Simulated sink terms for the same lysimeters showed similar trends as those measured ones (Figs. 6.22b, c; 6.23b, c; 6.24). For this reason, simulated fluxes and sink terms as a function of depth are not shown graphically.

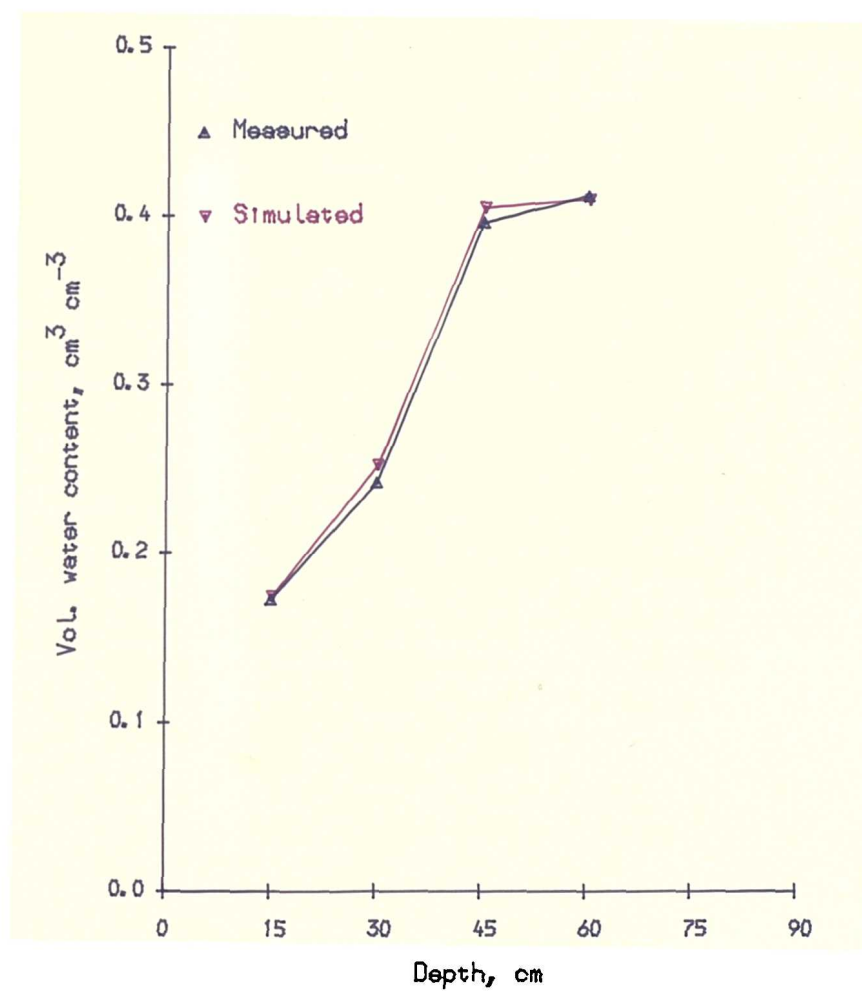


Fig. 6.29. (a) Measured and simulated water content as a function of depth for WT-60 at harvest (Bean).

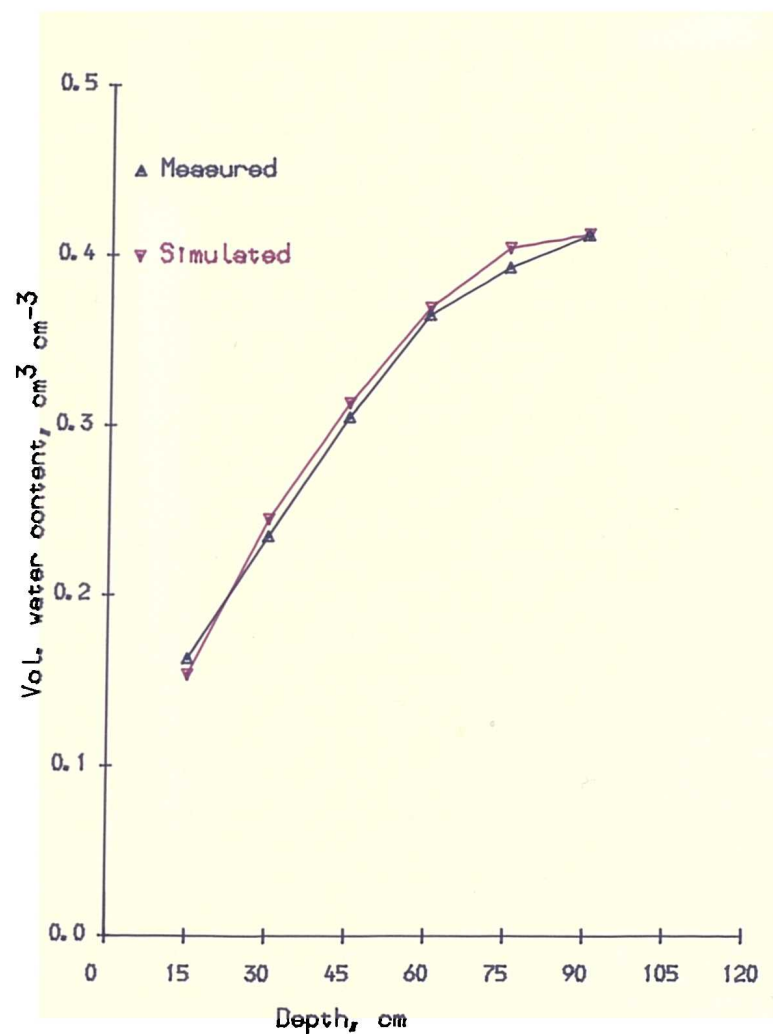


Fig. 6.29. (b) Measured and simulated water content as a function of depth for WT-90 at harvest (Bean).

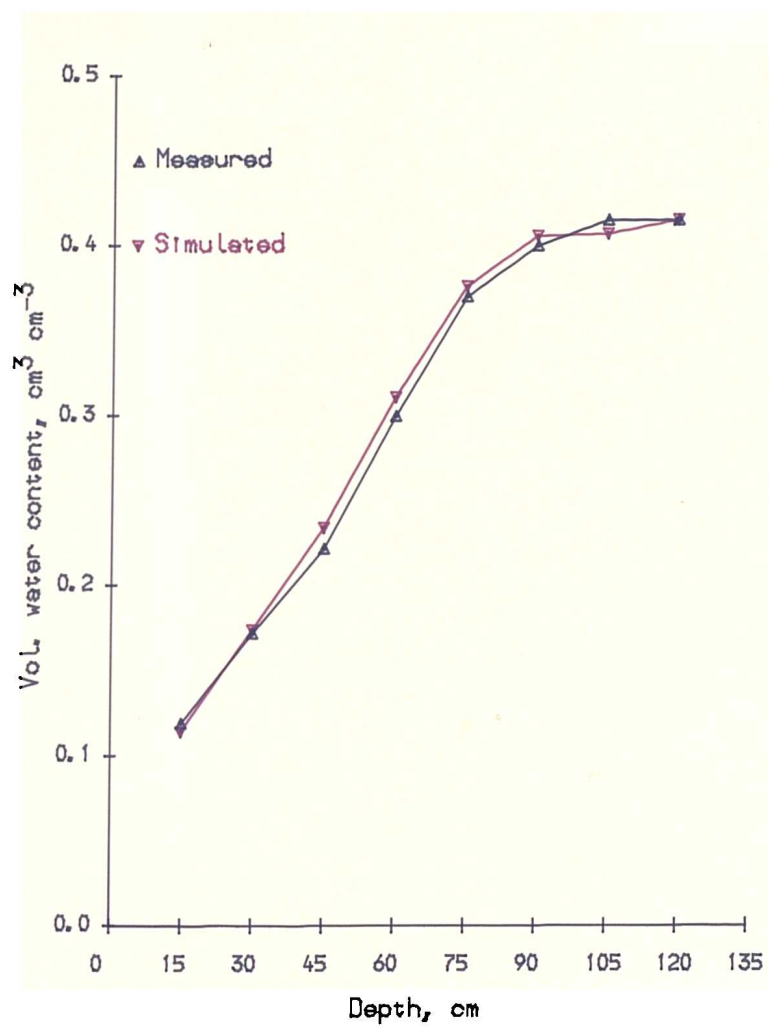


Fig. 6.29. (c) Measured and simulated water content as a function of depth for WT-120 at harvest (Bean).

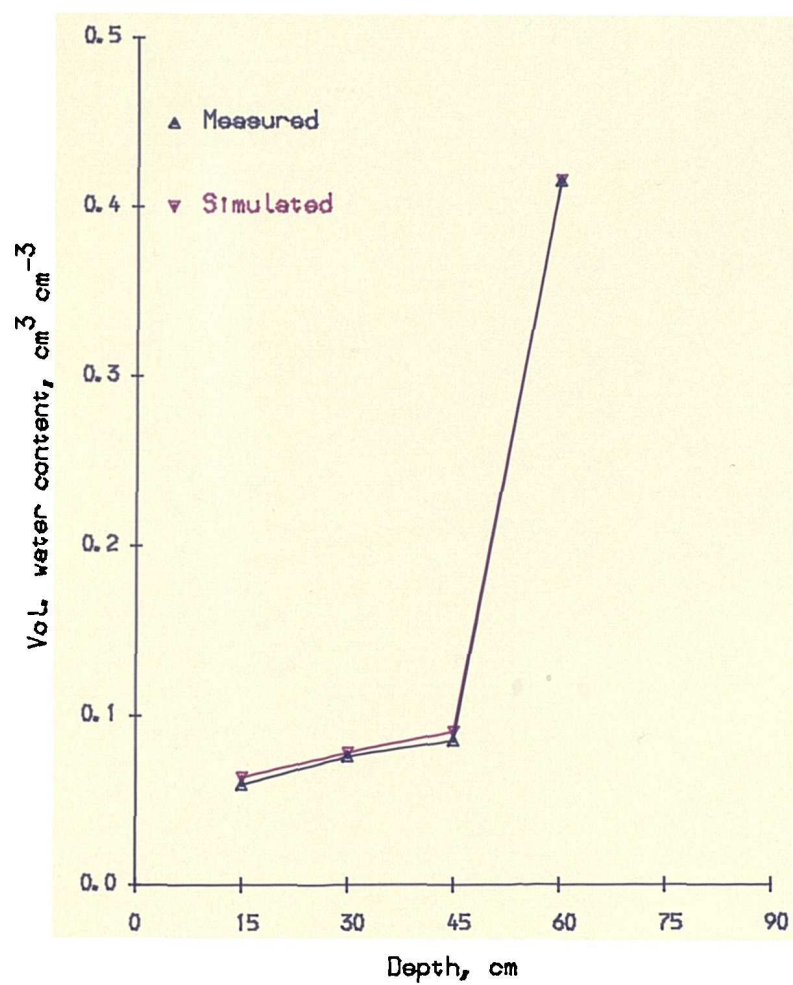


Fig. 6.30. (a) Measured and simulated water content as a function of depth for WT-60 at harvest (Barley).

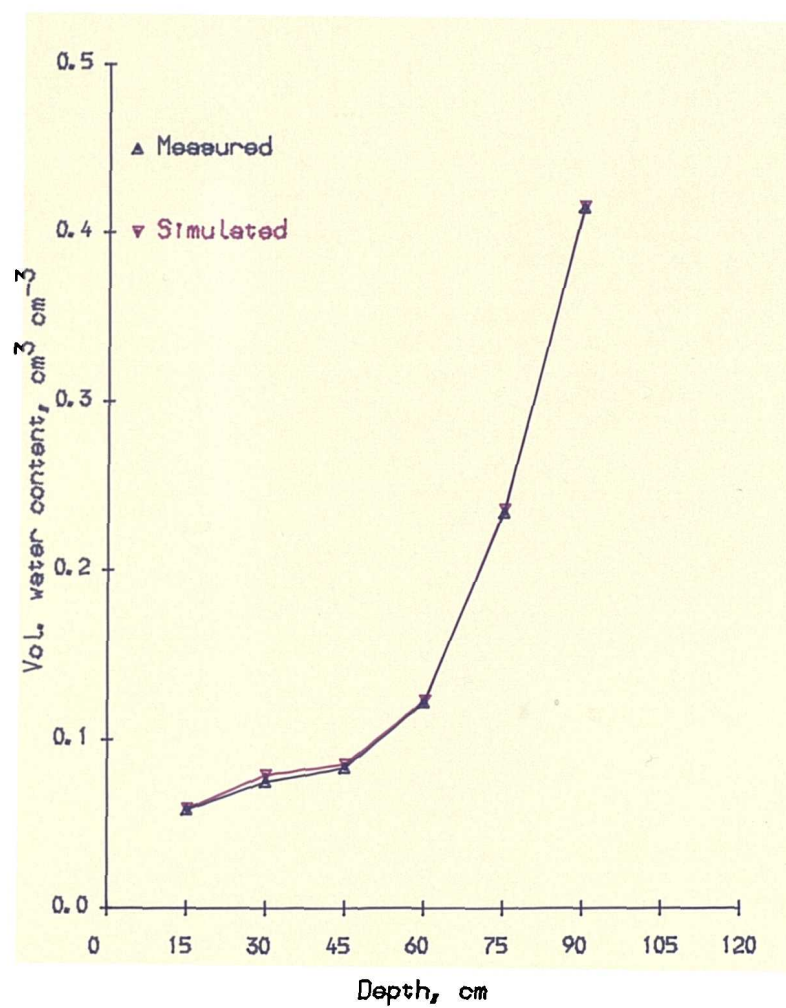


Fig. 6.30. (b) Measured and simulated water content as a function of depth for WT-90 at harvest (Barley).

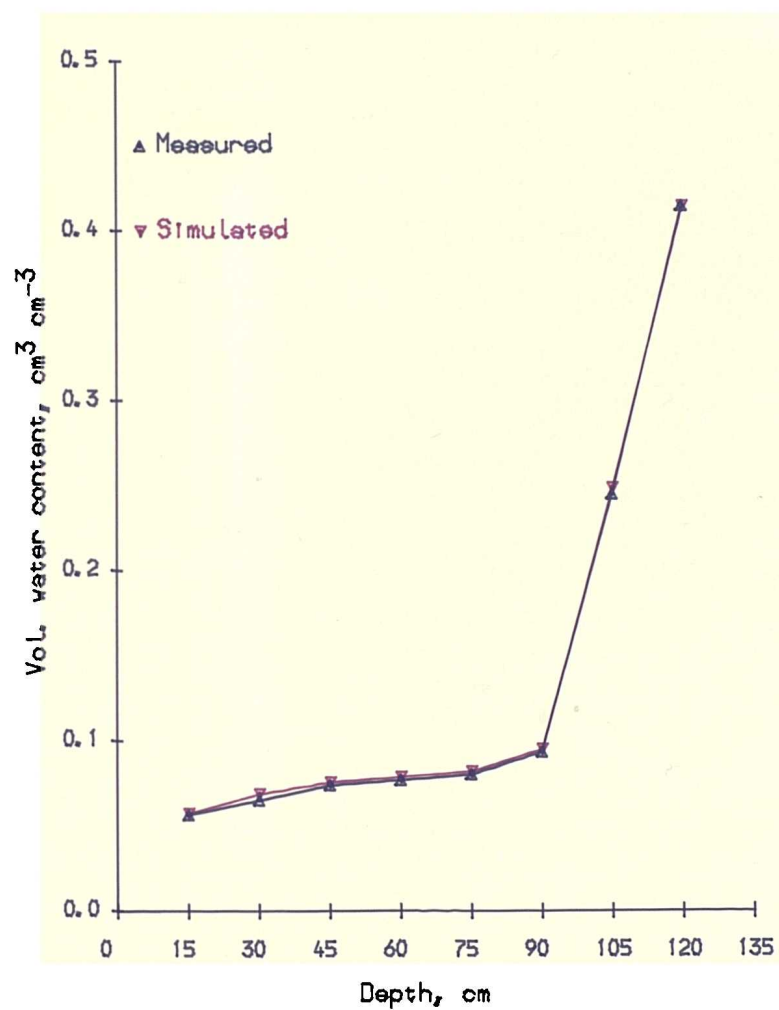


Fig. 6.30. (c) Measured and simulated water content as a function of depth for WT-120 at harvest (Barley).

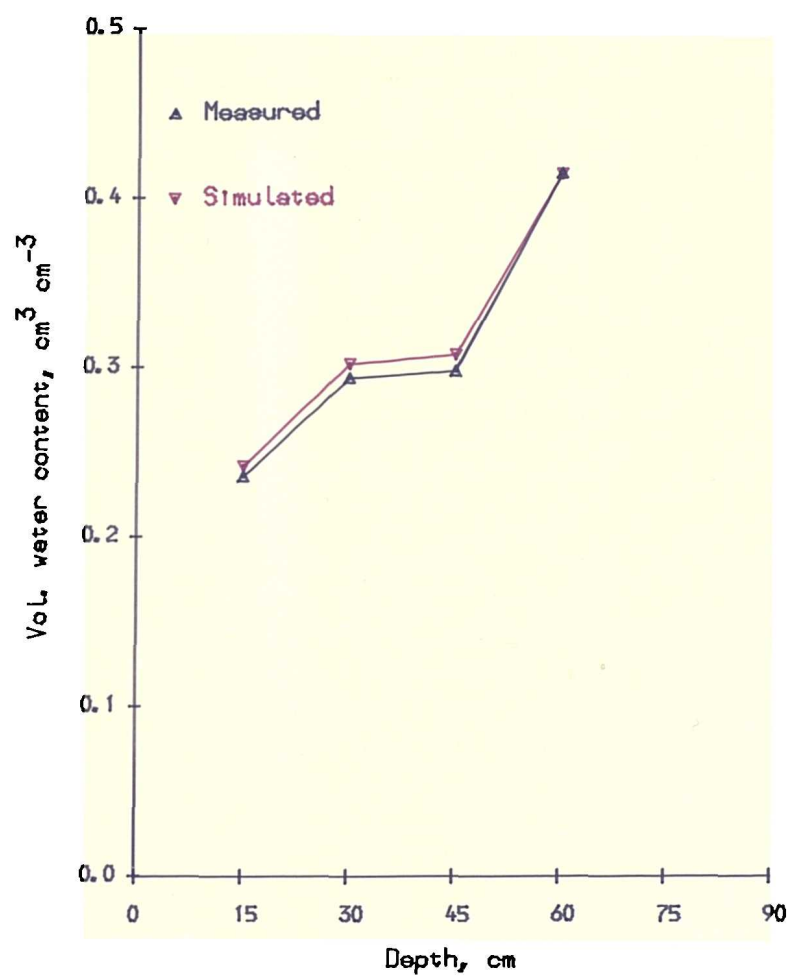


Fig. 6.31. (a) Measured and simulated water content as a function of depth for WT-60 at harvest (Lettuce).

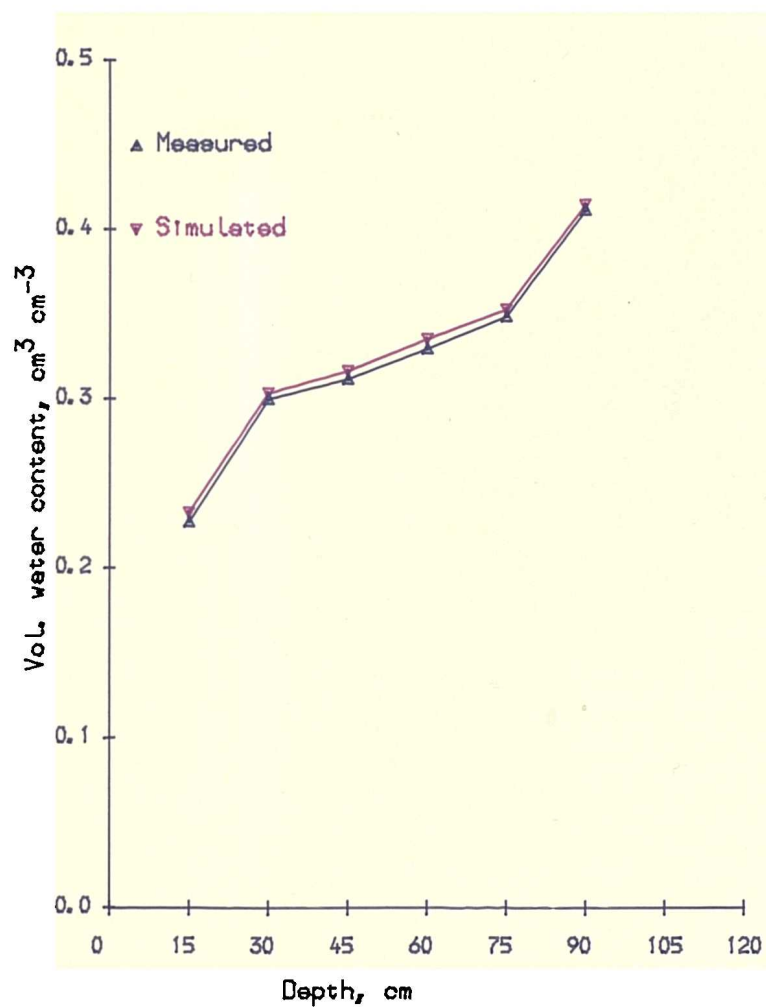


Fig. 6.31. (b) Measured and simulated water content as a function of depth for WT-90 at harvest (Lettuce).

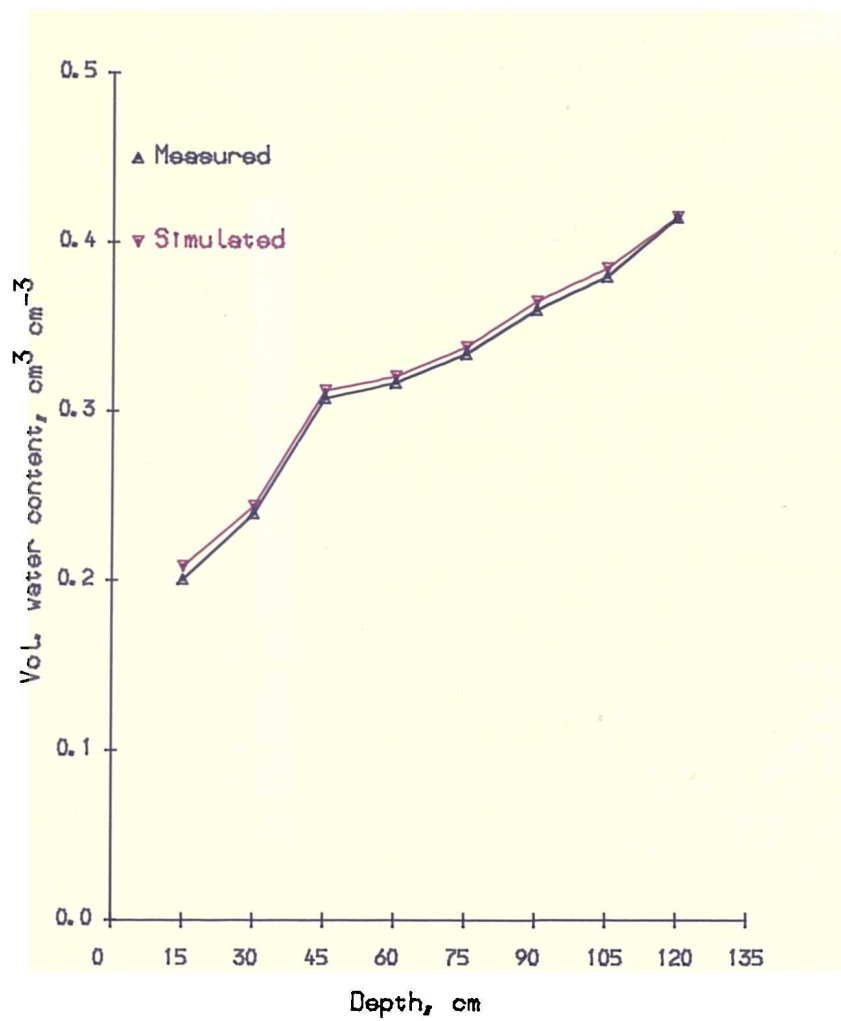


Fig. 6.31. (c) Measured and simulated water content as a function of depth for WT-120 at harvest (Lettuce).

Chapter VII

SUMMARY AND CONCLUSIONS

7.1 Soil Properties

The soil moisture characteristic for the entire moisture range was determined in the laboratory using suction plate, pressure plate and vapour equilibrium methods. The empirical three-straight-line semi-log models fitted well these laboratory determined soil moisture characteristics. The same straight-line semi-log models were used for predicting soil moisture content in the developed simulation model (CAPROW).

Unsaturated hydraulic conductivity of the experimental soil was determined from measurements of diffusivity on undisturbed cores in the laboratory, and *in situ* using both the drainage flux method and the measurements on soil-water depletion. Conductivity values obtained from the diffusivity measurements and measurements on the soil-water depletion agreed well, but were smaller than those obtained using the drainage flux method. Gardner's (1958) and Rijtema's (1965) conductivity functions were used to fit data. Gardner's conductivity function fitted the data well having a value of $n = 1.05$, within the investigated range of 1 for heavy soils and 4 for very coarse-textured soils.

7.2 Capillary Contribution

The study confirms that successful exploitation of the water table needs to have an initial equilibrium soil moisture profile irrespective of crop type, depth to water table and crop water demand. In this context, at the water table, hydraulic gradient $dH/dz < 0$ and continuous capillary rise will occur.

Because the initial soil moisture suction profile was not in equilibrium, there was no capillary rise in beans with water tables 90 and 120 cm deep and only a small amount (4.5% of E) with water table at 60 cm depth. The water table contributed to about 27.0, 16.4 and 11.4% of water use of barley for 60, 90 and

120 cm water table depths, respectively. For lettuce, the measured contribution of the water table to evapotranspiration was 34.7, 13.5 and 6.0%, respectively.

The results indicate that a properly managed water table is a potential resource of subirrigation for shallow, medium and deep-rooted crops.

7.3 Root Water Uptake

The water uptake by roots was evaluated using the sink term added to the continuity Equation (3.28). The sink term in bean and barley penetrated deeper after exhausting soil moisture in the surface layer. But in lettuce, the sink term was confined to the top layer (0-5 cm) up to harvest. Because there was an equilibrium soil moisture profile at the start of the experiment, the water table contributed directly to the crop water demand instead of the soil water store becoming exhausted in the top layers. In contrast to the hypothesis of Feddes and Zaradny (1978), the sink term is not constant as suction increases between anaerobiosis and the limiting point, for three different crops.

In bean and barley, it is apparent from the soil moisture suction profiles that the root grew downward faster than water could move up from the water table.

In barley, 10.8, 5.1 and 2.5% of roots near the water table were absorbing water from capillary fringe at 60, 90 and 120 cm water table depths, respectively.

7.4 Model Prediction

Prediction of soil moisture content using three-straight-line semi-log models for the moisture characteristic in CAPROW at harvest agreed well with the measured values for all crops.

There was a good agreement between cumulative measured and simulated capillary upward flux from the water table in barley and lettuce.

Simulated fluxes and sink terms as a function of time at different depths for 90 and 120 cm water tables showed similar trends as those measured under three different crops.

7.5 Future Extension

This study is on the contribution by the water table to crop water use under conditions of no surface water application. The same study could be extended to evaluate the physics of water table contribution when water is applied to the soil surface.

It should be mentioned here that the desorption curve $\theta(\psi)$ can only be used for drying. In the case of wetting and drying simultaneously, hysteresis has to be considered to avoid error. If there is hysteresis, the $K(\theta)$ function should be used instead of $K(\psi)$, from the direct measurement of θ instead of values inferred from ψ .

In field conditions, the water table is not constant at a particular depth, rather it is variable for each and every location. So the study could be further be extended to study the physics of the water table contribution under variable water table depths for differing root systems.

Appendix A

CALCULATION OF INFLOW TO ROOTS: Factor $A_f = 0.067$

Lysimeter diameter = 108.0 cm

Lysimeter area = $\pi r^2 = \pi \times 54^2 \text{ cm}^2$

Length of root in each 15 cm layer:

$$\begin{aligned} &= \text{Lysimeter Area} \times \text{depth} \times \text{root density} \\ &= \pi \times 54^2 \text{ cm}^2 \times 15 \text{ cm} \times \text{root density cm}(\text{root}) \text{ cm}^{-3}(\text{soil}) \\ &= 137400 \times \text{root density cm}(\text{root}) \end{aligned}$$

Volume of water extraction:

$$\begin{aligned} &= \text{Lysimeter Area} \times \text{Sink term} \\ &= \pi \times 54^2 \text{ cm}^2 \times \text{sink term cm}(\text{H}_2\text{O}) \text{ d}^{-1} \\ &= 9160 \times \text{Sink term cm}^3(\text{H}_2\text{O}) \text{ d}^{-1} \end{aligned}$$

Inflow to root = Volume of water extracted / Length of root

$$= 0.067 \times \frac{\text{Sink term}}{\text{Root density}} \text{ cm}^3(\text{H}_2\text{O}) \text{ cm}^{-1}(\text{root}) \text{ d}^{-1}$$

Appendix B

CAPROW SIMULATION PROGRAMME WRITTEN IN FORTRAN 77 DEVELOPED BY AHMAD ALI HASSAN, UNIVERSITY OF NEWCASTLE UPON TYNE, ENGLAND NE1 7RU, U. K.

```
*      SIMULATION OF CAPILLARY RISE AND ROOT WATER UPTAKE
*      (CAPROW) IN PRESENCE OF HIGH WATER TABLE.
*
*      GLOSSARY OF SYMBOLS
*
*      A  = CONSTANT OF GARDNER'S EQUATION
*      A1 = CONSTANT OF SUCTION vs THETA RELATION EQUATION
*           FROM SOIL MOISTURE CHARACTERISTIC.
*      A2 = SAME AS A1
*      A3 = SAME AS A1
*      AK = UNSATURATED HYDRAULIC CONDUCTIVITY (mm/day)
*      AMD= DEPTH OF MOISTURE EXTRACTION (mm)
*      AMD1= DEPTH MOISTURE EXTRACTION(AVERAGE) (mm/day)
*      AN = SAME AS A
*      B  = SAME AS A
*      B1 = SAME AS A1
*      B2 = SAME AS A1
*      B3 = SANE SA A1
*      D  = TENSIO METER DEEPTHS INCLUDING ZERO FOR SURFACE
*           AND WATER TABLE DEPTH (cm)
*      DD = DIFFERENCE OF DEPTH (cm) FOR CALCULATING AMD
*           AND AMD1.
*      DH = DIFFERENCE OF SUCTION HEAD (cm)
*      DTHETA = VOLUMETRIC MOISTURE EXTRACTION IN SPECIFIC
*              INTERVAL USED
*      DZ = DIFFERENCE OF GRAVITATIONAL HEAD (cm)
*      GMH = GEOMETRIC MEAN OF MATRIC SUCTION (cm)
*      H  = SOIL MATRIC SUCTION HEAD (cm)
*      H(K,L)= SUCTION HEAD WITH RESPECT TO LAYER AND TIME
```

```

*      IT = DAY OF OBSERVATIONS (day)
*      Q  = SOIL MOISTURE FLUX  (mm/day)
*      Q1 = SOIL MOISTURE FLUX OR FLUX FROM WATER TABLE (mm/day)
*      RD = ROOT DENSITY [ $cm(root)/cm^3(soil)$ ]
*      RI = ROOT INFLOW RATE [ $cm^3(water)/cm(root)/day$ ]
*      S  = SINK TERM (mm/day)
*      SQRT = SQUARE ROOT OF SUCTION HEAD
*      THETA = VOLUMETRIC MOISTURE CONTENT ( $cm^3\ cm^{-3}$ )
      PROGRAM MAIN
      DIMENSION D(50),IT(50),H(50,50),THETA(50,50),GMH(50,50),
*AK(50,50),S(50,50),DTHETA(50,50),DD(50),
*AMD(50,50),Q1(50,50),Q(50,50),RI(50,50),
*DZ(50),DH(50,50),AMD1(50,50),RD(50)
      READ(5,10)A,B,A1,B1,A2,B2,A3,B3,AN
10  FORMAT(9F8.3)
*
      DO 100 I=1,6
      READ(5,15) D(I)
15  FORMAT(F10.3)
100  CONTINUE
*
      DO 105 J=1,24
      READ(5,20)IT(J)
20  FORMAT(2X,I3)
105  CONTINUE
*
      DO 91 N=1,4
      READ(5,55)RD(N)
55  FORMAT(F10.2)
91  CONTINUE
*
      READ(5,25)((H(K,L),L=1,24),K=1,5)
25  FORMAT(6F10.3)
*

```



```

        WRITE(6,29)
29  FORMAT('  '/'  ',2X,'DAY',8X,'THETA')
*
        DO 120 K=1,5
        DO 125 L=1,24
        IF (H(K,L).GE.3165.0)GO TO 501
        IF (H(K,L).GT.25.0)GO TO 502
        IF (H(K,L).GT.0.0) THEN
        THETA(K,L)=B3-ALOG(H(K,L))/A3
        ELSE
        THETA(K,L)=0.415
        ENDIF
        GO TO 504
502  THETA(K,L)=B2-ALOG(H(K,L))/A2
        GO TO 504
501  THETA(K,L)=B1-ALOG(H(K,L))/A1
504  WRITE(6,30)IT(L),THETA(K,L)
        30  FORMAT(2X,I3,5X,F10.5)
125  CONTINUE
120  CONTINUE
*
        WRITE(6,32)
32  FORMAT('  '/'  ',2X,'DAY',4X,'D',7X,'AMD',7X,'AMD1')
        DO 130 I=1,5
        DD(I)=D(I+1)-D(I)
        DO 135 J=1,23
        DTHETA(I,J)=THETA(I,J)-THETA(I,J+1)
        IF(THETA(I,J).LE.0.109)THEN
        AMD(I,J)=0.0
        ELSE
        AMD(I,J)=DD(I)*DTHETA(I,J)*10.0
        ENDIF
        AMD1(I,J)=AMD(I,J)/(IT(J+1)-IT(J))
        WRITE(6,40)IT(J+1),D(I+1),AMD(I,J),AMD1(I,J)

```

```

40  FORMAT(2X,I3,2X,F5.2,2F10.5)
135  CONTINUE
130  CONTINUE
*
      WRITE(6,34)
34  FORMAT(/3X,'DAY',2X,'D',5X,'DZ',10X,'DH',10X,
          'GM',9X,'K',8X,'Q')
      N=5
      DO 140 J=1,24
      DO 145 I=1,N-1
      IF(I.LT.4)THEN
      GMH(I,J)=SQRT(H(I,J)*H(I+1,J))
      ELSE
      GMH(I,J)=(H(I,J)+H(I+1,J))/2.0
      ENDIF
      AK(I,J)=10.0*A/(B+GMH(I,J)**AN)
      DZ(I+1)=D(I+2)-D(I+1)
      DH(I,J)=H(I,J)-H(I+1,J)
      Q(I,J)=AK(I,J)*((DH(I,J)/DZ(I+1)-1.0))
      IF (Q(I,J).GT.0.0)THEN
      WRITE(6,45)IT(J),D(I+1),DZ(I+1),DH(I,J),
          GMH(I,J),AK(I,J),Q(I,J)
      ELSE
      WRITE(6,46)IT(J),D(I+1),DZ(I+1),DH(I,J),
          GMH(I,J),AK(I,J)
      ENDIF
45  FORMAT(2X,I3,2X,F5.2,1X,F5.2,F12.2,F12.2,
          2X,F10.8,2X,F10.8)
46  FORMAT(2X,I3,2X,F5.2,1X,F5.2,F12.2,F12.2,2X,F10.8)
145  CONTINUE
140  CONTINUE
*
      WRITE(6,4)
4  FORMAT(/3X,'DAY',4X,'D',10X,'H',10X,'Q',9X,'Q1')

```

```

DO 137 J=1,24
DO 138 I=1,4
IF(H(I,J).GE.15000.00)THEN
Q1(I,J)=0.0
ELSE
Q1(I,J)=Q(I,J)
ENDIF
WRITE(6,139)IT(J),D(I+1),H(I,J),Q(I,J),Q1(I,J)
139 FORMAT(2X,I3,2X,F5.2,2X,F12.2,2X,F10.8,2X,F10.8)
138 CONTINUE
137 CONTINUE
*
WRITE(6,31)
31 FORMAT(' '/' ',2X,'DAY',4X,'D',6X,'AMD1',6X,'Q1',8X,'S')
* CAPILLARY FLUXES FROM WATER TABLE ON DAILY BASIS (mm/day)
READ(5,57)(Q1(5,M),M=1,24)
57 FORMAT(6F10.3)
*
DO 160 M=5,23
DO 155 L=1,4
IF(L.EQ.1.AND.Q1(L+1,M).LE.0.0)GO TO 101
IF(L.EQ.1.AND.Q1(L+1,M).GT.0.0)GO TO 102
S(L,M)=Q1(L+1,M)-Q1(L-1,M)+AMD1(L,M-1)
GO TO 103
102 S(L,M)=Q1(L+1,M)+AMD1(L,M-1)
GO TO 103
101 S(L,M)=AMD1(L,M-1)
103 IF(Q1(L,M).GE.0.0.AND.S(L,M).GT.0.0)THEN
WRITE(6,50)IT(M),D(L+1),AMD1(L,M-1),Q1(L,M),S(L,M)
ELSE
WRITE(6,51)IT(M),D(L+1),AMD1(L,M-1),Q1(L,M)
50 FORMAT(2X,I3,2X,F5.2,3F10.5)
51 FORMAT(2X,I3,2X,F5.2,2F10.5)
ENDIF

```

```

155  CONTINUE
160  CONTINUE
*
    WRITE(6,42)
42   FORMAT('  '/'  ',2X,'DAY',4X,'D',7X,'RI')
    DO 165 M=5,23
    DO 170 L=1,4
    IF(S(L,M).GT.0.0)THEN
    RI(L,M)=0.067*(S(L,M)/(RD(L)*10.0))
    WRITE(6,180)IT(M),D(L+1),RI(L,M)
    ELSE
    WRITE(6,200)IT(M),D(L+1)
180  FORMAT(2X,I3,2X,F5.2,F10.5)
200  FORMAT(2X,I3,2X,F5.2)
    ENDIF
170  CONTINUE
165  CONTINUE
    RETURN
    END

```

REFERENCES

1. ACHARYA, C. L. and F. A. DAUDET. (1980). Some difficulties in the interpretation of experimental outflow curves for hydraulic conductivity determinations. *Geoderma* 23:285-297.
2. ALEXANDER, L. and R. W. SKAGGS. (1986). Predicting unsaturated hydraulic conductivity from the soil water characteristics. *Trans. ASAE* 29:176-184.
3. ALLMARAS, R. R., W. W. NELSON and W. B. VOORHEES. (1975). Soybean and corn rooting in Southwestern Minnesota: II. Root distributions and related water inflow. *Soil Sci. Soc. Am. Proc.* 39:771-777.
4. ALVINO, A. and G. ZERBI. (1986). Water-table level effect on the yield of irrigated and unirrigated grain maize. *Trans. ASAE* 29(4): 1086-1089.
5. ANAT, A., H. R. DUKE and A. T. COREY. (1965). Steady upward flow from water tables. *Colorado State Univ. Hydrol. Paper No. 7*, June.
6. ARYA, L. M., D. A. FARREL and G. R. BLAKE. (1975). A field study of soil water depletion patterns in presence of growing soybean roots: I. Determination of hydraulic properties of the soil. *Soil Sci. Soc. Am. Proc.* 39:424-430.
7. AVERJANOV, S. F. (1950). About permeability of subsurface soils in case of incomplete saturation. p.19-21. in *English Collection*, Vol. 7, (1950), as quoted by P. Ya Palubarinova., 1962. The theory of ground water movement. (English translation by I. M. Roger De Wiest, Princeton University Press).
8. AVERY, B. W. and C. L. BASCOMB. (1982). Soil survey laboratory methods. *Soil Survey Technical Monograph No. 6*. Harpenden, U. K.
9. BABABE, B. (1987). Soil hydraulic conductivity and its influence on water water status of *Lolium perenne*, *L. seedlings*. Ph. D. Thesis. University of Newcastle upon Tyne.

10. BARTELLI, L. J. and D. B. PETERS. (1959). Integrating soil moisture characteristics with classification units of some Illinois Soils. *Soil Sci. Soc. Am. Proc.* **23**:149-151.
11. BENZ, L. C., E. J. DOERING and G. A. REICHMAN. (1985). Water table and irrigation effects on corn and sugar beet. *Trans. ASAE* **28**(6):1951-1956.
12. BENZ, L. C., E. J. DOERING and G. A. REICHMAN. (1985). Alfalfa yields and evapotranspiration in response to static water tables and irrigation. *Trans. ASAE* **28**(4):1178-1185.
13. BLACK, T. A., W. R. GARDNER and G. W. THURTELL. (1969). The prediction of evaporation, drainage and soil water storage for a bare soil. *Soil Sci. Soc. Am. Proc.* **38**:885-888.
14. BLAKE, G. R. and K. H. HARTGE. (1986). Bulk density. In *Methods of Soil Analysis, Part I*, pp.363-375. *ASA monograph No. 9* (2nd ed.).
15. BOUMA, J. (1983). Use of soil survey data to select measurement techniques for hydraulic conductivity. *Agric. Water Management* **6**:177-190.
16. BRADY, N. C. (1974). *The nature and properties of soils* (8th ed.). Macmillan, New York.
17. BROOKS, R. H. and A. T. COREY. (1964). Hydraulic properties of porous media. *Hydrology Paper 3*, Colorado State Univ., Fort Collins, CO.
18. BRUCE, R. R. and A. KLUTE. (1956). The measurement of soil moisture diffusivity. *Soil Sci. Soc. Am. Proc.* **20**:458-462.
19. BUCKINGHAM, E. (1907). Studies on the movement of soil moisture. *U. S. Dept. Agr. Bur. Soils Bull.* **38**:29-61.
20. CAMPBELL, G. S. (1985). *Soil physics with basic : Transport models for soil-plant systems*. Elsevier Scientific Publishing Co., Amsterdam.
21. CAMPBELL, R. B. and G. T. SEABORN. (1972). Yield of flue-cured tobacco and levels of soil oxygen in lysimeters with different water table depths. *Agron. J.* **64**:730-733.

22. CAMPBELL, R. E., W. E. LARSON, T. S. AASHEIM and P. L. BROWN. (1960). Alfalfa response to irrigation frequencies in the presence of a water table. *Agron. J.* 52:437-441.
23. CHANG, J. H. (1968). *Climate and Agriculture*. Aldine, Chicago.
24. CHILDS, E. C. (1940). The use of soil moisture characteristics in soil studies. *Soil Sci.* 50:239-252.
25. CHILDS, E. C. and N. COLLIS-GEORGE. (1950). The permeability of porous materials. *Proc. Roy. Soc. London.* 201A, 392-405.
26. CLAPP, R. B. and G. M. HORNBERGER. (1978). Empirical equations of some hydraulic properties. *Water Resour. Res.* 14:601-604.
27. COWAN, I. R. (1965). Transport of water in the soil-plant-atmosphere system. *J. appl. Ecol.* 2:221-239.
28. DAVIDSON, J. M., D. R. NIELSEN and J. W. BIGGAR. (1966). The dependence of soil water pressure and release upon the applied pressure increment. *Soil Sci. Soc. Am. Proc.* 30:298-304.
29. DE JONG, E. (1976). Moisture retention of selected Saskatchewan soils. In *Soil Plant Nutrient Res. Report*, compiled by D. A. Rennie, Sask. *Inst. of Ped., Rep. No. 6.* 100p.
30. DE JONG, E., C. A. CAMPBELL and W. NICHOLAICHUK. (1983). Water retention equations and their relationships in soil organic matter and particle size distribution for disturbed samples. *Can. J. Soil Sci.* 63:291-302.
31. DUNHAM, R. J. and P. H. NYE. (1973). The influence of soil water content on the uptake of ions by roots I. Soil water content gradients near a plane of onion roots. *J. appl. Ecol.* 10:585-598.
32. DOERING, E. J. (1965). Soil-water diffusivity by the one-step method. *Soil Sci.* 99:322-326.

33. FEDDES, R. A. (1968). The use of lysimeter data in the determination of capillary rise, available water, and actual evapotranspiration of three soil profiles. *Proc. Reg. Training Seminar Agromet.*, pp.107-124. Wageningen, Netherlands.
34. FEDDES, R. A. (1971). Water, heat and crop growth. *Comm. Agric. Univ. Wageningen*, 71-72, 184p. (Thesis).
35. FEDDES, R. A. and P. E. RIJTEMA. (1972). Water withdrawal by plant roots. *J. Hydrology* 17:33-59.
36. FEDDES, R. A., E. BRESLER and S. P. NEUMAN. (1974). Test of modified numerical model for water uptake by root systems. *Water Resour. Res.* 10(6):1199-1206.
37. FEDDES, R. A., P. KOWALIK, K. KOLINSKA-MALINKA and H. ZARADNY. (1976). Water dependent root extraction function. *J. Hydrology* 31:13-26.
38. FEDDES, R. A., P. J. KOWALIK and H. ZARADNY. (1978). Simulation of field water use and crop yield. *Pudoc*, Wageningen, Netherlands.
39. FEDDES, R. A. and H. ZARADNY. (1978). Numerical model for transient water flow in non-homogeneous soil-root systems with groundwater influence. *Institute for Land and Water Management Research*, Wageningen, Netherlands.
40. GARDNER, W. R., O. W. ISRAELSEN, N. E. EDLEFSEN and N. S. CLYDE. (1922). The capillary potential function and its relation to irrigation practice. *Soil Sci.* 11:215-232.
41. GARDNER, W. R. (1956). Calculation of capillary conductivity from pressure plate outflow data. *Soil Sci. Soc. Am. Proc.* 20:317-320.
42. GARDNER, W. R. (1958). Some steady-state solutions of the unsaturated moisture flow equation with application to evaporation from a water table. *Soil Sci.* 85:228-232.
43. GARDNER, W. R. and M. FIREMAN. (1958). Laboratory studies of evaporation from soil columns in the presence of a water table. *Soil Sci.* 85:244-249.

44. GARDNER, W. R. (1960). Dynamic aspects of water availability to plants. *Soil Sci.* 89:63-73.
45. GARDNER, W. R. (1962). Note on the separation and solution of diffusion type of equation. *Soil Sci. Soc. Am. Proc.* 26:404.
46. GARDNER, W. R. (1964). Relation of root distribution to water uptake and availability. *Agron. J.* 56:35-41.
47. GARDNER, W. R., D. HILLEL and Y. BENYAMINI. (1970). Post irrigation movement of soil water I. Redistribution. *Water Resour. Res.* 6 :851-861.
48. GILLHAM, R. W., A. KLUTE and D. F. HEERMANN. (1976). Hydraulic properties of porous medium : Measurements and empirical representation. *Soil Sci. Soc. Am. J.* 40:203-207.
49. GILLHAM, R. W., A. KLUTE and D. F. HEERMANN. (1979). Measurement and numerical simulation of hysteretic flow in a heterogeneous porous medium. *Soil Sci. Soc. Am. J.* 43:1061-1067.
50. GREEN, W. H. and G. A. AMPT. (1911). Studies on soil physics I. The flow of air and water through soils. *J. Agric. Sci.* 4:1-24.
51. GREEN, W. H. and G. A. AMPT. (1913). Studies on soil physics II. The permeability of an ideal soil to air and water. *J. Agric. Sci.* 5:1-26.
52. GREEN, R. E., L. R. AHUJA and S. K. CHONG. (1986). Hydraulic conductivity, diffusivity, and sorptivity of unsaturated soils : Field methods. In *Methods of Soil Analysis, Part I*, pp.771-798. *ASA monograph No. 9* (2nd ed.).
53. GREGORY, P. J., M. MCGOWAN and P. V. BISCOE. (1978). Water relations of winter wheat 2. Soil water relations. *J. agric. Sci.* 91:103-116.
54. GREGORY, P. J. (1988). Growth and functioning of plant roots. In *Russell's soil conditions and plant growth*, edited by *Alan Wild (11th ed.)*. pp. 113-167. Longmann Scientific and Technical, London.

55. GUPTA, S. C. and W. E. LARSON. (1979). Estimating soil water retention characteristics from particle size distribution, organic matter percent, and bulk density. *Water Resour. Res.* 15:1633-1635.
56. HADAS, A. and D. HILLEL. (1968). An experimental study of evaporation from uniform columns in the presence of a water table. *Trans. 9th. Congr. Int. Soc. Soil Sci.* 1:67-74.
57. HAINES, W. B. (1930). Studies in the physical properties of soil: 5. The hysteresis effect in capillary properties and the modes of moisture distribution associated therewith. *J. Agri. Sci.* 20:97-116.
58. HARTMANN, R. and M. DE BOODT. (1973). Steady rate of capillary rise from a shallow water table in the flemish sandy area. *Meded. Fac. Landbouwwet. Gent* 38(4):2081-2089.
59. HARTMANN, R. (1984). Evaluation of the field water balance. Laboratory of soil physics report. *Rijksuniversiteit Gent*. Belgium.
60. HASSAN, A. A. (1986). Tensiometer: Application of measurements. *Irrigation and Water Management Division, Bangladesh Institute of Nuclear Agriculture. Report IWM-I-86.*
61. HAVERKAMP, R. and M. VAUCLIN. (1979). A note on estimating finite difference interblock hydraulic conductivity values for transient unsaturated flow problems. *Water Resour. Res.* 15(1):181-187.
62. HILLEL, D. and Y. BENYAMINI. (1973). Experimental comparison of infiltration and drainage methods for determining unsaturated hydraulic conductivity of a soil in situ. In *IAEA: Isotope and radiation techniques in soil physics and irrigation studies*, Vienna. pp. 271-275. IAEA.
63. HILLEL, D., C. G. E. M. VAN BEEK and H. TALPAZ. (1975). Macroscopic scale model of soil water and salt movement to plant roots. *Soil Sci.* 120:385-399.

64. HILLEL, D. and H. TALPAZ. (1976). Simulation of root growth and its effect on the pattern of soil water uptake by a non-uniform root system. *Soil Sci.* **121**:307-312.
65. HILLEL, D. (1980). Applications of Soil Physics. *Academic Press*, New York.
66. HOA, N. T., R. GAUDU and C. THIRROT. (1977). Influence of the hysteresis effects on transient flow in saturated-unsaturated media. *Water Resour. Res.* **13**:992-996.
67. IRWIN, R. and J. R. RANDOLPH. (1958). Root growth near tensiometer cups as a cause of diurnal fluctuations of readings. *Soil Sci.* **85**:167-171.
68. JACOBSEN, B. F. (1973). Interrelations of soil physical characteristics. *Acta Agric. Scand.* **23**:165-172.
69. JACKSON, R. J. (1962). Study of laboratory methods for assesment of soil structure with special reference to opencast sites. *Ph. D. Thesis*. King's College, Durham, U. K.
70. JAMISON, V. C. and E. M. KROTH. (1958). Available moisture storage capacity in relation to textural composition and organic matter content of several Missouri soils. *Soil Sci. Soc. Am. Proc.* **22**:189-192.
71. KEEN, B. A. (1919). A note on the capillary rise of water in soils. *J. Agric. Sci.* **9**:396-399.
72. KLUTE, A. (1972). The determination of the hydraulic conductivity and diffusivity of unsaturated soils. *Soil Sci.* **113**:264-276.
73. KLUTE, A. (1986). Water retention: Laboratory methods. In *Methods of Soil Analysis, Part I*, pp.635-660. *ASA monograph No. 9* (2nd ed.).
74. KLUTE, A. and C. DIRKSEN. (1986). Hydraulic conductivity and diffusivity: Laboratory methods. In *Method of Soil Analysis, Part I*, pp.687-734. *ASA monograph no. 9* (2nd ed.).

75. KOOL, J. B., J. C. PARKER and M. Th. VAN GENUCHTEN. (1985). Determining soil hydraulic properties from one-step outflow experiments by parameter estimation I. Theory and numerical studies. *Soil Sci. Soc. Am. J.* 49:1348-1353.
76. KOOL, J. B. and J. C. PARKER. (1987). Development and evaluation of closed-form expression for hysteretic hydraulic properties. *Water Resour. Res.* 23:105-114.
77. KOVDA, V. A. and C. VAN DEN BERG. (1973). Reclamation of saline and alkali soils. In: *Irrigation, Drainage and Salinity, an international source book*, eds. V. A. KOVDA, C. VAN DEN BERG and R. M. HAGEN, UNESCO/FAO, Hutchinson, London, pp.430-480.
78. LAL, P. and K. C. SHARMA. (1974). Contribution of groundwater in the evapotranspiration demand of wheat crop. *Indian J. Agric. Sci.* 44(10):635-639.
79. LAMBERT, J. R. and F. W. T. PENNING DE VRIES. (1973). Dynamics of water in the soil-plant-atmosphere system: A model named Torika. In *Physical Aspects of Soil Water and Salts in Ecosystems*, pp.257-273. Springer-Verlag, Berlin.
80. LAMBERT, J. R., D. N. BAKER and C. J. PHENE. (1976). Dynamic simulation of processes in the soil undergoing row crops: RHIZOS. In *Proceedings of US/USSR Conference on the Use of Large Scale Computers in Agriculture*, October, 1976.
81. LANG, A. R. G. and W. R. GARDNER. (1970). Limitations to water flux from soils to plants. *Agron. J.* 62:693-695.
82. LAWLOR, D. W. (1972). Growth and water use of *Lolium perenne* I. Water transport. *J. appl. Ecol.* 9:70-98.
83. LEMBKE, W. D. (1969). The capillary fringe above a falling water table in drainage of a lake plain soil. *Trans. ASAE* 12(4):559-563.

84. LUND, Z. F. (1959). Available water holding capacity of alluvial soils in Louisasa. *Soil Ssi. Soc. Am. Proc.* **23**:1-3.
85. MALIK, R., V. V. N. MURTY and N. K. NARDA. (1989). Macroscopic scale soil moisture dynamics model for a wheat crop. *Irrigation Sci.* **10**:141-151.
86. MARSH, B. B. (1971). Measurement of length in random arrangement of lines. *J. appl. Ecol.* **8**:265-267.
87. MARSHALL, T. J. and J. W. HOLMES. (1988). Soil Physics (2nd ed.). *Cambridge Univ. Press*, London.
88. MEMON, N. A., C. A. MADRAMOOTOO, S. O. PRASHER and R. S. BROUGHTON. (1986). A method for estimating the steady upward flux from a water table. *Trans. ASAE* **29**(6):1646-1649.
89. McGOWAN, M. (1973). Depth of water extraction by roots: Application to soil-water balance studies. In *IAEA: Isotope and Radiation techniques in soil physics and irrigation studies*, Vienna. pp.435-445. IAEA.
90. McQUEEN, I. S. and R. F. MILLER. (1974). Approximating soil moisture characteristics from limited data : empirical evidence and tentative model. *Water Resour. Res.* **10**:521-527.
91. MISRA, R. D., K. C. SHARMA, B. C. WRIGHT and V. P. SINGH. (1969). Critical stages in irrigation requirement of wheat variety *Lerma Rojo*. *Indian J. Agric. Sci.* **39**(9):898-906.
92. MODGAL, S. C., A. JOSEPH and S. S. GOEL. (1968). Effect of soil moisture regimes and nitrogen levels on the performance of Indian and Mexican wheats under Tarai conditions of UP. *Proc. Symp. Wat. Managt. Udaipur* **118**:26.
93. MOLZ, F. J. (1971). Interaction of water uptake and root distribution. *Agron. J.* **63**:608-610.
94. MOLZ, F. J. and I. REMSON. (1970). Extraction term models of soil moisture use by transpiring plants. *Water Resour. Res.* **6**(5):1346-1356.

95. MOLZ, F. J. and I. REMSON. (1971). Application of an extraction term model to the study of moisture flow to plant roots. *Agron. J.* 63:72-77.
96. MOLZ, F. J. and G. M. HORNBERGER. (1974). Water transport through plant tissue in the presence of diffusible solute. *Soil Sci. Soc. Am. Proc.* 37:833-837.
97. MOLZ, F. J. and E. IKENBERRY. (1974). Water transport through plant cells and cell walls: Theoretical development. *Soil Sci. Soc. Am. Proc.* 38:699-704.
98. MOLZ, F. J., I. REMSON, A. A. FUNGAROLI and R. L. DARKE. (1968). Soil moisture availability for transpiration. *Water Resour. Res.* 4:1161-1169.
99. MOLZ, F. J. (1975). Potential distribution in the soil-root system. *Agron. J.* 67:726-729.
100. MOLZ, F. J. (1976). Water transport in the soil-root system: Transient analysis. *Water Resour. Res.* 12:805-807.
101. MOORE, R. E. (1939). Water conduction from shallow water tables. *Hilgardia* 12:383-426.
102. MUALEM, Y. (1974). Hydraulic properties of unsaturated porous media: a critical review and new models of hysteresis and prediction of the hydraulic conductivity. *Technion, Proj. no. 38/74 (report). Israel Institute of Technology, Haifa.*
103. MUALEM, Y. (1976b). Hysteretical models for prediction of the hydraulic conductivity of unsaturated porous media. *Water Resour. Res.* 12:1248-1254.
104. MUALEM, Y. and E. E. MILLER. (1979). A hysteresis model based on the explicit domain dependence function. *Soil Sci. Soc. Am. J.* 43:1067-1073.
105. MUALEM, Y. (1986). Hydraulic conductivity of unsaturated soils: Prediction and formulas. In *Methods of Soil Analysis, Part I*, pp.780-823. *ASA monograph No. 9* (2nd ed.).
106. NARDA, N. K. and R. B. CURRY. (1981). Soyroot - a dynamic model of soybean root growth and water uptake. *Trans. ASAE* 24:651-662.

107. NEWMAN, E. I. (1966). A method of estimating the total length of root in a sample. *J. appl. Ecol.* **3**:134-145.
108. NIELSEN, D. R. and J. W. BIGGAR. (1961). Measuring capillary conductivity. *Soil Sci.* **92**:192-193.
109. NIELSEN, D. R., J. M. DAVIDSON, J. W. BIGGAR and R. J. MILLER. (1964). Water movement through Panoche clay loam soil. *Hilgardia* **35**:491-506.
110. NIELSEN, D. R., J. W. BIGGAR and K. T. ERH. (1973). Spatial variability of field-measured soil-water properties. *Hilgardia* **42**:215-260.
111. NIKOLSKI, Y. N. (1977). The dependence of irrigation requirements on water table depth in drained lands. *Agric. Water Management* **1**:191-196.
112. NIMAH, M. N. and R. J. HANKS. (1973). Model for estimating soil water, plant and atmospheric interrelations I. Description and sensitivity. *Soil Sci. Soc. Am. Proc.* **37**:522-527.
113. OGATA, GEN., L. A. RICHARDS and W. R. GARDNER. (1960). Transpiration of alfalfa determined from water content changes. *Soil Sci.* **80**:179-182.
114. PARKER, J. C., J. B. KOOL and M. Th. VAN GENUCHTEN. (1985). Determining soil hydraulic properties from one-step out-flow experiments by parameter estimation II. Experimental studies. *Soil Sci. Soc. Am. J.* **49**:1354-1359.
115. PARLANGE, N. Y. and D. AYLLOR. (1972). Theory of water movement in soils 9. The dynamics of capillary rise. *Soil Sci.* **114**:79-81.
116. PHILIP, J. R. (1957a). The physical properties of soil water movement during the irrigation cycle. *Trans. 3rd Cong. Interim. Comm. Irr. Drain., Question* **8**:125-154.
117. PHILIP, J. R. (1957b). The theory of infiltration: 3. Moisture profiles and relation to experiment. *Soil Sci.* **84**:163-178.

118. PHILIP, J. R. (1966). The dynamics of capillary rise. In *UNESCO symposium on water in the unsaturated zone* pp.559-564.
119. POULOVASSILIS, A. (1962). Hysteresis of pore water: an application of the concept of independent domains. *Soil Sci.* **93**:405-412.
120. POULOVASSILIS, A. (1970). The effect of the entrapped air on the hysteresis curves of a porous body and its hydraulic conductivity. *Soil Sci.* **109**:154-162.
121. RAGAB, R., J. FEYEN and D. HILLEL. (1981). Comparative study of numerical and laboratory methods for determining the hydraulic conductivity function of a sand. *Soil Sci.* **131**:375-388.
122. RAGAB, R. A. and F. AMER. (1986). Estimating water table contribution to the water supply of maize. *Agric. Water Management* **11**:221-230.
123. RAATS, P. A. C. and W. R. GARDNER. (1974). Movements of water in the unsaturated zone near water table. In *Drainage for Agriculture*. pp.311-355. *ASA monograph No. 17*.
124. REICOSKY, D. C., R. J. MILLINGTON, A. KLUTE, and D. B. PETERS. (1972). Patterns of water uptake and root distribution of soybeans in the presence of a water table. *Agron. J.* **64**:292-297.
125. REICOSKY, D. C. and J. T. RITCHIE. (1976). Relative importance of soil resistance in root water absorption. *Soil Sci. Soc. Am. J.* **40**:293-297.
126. RICHARDS, L. A. (1931). Capillary conduction of liquids through porous mediums. *Physics* **1**:318-333.
127. RICHARDS, L. A. and O. R. NEAL. (1936). Some field observation with tensiometers. *Soil Sci. Soc. Am. Proc.* **1**:71-91.
128. RICHARDS, L. A. (1965). Physical conduction of water in soil. In *Methods of Soil Analysis, Part I*, pp.125-151. *ASA monograph No. 9 (1st ed.)*.
129. RICHARDS, L. A., W. R. GARDNER and G. OGATA. (1956). Physical processes in determining water loss from soil. *Soil Sci. Soc. Am. Proc.* **20**:310-314.

130. RIJTEMA, P. E. (1959). Evapotranspiration in relation to suction and capillary conductivity. Plant water relationships in arid and semi arid conditions. *Proc. Madrid Symp. Arid Zone Research, Unesco*, pp.99-106.
131. RIJTEMA, P. E. (1965). An analysis of actual evapotranspiration. *Agr. Res. Rep. 659*. 179 pp., Pudoc, Wageningen, Netherlands.
132. RIPPLE, C. D., J. RUBIN and T. E. A. VAN HYLKAMA. (1972). Estimating steady-state evaporation rates from bare soils under conditions of high water table. *U.S. Geol. Survey, Water Supp. Paper 2019-A*.
133. RITCHIE, J. T. (1972). Model for predicting evaporation from a row crop with incomplete cover. *Water Resour. Res.* 8:1204-1213.
134. ROGOWSKI, A. S. (1971). Watershed physics : model of the soil moisture characteristics. *Water Resour. Res.* 7:1575-1582.
135. ROSE, C. W., W. R. STERN and J. E. DRUMMOND. (1965). Determination of hydraulic conductivity as a function of depth and water content for soil in situ. *Aust. J. Soil Res.* 3:1-9.
136. ROSE, C. W. and W. R. STERN. (1967). Determination of withdrawal of water from soil by crop roots as a function of depth and time. *Aust. J. Soil Res.* 5:11-19.
137. ROSE, D. A. (1963a). Water movement in porous materials. I. Isothermal vapour transfer. *Brit. J. Appl. Phys.* 14:256-262.
138. ROSE, D. A. (1968b). Water movement in porous materials III. Evaporation of water from soil. *Brit. J. Appl. Phys. (J. Phys. D.)*, Ser. 2, 1:1779-1791.
139. SALTER, P. J., G. BERRY and J. B. WILLIAMS. (1966). The influence of texture on the moisture characteristics of soils II. Quantitative relationships between particle size, composition, and available water capacity. *J. Soil Sci.* 17:93-98.
140. SCHOFIELD, R. K. (1935). The p^F of the water in soil. *Trans. 3rd Congr. Int. Soc. Soil Sci.* 2:37-48.

141. SHARMA, K. C. and M. SINGH. (1971). Optimum time of first irrigation for dwarf wheats in Tarai soils with high water table. *Indian J. Agron.* 16:271-275.
142. SHAYKEWICH, C. F. and M. A. ZWARICH. (1968). Relationship between soil physical constants and soil physical components of some Manitoba soils. *Can. J. Soil Sci.* 48:199-204.
143. SHAYKEWICH, C. F. and L. STROOSNIJDER. (1977). The concept of matric flux potential applied to simulation of evaporation from soil. *Neth. J. Agric. Sci.* 25:63-82.
144. SHIH, S. F. and G. S. RAHI. (1985). Evapotranspiration, yield, and water table studies of celery. *Trans. ASAE* 28(4):1212-1218.
145. SHIH, S. F. (1985). Yield of sweet corn grown with shallow water table. *Trans. ASAE* 28(5):1578-1582.
146. SHIH, S. F. (1986). Evapotranspiration, water use efficiency, and water table studies of sweet sorghum. *Trans. ASAE* 29(3):767-773.
147. SKAGGS, R. W. (1978). A water management model for shallow water table soils. *Report No. 134*, Water Resources Research Institute of the University of North Carolina, Raleigh.
148. SLATYER, R. O. (1967). *Plant-Water Relationships*. Academic Press, London.
149. SLAVIK, B. (1974). *Methods of studying plant water relations*. Springer-Verlag, New York.
150. SPOSITO, G. and W. A. JURY. (1986). Fundamental problems in the stochastic convection-dispersion model of solute transport in aquifers and field soils. *Water Resour. Res.* 22:77-88.
151. STEWART, E. H., J. E. BROWNING and E. O. BURT. (1969). Evapotranspiration as affected by plant density and water table depth. *Trans. ASAE* 12(5):646-647.

152. STONE, L. R., L. HORTON AND T. C. OLSON. (1973). Water loss from an irrigated sorghum field 2. Evapotranspiration and root extraction. *Agron. J.* 65:495-497.
153. STUFF, R. G. and R. F. DALE. (1978). A soil moisture budget model accounting for shallow water table influences. *Soil Sci. Soc. Am. J.* 42:637-643.
154. TALSMA, T. (1963). The control of saline ground water. *Med. Landb. Wageningen* 63(10):1-68.
155. TALSMA, T. (1970). Hysteresis in two sands and the independent domain model. *Water Resour Res.* 6:964-970.
156. TAYLOR, H. M. and B. KLEPPER. (1971). Water uptake by cotton roots during an irrigation cycle. *Aust. J. biol. Sci.* 24:853-859.
157. TAYLOR, H. M. and B. KLEPPER. (1978). The role of rooting characteristics in the supply of water to plants. *Adv. Agron.* 30:99-128.
158. TENNANT, D. (1975). A test of a modified line intersect method of estimating root length. *J. Ecology* 63:995-1001.
159. TOPP, G. C. (1969). Soil water hysteresis measured in sandy loam compared with the hysteretic domain model. *Soil Sci. Soc. Am. Proc.* 30:156-162.
160. TOPP, G. C. (1971). Soil-water hysteresis : The model theory extended to pore interaction conditions. *Soil Sci. Soc Am. J.* 33:645-651.
161. TORRES, J. S. and R. J. HANKS. (1989). Modelling water table contribution to crop evapotranspiration. *Irrigation Sci.* 10:265-279.
162. VACHAUD, G. and J. L. THONY. (1971). Hysteresis during infiltration and redistribution in a soil column at different initial water content. *Water Resour. Res.* 7:111-127.
163. VAN BAVEL, C. H. M., G. B. STIRK and K. J. BRUST. (1968a). Hydraulic properties of a clay loam soil and the field measurement of water uptake by

- roots I. Interpretation of water content and pressure profiles. *Soil Sci. Soc. Amer. Proc.* **32**:310-317.
164. VAN BAKEL, P. J. T. (1981). Unsaturated zone and evapotranspiration. *Tech. Bull. 7, Institute for Land and Water Management Research, Wageningen, Netherlands.*
165. VAN DEN HONERT, T. H. (1948). Water transport in plants as catenary process. *Disc. Faraday Soc.* **3**:146-153.
166. VISSER, W. C. (1959). Crop growth and availability of moisture. *Tech. Bull. No. 6, Institute for Land and Water Management Research, Wageningen, Netherlands.*
167. VISSER, W. C. (1969a). The relation between lithological properties and the shape of the desorption curve. In *UNESCO symposium on water in the unsaturated zone.* pp.305-311.
168. VISSER, W. C. (1969b). An empirical expression for the desorption curve. In *UNESCO symposium on water in the unsaturated zone.* pp.329-335.
169. WALLENDER, W. W., D. W. GRIMES, D. W. HENDERSON and L. K. STROMBERG. (1979). Estimating the contribution of a perched water table to the seasonal evapotranspiration of cotton. *Agron. J.* **71**:1056-1060.
170. WATSON, K. K. (1966). An instantaneous profile method for determining the hydraulic conductivity of unsaturated porous materials. *Water Resour. Res.* **2**:709-715.
171. WHISLER, F. D., A. KLUTE and R. J. MILLINGTON. (1970). Analysis of radial, steady state solution and solute flow. *Soil Sci. Soc. Am. Proc.* **34**:382-387.
172. WHISLER, F. D., A. KLUTE and R. J. MILLINGTON. (1968). Analysis of steady state evapotranspiration from a soil column. *Soil Sci. Soc. Am. Proc.* **32**:167-174.

173. WILLIAMS, J., R. E. PREBBLE, W. T. WILLIAMS and C. T. HIGNETT. (1983). The influence of texture, structure, and clay mineralogy on the soil moisture characteristics. *Aust. J. Soil Res.* 21:15-32.
174. WILLATT, S. T. and H. M. TAYLOR. (1978). Water uptake by soybean roots as effected by their depth and soil water content. *J. Agric. Sci., Camb.* 90:205-213.
175. WIND, G. P. (1955). A field experiment concerning capillary rise of moisture in a heavy caly soil. *Neth. J. Agric. Sci.* 3:60-69.
176. YOUNGS, E. G. (1960). The hysteresis effect in soil moisture studies. *Trans. 7th Congr. Int. Soc. Soil Sci.* 1:107-113.
177. YANG, S. J. and E. DE JONG. (1972). Effect of aerial environment and soil water potential on the transpiration and energy status of water in wheat plants. *Agron. J.* 61:571-578.
178. ZHANG, W. (1968). Methods for estimating the evaporation from shallow water table in drainage design formulas. *Hydraulic design in water resources engineering: Land drainage - Proceedings of the 2nd international Conference*, Southampton University, U.K. pp.63-73.